

# Use of MOS Gas Sensors with Temperature Modulation-Specified Detection Point for Potential Identification of Soil Status Using Electronic-Nose Principle

メタデータ	言語: eng 出版者: 公開日: 2017-10-05 キーワード (Ja): キーワード (En): 作成者: メールアドレス: 所属:
URL	<a href="http://hdl.handle.net/2297/45400">http://hdl.handle.net/2297/45400</a>

This work is licensed under a Creative Commons Attribution-NonCommercial-ShareAlike 3.0 International License.



# **DISSERTATION**

## ***Use of MOS Gas Sensors with Temperature Modulation-Specified Detection Point for Potential Identification of Soil Status using Electronic-Nose Principle***

**Graduate School of  
Natural Science & Technology  
Kanazawa University**

**Division of  
Electrical Engineering and Computer Science**

**Student ID: 1223112011  
Name: Arief Sudarmaji  
Chief advisor: Prof. Akio Kitagawa  
March 2016**

# CONTENTS

LIST OF FIGURES .....	iii
LIST OF TABLES .....	vii
ABSTRACT .....	ix
Chapter 1. Introduction.....	1
1.1.    Background Overview .....	1
1.2.    Research Objectives .....	5
1.3.    Dissertation Organization .....	6
Chapter 2. Fundamental Literature Review .....	9
2.1.    Soil Smell and Potential Gases in Soil Atmosphere .....	9
2.2.    Principle of E-Nose Technology .....	11
2.3.    Sample Handling and Measurement Methods .....	14
2.4.    MOS Gas Sensors Technology for E-Nose .....	17
2.5.    Pattern Recognition Tools in E-Nose (PARC) .....	21
Chapter 3. Temperature Modulation with Specified Detection Point on Array MOS Gas Sensors.....	25
3.1.    Introduction.....	25
3.2.    Design of Rectangular Temperature Modulation-SDP.....	26
3.3.    Experimental Design.....	28
3.4.    Results and Discussion.....	31
3.4.1. The Modulation and Sensor Response under Modulation.....	31
3.4.2. Environmental Circumstances and Initial Response.....	35
3.4.3. Selectivity Evaluation. ....	37

Chapter 4. Potential Use of Temperature Modulation-SDP on MOS Gas Sensors in Self-made E-Nose to Indicate Additional Nutrient in Soil .....	43
4.1. Introduction .....	43
4.2. Experimental Materials and Methods .....	44
4.2.1. The Self-made Electronic-Nose .....	44
4.2.2. Soil Preparation and Treatment .....	46
4.2.3. Soil Gaseous Sampling and Headspace Condition. ....	47
4.2.4. Measurement Procedures. ....	49
4.3. Results and Discussion.....	51
4.3.1. Initial Measurement. ....	51
4.3.2. Sensor Responses and soil gaseous profiles. ....	52
4.3.3. Soil Discrimination under different nutrient addition. ....	55
Chapter 5. Conclusion.....	59
5.1. Conclusions.....	59
5.2. Future Works. ....	61
Acknowledgments .....	63
References .....	65
Publication List.....	79
Appendix .....	81

## LIST OF FIGURES

Fig. 2.1. Historical research of development of e-nose based system (Turner & Magan 2004). .....	11
Fig. 2.2. Section through human nose representing some components of the olfactory system, adapted from Nagle et al. (1998) and Patel (2014). .....	12
Fig. 2.3. Representing components mimics the functional units in human olfactory system (Turner & Magan 2004). .....	13
Fig. 2.4. Principles of static headspace when (a) equilibration and (b) sample delivery. SC=sample container, TH=thermostating, adapted from Nakamoto (2003). ...	15
Fig. 2.5. Principle of Purge and Trap method in GC, (a) the adsorption of volatiles from the sample and (b) the desorption from the adsorption by back-flushing of the heated trapped volatiles, adapted from Nakamoto (2003). .....	16
Fig. 2.6. Principle of (a) the static system and (b) the sampling of sample flow system, adapted from Nakamoto (2003). .....	16
Fig. 2.7. Basic elements of MOS gas sensor, adapted from Patel (2014). .....	18
Fig. 2.8. The basic construction of (a) the sintering-type and (b) thin-film type of the MOS gas sensors, adapted from Yamazoe et al. (2003). .....	18
Fig. 2.9. (I) Schematic depiction of ionosorption in structural and band model for atmospheric O <sub>2</sub> interaction and CO gas sensing by SnO <sub>2</sub> where (a) with or (b) without CO existence (Wang et al. 2010), while (II) is the simplified model (Puzzovio 2008). .....	21
Fig. 2.10. Scheme of classification of multivariate analysis used in e-nose application (Patel 2014). .....	22

Fig. 2.11. Descent in weight space for (a) small learning rate, (b) large learning rate, and (c) large learning rate with momentum (Du & Swamy 2014). .....	23
Fig. 2.12. The architecture of neural network with single hidden layer, adopted from Du & Swamy (2014). .....	24
Fig. 3.1. Schematic-based comparison of typical working mode of MOS gas sensor: A. static temperature modulation, B. temperature modulation, and C. temperature modulation with specified detection point, where $V_H$ =voltage of heater, $V_C$ =voltage of sensing element, and $V_o$ =voltage of output. ....	26
Fig. 3.2. The signal of (a) required modulation of TGS 2444 and (b) the designed temperature modulation-SDP. ....	27
Fig. 3.3. Schematic of temperature modulation-SDP for array (a) TGS sensor and (b) FIS sensor with $V_H$ is heater voltage, $V_C$ is sensing circuit voltage, $S_{VH}$ is modulation signal for $V_H$ , and $S_{VC}$ is modulation signal for $V_C$ . ....	28
Fig. 3.4. Diagram block of system based on PSOC CY8C28445-24PVXI with pins configuration. ....	29
Fig. 3.5. Diagram of sample flow system (dynamic chamber) measurement to measure 3 various liquids (ammonia, ethanol, and toluene). ....	29
Fig. 3.6. Captured signal on MOS gas sensors under applied modulation of 0.25 Hz with duty cycle 25%, 50% and 75%, where: $V_{OH}$ (top)= 2V/div of FIS; $V_{OH}$ (top)= 2V/div of TGS; $V_{OC}$ (middle) =5V/div; Time of detection Point (below) =5V/div; Time-Div= 1s. ....	32
Fig. 3.7. Response of (a) TGS 2444, and the others (TGS2602, TGS830, FISAQ1, FISSB30 and FIS12A) operated on (b) modulation 0.25 Hz, (c) modulation 1 Hz, and (d) modulation 4 Hz to air (no gas), ammonia, ethanol, and toluene gas.	

.....	33
Fig. 3.8. Change of chamber environment (temperature, relative humidity, and oxygen concentration) after 30 minutes initial action. ....	35
Fig. 3.9. Initial action responses of MOS sensors Resistance during 30 minutes after ready state conditioning (1 minute) of each MOS gas sensors: (1)=TGS-2602, (2)=TGS-825, (3)=FIS-12A, (4)=FIS-AQ1, and (5)=FIS-SB30 on modulation frequency: 0.25Hz (dotted), 1Hz (dashed) and 4Hz (solid). All modulation were on 50% duty cycle.....	37
Fig. 3.10. The resistance responses of the SnO <sub>2</sub> sensor on 200 ppm H <sub>2</sub> pulses at various operating temperatures (Malyshev & Pislyakov 2008). ....	37
Fig. 3.11. Sensitivity variation of each MOS gas sensors and modulation upon exposure to various gases after (a) 15 minutes and (b) 30 minutes quasi-steady state ...	39
Fig. 3.12. Visualization of PCA plot of selected temperature modulation-SDP Vs without Modulation using 3 major PCs. ....	40
Fig. 3.13. Comparison of selectivity performance of array sensors among temperature modulation-SDP to distinguish three gases based on distance of Principal Component's score after 15 minutes and 30 minutes quasi-steady state. ....	40
Fig. 4.1. Measurement diagram of soil vapor fingerprint based on e-nose principle. ..	45
Fig. 4.2. Static headspace design for saturated soil samples.....	47
Fig. 4.3. Headspace conditioning with heating and stirring using The Corning PC-420D in SH sampling, the layout of Corning modified from (Corning Inc. 2007). ..	49
Fig. 4.4. Experimental setup to capture the soil gaseous compounds using static headspace extraction in sample flow system (close) measurement. ....	50
Fig. 4.5. Measurement steps to indicate the nutrient level based on soil gaseous profiles.	

.....	51
Fig. 4.6. The response of TGSs and FISs to soil samples (sandy loam soil and sand soil) without compost addition under 0.25 Hz; 75% modulation in 5 minutes. ....	51
Fig. 4.7. 0.25 Hz; 75% Modulation signals of TGS and FIS, orange: $S_{VH}$ , blue: $S_{VC}$ , and purple: time of detection point, captured by Oscilloscope Tektronix TDS 2024B: 5V/div except for $S_{VH}$ of FIS at 2V/div (Sudarmaji & Kitagawa 2015).....	52
Fig. 4.8. Variation of baseline resistance expressed in standard deviation from mean value during measurement. ....	53
Fig. 4.9. Individual Sensitivity of sensor, average of 5 replicates, to 3 level of compost adding in different soil, 1:TGS2444, 2:TGS2602, 3: TGS825, 4: FISAQ1, 5: FISSB30, and 6: FIS12A. ....	54
Fig. 4.10. Experiment result of TGS 825 responses to compost dose (Ton/Ha) in sandy loam and sand soil for 5 replicates.....	55
Fig. 4.11. PCA plot between sandy loam and sand soil in without compost addition. .	56
Fig. 4.12. PCA plot between sandy loam and sand soil both without compost addition, and soil gaseous pattern projection mapped in 2 PCs for each soil sample to differ the level of compost addition of (b) sand, (c) sandy loam, (d) irrespective of soil type.....	57



# LIST OF TABLES

Table 2.1. Doped additive materials in semiconductor oxide-based gas sensors (Yamazoe et al. 2003).....	19
Table 3.1. Properties of analyte liquids and their calculated portion in prepared solution. .....	31
Table 3.2. Selected temperature modulation-SDP of MOS gas sensors based on their sensitivities for 15 minutes and 30 minutes quasi-steady state prior measurement. ....	38
Table 3.3. Euclidean distance between Principal Component score of no modulation vs. selected modulation of 15 minutes and 30 minutes quasi-steady state.....	40
Table 3.4. Solubility, determined by Henry's Law constant, among Ammonia, Ethanol, and Toluene. (Sander 2015) .....	41
Table 4.1. MOS gas sensors used and typical gas target <sup>*)</sup> .....	45
Table 4.2. Properties of samples of soil, fertilizer, water, and static headspace condition. .....	49
Table 4.3. Sensor chamber circumstances during $R_0$ and $R_g$ measurement. ....	53
Table 4.4. Cumulative proportion of 3 PCs resulted from 6 sensors used. ....	58
Table 4.5. MSE achieved by 6 neuron of hidden layer to discriminate 3 level of compost addition in soil. ....	58

*This page is intentionally left blank*

## ABSTRACT

The dissertation presents a potential use of array MOS gas sensors which driven by new temperature modulation technique in a self-made e-nose system to identify soils in certain status (i.e. the presence of nutrient addition) by capturing the soil gaseous profiles. Soils is a complex mixture that composed mostly of minerals and organic materials, water, air, and countless organisms. Many gases, mostly volatile organic compounds, are found at soil atmosphere which their type and the concentrations produced may be differ because of differences in community composition of microbes and material contained. And also the presence of particular smell molecules of soil might affect the generated gases and volatiles.

It is introduced the new technique namely temperature modulation with specified detection point (temperature modulation-SDP) which applied to drive the array of MOS gas sensor. Basically, it is similar with general temperature modulation, yet it also modulates the sensing unit concurrently and in same phase with the modulation on the heater unit. The SDP means the output detection (acquiring) of MOS gas sensor is put at specified point (i.e. at middle of sensing unit modulation). In first investigation, the rectangular (square) modulation was successfully designed and it led to response more distinct and sloping at lower frequency. It could increase the sensitivity and selectivity either on single or array sensors rather than static temperature. By applying selected temperature modulation-SDP, The PCA plot showed that it provided more than 60% increment of selectivity compared with static temperature in discriminating 3 gases (Toluene, Ethanol and Ammonia).

By using the same gas sensors, the technique was then tested on their sensing performance to such a complex mixture, soil gaseous compound. The self-made e-nose was employed to identify two soils (sandy and loam sand) and the presence of nutrient addition at different dose. It consists of (a) 6 MOS gas sensors

(TGS2444, TGS2602, TGS825, FISAQ1, FISSB30, and FIS12A) which driven and acquired wirelessly to a computer through (b) an interface system based on PSoC CY8C28445-24PVXI, and (c) Principal Component Analysis (PCA) and Neural Network (NN) as preprocessing and pattern recognition units respectively. The soil odors and volatiles were accumulated using a static headspace under both thermostating and agitating in certain condition for optimizing the equilibration. The soil gaseous profiles were presented in PCA plots and the patterns were trained by back-propagation algorithm which employs a log-sigmoid activation function and updates the weights using search-then-converge schedule. The results indicate that the temperature modulation-SDP in the e-nose system could differentiate clearly the soil type and indicate the presence of nutrient addition in soil and their level as well since they could response and has different sensitivity according to the samples, providing (unique) soil gaseous profiles. An optimum architecture of 3-layer (3-6-3) NN was obtained to discriminate among the pre-described three categorized fertilizer levels (without, normal, and high dose) in soil sample with PCA as data preprocessor of sensor outputs. The PCA helps improving the NN classification to differ level of compost addition in soil. As an instance on gaseous profile of sand soil, the training resulted in the MSE (mean square error) respectively  $4.20 \times 10^{-4}$  and  $3.49 \times 10^{-3}$  for the with PCA system and without PCA.

**Keywords:** Soil gases, MOS gas sensor, temperature modulation, specified detection point, E-nose application.

# Chapter 1. Introduction

## 1.1. Background Overview

Practical application of precision agriculture aims not only to optimize the crop productions and increase the economic takings to farmer consequently, but also able to reduce the negative environmental impact due to farming activities. More precise and appropriate resources management either temporally and spatially may reduce their under or over application, thereby ensuring optimum result for any given unit of land (Lee et al. 2010). Hence, a rapid and accurate information concerning the spatial variabilities within fields is required to achieve the philosophy of precision agriculture (e.g. for specialty crops) which one of this variabilities is soil status information which plays important role in further precision farming application (Sudduth et al. 1997; Lee et al. 2010). Good practice in soil management and land-use will prevent deep degradation of soil quality which mainly caused by excessive application of pesticides, herbicides, and commercial fertilizer (Doran 2002). The uncontrolled and over use of fertilizer has been cited as a source of contamination of surface and groundwater (Vadas et al. 2004). Moreover, an arbitrary management practices can influence atmospheric quality through changes in the soil's capacity to produce/consume direct or indirectly important atmospheric gases such as ammonia ( $\text{NH}_3$ ), carbon dioxide ( $\text{CO}_2$ ), carbon monoxide ( $\text{CO}$ ), nitric oxide ( $\text{NO}$ ), nitrous oxide ( $\text{N}_2\text{O}$ ), and methane ( $\text{CH}_4$ ) (Li 2000; Mosier 1998).

Ideally, application rates should be adjusted based on estimates of the requirements for optimum production at each location because there is high spatial variability of nutrient within individual agricultural fields (Page et al. 2005). Therefore, the ability of instrument to be applied in the in-situ measurement is main point to quantify soil variables where information on the state of the soil can be in line with immediate responds of the device system (Hellebrand et al. 2002). Otherwise, the other possibility is the separation in time of sensing and control action by the condition will not changes essentially or the change can be calculated accurately. Both are required the sensors in each case, since all actions must be based on reliable necessary information.

Besides some physical environment parameters of soil (such as temperature, water

content and pH), the emitted gasses from soil has been investigated and become more attracting due to concerning the climate change and other potential analysis, such as potential indication or early detection of the soil status related to the use of additional nutrients. This is possible since odorous compounds result from decomposition of matter (Vass et al. 2008; Scaglia et al. 2011), and some strong evidences which pointed that resulted gases and volatile organic compounds (VOCs) in the soil atmosphere in vary widely types and relative concentrations (Wheatley et al. 1996; Peñuelas et al. 2014) might be produced due to fertilizer adding and microbial activity (De Cesare et al. 2011) which influenced by environment conditions (Milchunas et al. 1988; Sherlock et al. 1994; Smith et al. 2003). Moreover, also there are known smell molecules in soil, namely geosmin and methylisoborneol (Wang & Cane 2008; Mei Wang & Cane 2008; Green et al. 1975), which would influence the soil gaseous profile resulted in soil atmosphere.

The Gas Chromatography/Mass Spectrometry (GC/MS) technique is a well-known and established method to identify and quantify accurately the soil gaseous and volatile compounds as important soil status in many purposes and applications, including nutrient components determination (Smith & Dowdell 1973; Carter & Gregorich 2008). However, it is difficult to take the advantages of GC/MS for rapid or in-situ measurement. It becomes less favored since the large labor requirements (e.g. sample preparation, mixed with an extracting material and skilled operation of the extraction unit), the expense and time needed, making inefficient (Rappert & Müller 2005). Therefore it is needed fast and reliable sensors and measuring techniques to obtain the soil gaseous profiles.

In gas sensor technology, some advance and wide inventions of technologies of gas sensor are chemo-resistive (Metal Oxide Semiconductor, MOS) sensors, electrochemical (Galvanic Fuel Cell) sensors and non-dispersive infrared radiation absorption (NDIR) (Aleixandre & Gerboles 2012). Particularly, the established and fabricated in MOS gas sensor (such as by Figaro, Inc. and FIS, Inc.) has lead fabricated small size, robust, and low cost sensor with various sensitivity and fairly stable to be applied successfully in agricultural fields for many purposes (Wilson & Baietto 2009; Berna 2010), including soil application (Rincón et al. 2010; Del et al. 2007). Yet, despite their many distinctive quality factors, MOS gas sensors also likely to have a drift (Hierlemann & Gutierrez-Osuna 2008) and poor selectivity (cross-sensitivity) to other gases which might render unreliable signal and affect the baseline and the sensitivity of sensor (Bermak et al. 2005;

Carlo & Falasconi 2012). The drift is caused from variation of temperature and humidity (Meixner & Lampe 1996) which changes the baseline of the sensor signal shifts which are potentially resulted from use of static temperature on gas sensor and mounting the sensor in chamber. The static temperature, consequently by given static/direct voltage, only provides one dimensional response (i.e. the changes in direct resistance) and there is no other information about the response reactions. This is inadequate for distinguishing between the response to a target and those to other interfering gases (Nakata et al. 2006; Huang et al. 2004). Each metal-oxide sensor is primary selective to one certain gas but its cross-sensitivity to other gases is not negligible (Wilson & Baietto 2009) and also known that the performance of almost all types of SnO<sub>2</sub> sensors is sensitive to the temperature of operation (Wang et al. 2010).

As reported by Lee & Reedy (1999), temperature modulation through oscillation of heater voltage, also some called dynamic measurement technique, has been most potential promising and established technique of temperature modulation than temperature transient or pulsed techniques to be applied on MOS gas sensors. Temperature modulation alters the kinetic of the sensor through changes in the operational temperature of device. The operating modulation voltage, also consequently the operating temperature, of the sensor changes periodically either by square (rectangular) or triangular or sine waveform (Huang et al. 2004). Lee & Reedy (1999) also reported that since a cyclic temperature variation lead different rates of reaction of various analyte gases, it can give a unique response for each gas. The response of temperature modulation is more distinct and informative than static temperature. By using rectangular waveform, Dutta & Bhuyan (2012) has determined the optimal frequency applied for each sensor using theory of system identification based on best fit transfer function, pole-zero plot and the overshoot percentage. In agricultural application, Huang et al. (2003) applied the rectangular temperature modulation to distinguish the presence of two pesticide gases, acephate and trichlorphon (binary gas mixture), in the ambient atmosphere.

In advance, it is successfully developed a new technique based on temperature modulation to increase selectivity and sensitivity of MOS gas sensor and named it Temperature Modulation-Specified Detection Point (SDP) (Sudarmaji & Kitagawa 2015). This technique together with Principle Component Analysis (PCA) provided 64.7% higher selectivity than the static temperature modulation on array gas sensors to

distinguish 3 gases resulted from each liquid (ammonia, ethanol, and toluene). Thus, this technique is highly potential be employed in an application using principle of electronic-nose (e-nose) which therein widely utilizes a PCA.

The favorable method which could overcome the disadvantages of using single MOS gas sensor, is that called electronic nose (e-nose). The primary advantage of E-noses is the presence of an array of sensors coated with differentially and partially specific sensitive materials which can interact with single analytes belonging to the same chemical class but not highly specific for a single substance, it can also interact with substances belonging to other chemical classes (cross-selectivity), despite on a lower extent (overlapping responses) (Nanto & Stetter 2003). This technology have been made ever since the early 1980s when researchers at the Warwick University (Coventry, England) developed sensor arrays for odor detection based on conductivity changes, i.e. initially using metal oxide sensors and later exploring the polymer-based sensor (Nagle et al. 1998),.

E-nose which mimic the human sense of smell capable to analyze complex mixtures of gases and volatiles (odors or aromas) in atmospheres. Typically, a sampling unit delivers the odor molecules to a test chamber in which the sensor array is based; the interaction between the sensors and the volatile compounds produce a change in the sensors response; this change is then interpreted by a pattern recognition system, in order to obtain uniquely an olfactory fingerprint of the analyzed sample. To maximize the use of e-nose technology, a neural network is installed, which act might like the memory in our brain, creating a library of sensor responses, also known as sensor profiles.

E-nose normally will not get tired nor be sensitized to particular smells and it also does not required comfortable or safe working conditions. It can sample the environment continuously, or at least frequently, and give a rapid feedback of the results. It is desirable even if the accuracy is not as good as that of the corresponding laboratory instrument in a controlled circumstance. Normally, the laboratory-based method is laborious and time consuming. E-nose also become attractive method and many applied by detecting the volatile changes, like the physical properties and quality of fruits and vegetables can be evaluated to substitute trained human panelists (Lee et al. 2010).

In agriculture field, many results give the strong evidences of successful system applications based on e-nose principle such as assessment of agriculture products quality



(freshness, ripeness, contamination, spoilage), cultivar selection, preservation treatments, variety characteristics, plant pathology, and plant identification (Wilson & Baietto 2009). Bastos & Magan (2006) applied electronic nose technology to detect and monitor the early microbial activity in water as well as for monitoring geosmin production in different water types by using normalized divergence data were analyzed using principal component analysis (PCA) and discriminant function analysis (DFA), thus help preventing off-odors and tastes occurrences. Then in (2007), they employed non-specific polymer sensor array to differentiate between soil types, and between soil samples under different temperature and water potential conditions. Following the addition of glucose or wheat straw into soil, a temporal discrimination between soil volatile fingerprints was obtained as response to nutrients, as well as between treated and untreated controls.

Especially in soil analysis as reported by De Cesare et al. (2011), a relevant and successful example of e-nose application on soil cases have been developed in recent years such as ammonium detection through ammonia measurement. They themselves measured the microbial activity in silty clay loam soil to distinguish different metabolic and growth phases of the inoculated bacteria during incubation and to discriminate between inoculated and non-inoculated ecosystems. The growth and activity of microbial was accelerated by adding nutrient solutions (organic and inorganic C, N, P and S sources) into soil which incubated for 23 days.

By those facts, E-nose technology which employs array of MOS gas sensors driven by the advanced temperature modulation technique was used to measure the gases and volatiles from conditioned soil sample and environment in order to indicate the soil status with different condition due to nutrient addition. It tests the potential of the temperature modulation-SDP technique based on the sensitivity and selectivity of sensor responses to the influence of soil type and nutrient addition. I tested two soils (sandy loam and sand) with the following addition of commercial compost in different dose (without, normal, and high).

## **1.2. Research Objectives**

One of essential aspects on Precision Agriculture is rapid availability of soil status, including the information relates to the soil gases and volatiles due to application of

additional nutrient in soil. It affects plant growth and contributes to environmental changes as well, also can change over time due to its circumstances conditions. It is therefore important to early detect and assess changes in soil, in order to support the way to optimize and overcome those changes respectively. This research explores qualitatively the potential of soil gaseous profiles acquired from an array MOS gas sensors rapidly for early information of soil condition since there expected gases and volatiles emitted from soil which correlated and effected with soil material contents.

Based on qualitative soil gaseous analysis, this project aims to examine the potential use of MOS gas sensors which driven by temperature modulation-SPD in an e-nose-based system for early and rapid indication of soil status relates to soil type and nutrient addition. It was tested the sensor responses characterization and ability of the e-nose for that such purpose by applying the fit modulation and generating the gaseous profiles in static headspace under particular controlled environment condition. Therefore, the objectives of this research are as follow:

- a. To design a temperature modulation-SDP technique that can drive a single or array gas sensor in e-nose application.
- b. To test the performance of the temperature modulation-SDP on the sensitivity and selectivity of MOS gas sensors on different sample of gases;
- c. To build a self-made e-nose system based on MOS gas sensors driven by temperature modulation-SDP for capturing the soil gaseous profile and indicating the soil type and nutrient addition in different dose.

### **1.3. Dissertation Organization**

In general, there are two main discussion in this dissertation, firstly a new development technique of temperature modulation on MOS gas sensor and secondly its potential implementation on agricultural field, especially in soil status due to the presence of additional nutrient in order to support precision agriculture eventually. The overall research was conducted laboratory based at Micro Electronic Research Laboratory of Kanazawa University.

The dissertation is organized into five chapters. Chapter 1 generally presents the logical motivations of this study as to the importance of knowing the soil status relates to

the use of additional nutrient that possibly obtained early by analyzing the soil gas profile acquired from the gas sensor that run by a particular technique. The term of temperature modulation with specified detection point (SDP) is introduced as our first work to drive MOS gas sensors in order to increase their selectivity and sensitivity. Chapter 2 provides the overview of fundamental literatures related to the aspects of this study. It includes the soil smell and potential gases in soil atmosphere, the principle of e-nose technology, and e-nose apparatus such as the method of sample handling and measurement in e-nose, MOS gas sensors technology for e-nose, and pattern recognition tools in e-nose. Chapter 3 describes in detail the main technique in this study, The Temperature Modulation-SDP. It drives the MOS gas sensors used in an e-nose to differentiate three volatile gases from their liquids. It covers the schematic designs and measurement steps, the responses resulted, the effect of modulation to circumstance conditions of sensors, and the selectivity performance. And, as the purpose of this dissertation, Chapter 4 discusses about the test or implementation of the temperature modulation-SDP technique to indicate nutrient addition in soil by using self-made e-nose with the same sensors, circuitry and measurement principle in Chapter 3. Finally in Chapter 5, I give a summary and some scopes of future work for this research which associated with the modulation itself to broader type of gas sensor for increase the , and other promising applications in soil/agriculture field.

*This page is intentionally left blank*

## **Chapter 2. Fundamental Literature Review**

### **2.1. Soil Smell and Potential Gases in Soil Atmosphere**

The smell of soil is due to the smell of two small molecules produced by small organisms. These small molecules are known as geosmin and methylisoborneol which mostly produced by bacteria belonging to the most genus *Streptomyces* that involves a number of enzymes, one of key enzymes is germacradienol synthase (Wang & Cane 2008; Mei Wang & Cane 2008; Green et al. 1975). The smell of these compounds can cause reduced quality of drinking water. They also have been found to reduce the quality of fish in freshwater aquacultures as the odors penetrate and accumulate in the fish, thereby lowering the commercial value. *Streptomyces* are ubiquitous, gram-positive soil bacteria that are known to produce of majority of pharmaceutically useful compounds (Wang & Cane 2008).

The Volatile Organic Compounds (VOC) were the most documented of gases in the soil atmosphere to vary widely in type and relative concentrations which strongly produced by microbial activity or metabolism, such as fungi, bacteria, and actinomycetes (Insam & Seewald 2010; Leff & Fierer 2008; Wheatley et al. 1996; Stahl & Parkin 1996). Generally, soil volatiles are identify and quantify traditionally using Gas Chromatography (GC) or Mass Spectrometry (MS), but they are effective, reliable and low cost, they can be time consuming, especially in time many replicates are necessary (Nagle et al. 1998; Insam & Seewald 2010). And, microbial and chemical processes that occur in the soil affect global change through their impact upon the concentrations of greenhouse/emission gases (e.g., CO<sub>2</sub>, CH<sub>4</sub>, N<sub>2</sub>O, NH<sub>3</sub>, and O<sub>3</sub>) in the atmosphere. Soil processes contribute highly variable in space and time, about 30% of NO<sub>x</sub>, 70% of N<sub>2</sub>O, 20% of NH<sub>3</sub> and 30% of annual global CH<sub>4</sub> emissions to the atmosphere (Mosier 1998).

Wheatley et al. (1996) analyzed the headspace of silty-clay loam soil at 50% water holding capacity using GC. They have identified 35 volatile organic compounds (27 in aerobic and 13 in anaerobic soil), with the predominant groups being Sulphur compounds (75%), aromatics (15%), ketones (4%), followed by alcohols/ aldehydes and some unidentified volatile organic compounds. Their relative concentrations changed when

nitrogen sources were added to soil, and the types of volatiles identified also varied when incubation conditions became more anaerobic (Wheatley et al. 1996). Yet, there is still very little information regarding the impact of key factors such as temperature, water potential, nutrients and even pesticides on soil microbial volatile production patterns.

Similarly, a relevant study by Stahl & Parkin (1996) investigated whether soils (silty clay loam) populated by varied microbial communities produced different types and concentrations of VOCs. Adding selective nutritional substrates and inhibitors into soil they found that the greatest amount of VOCs was produced in soil dominated by actinomycetes and bacterial populations. They also found that relating the nature of the microbial community to soil VOC emissions is complicated and the terpenes were the most common volatiles which commonly produced by plant roots.

Moreover Insam & Seewald (2010) gave many reported literatures on produced VOCs in soil due to microbial activities, in which mostly identified and quantified by GC/MS methods. Volatile organic compounds are produced in a high diversity in soils, some of them reflecting physiological properties or the presence of certain species. In different soils or under varying environmental conditions, the amounts and the type of VOCs produced may differ because of differences in community composition or nutrient availability. They stated determination of total VOC production or at least of a certain fraction results in VOC emission patterns (VOC fingerprints).

Hydrogen sulfide ( $H_2S$ ) also allows produced by some bacterial actions upon organic matter with the aid of the sulfates oxygen contained as an oxidation in low oxygen level (like flooded soil) which depends on ambient conditions such as temperature, humidity, and the concentration of certain metal ions (Elion 1927; Chou et al. 2014). And, soils may absorb amounts of  $H_2S$  from the air through atmospheric deposition, migration of mobilized pore water, or sulfuric material from spills and leaks, then retaining most of it in the form of elemental sulfur as sediment (Chou et al. 2014).  $H_2S$  is also found during flooding and water logging of wet land soils, hydrogen sulfide ( $H_2S$ ) is produced as a metabolic end product by prokaryotes that oxidize organic compounds using sulfate as a terminal electron acceptor (Lamers et al. 2013).

## 2.2. Principle of E-Nose Technology

The understanding of the process of human olfaction has led the development of e-nose technology and increased the interest in E-nose based research (a historical research perspective of e-nose shown in Fig. 2.1). Firstly, a brief overview of the mechanism involved in the human olfaction will provide a clear concept of the principle of e-nose.

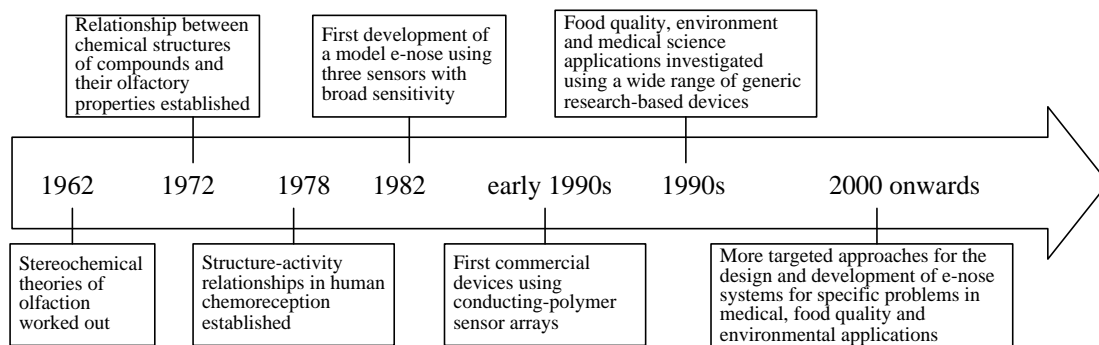


Fig. 2.1. Historical research of development of e-nose based system (Turner & Magan 2004).

The human olfaction system consists of three essential elements: (a) an array of olfactory receptors located in the olfactory epithelium at the roof of the nasal cavity between the eyes; (b) the olfactory bulb based, above it; and (c) the olfactory cortex, portions of the cerebral cortex that receive direct projections from the olfactory bulb collectively (Nagle et al. 1998; Patel 2014; Schiffman & Pearce 2003). As shown in Fig. 2.2, it begins with sniffing when odorant molecules are inhaled through the nostrils and enter the nasal cavity, they contact with the array of olfactory neuron, which moves air samples that contain molecules of odors to the thin mucus layer lining the olfactory epithelium in the upper portion of the nasal cavity. The odor molecules interact with the membrane bound receptor proteins of the olfactory receptor cells. Each neuron contains specialized receptor proteins bound to its cell membranes, which interact with the odorant molecules generating a series of nerve impulses. The number of different membrane-bound receptor proteins is estimated to be between 100 and 1000, with overlapping sensitivity and selectivity (Craven et al. 1996; Nagle et al. 1998). Although each neuron appears to express only one type of protein, the number of neurons within the array is large (approximately 100 million) and therefore, it responds to a wide range of different odorant molecules without being specific towards any particular molecule (Craven et al.

1996). Hence our sense of smell is able to recognize and discriminate a wide range of odors with high sensitivity and accuracy, even when present at *parts per trillion* levels (Craven et al. 1996).

Then, those electrical signals feed into the olfactory bulb where they are pre-processed in order to reduce noise by compressing the signals and amplifying the output, and simplify the neuron output, converting them into the form of a signature (Craven et al. 1996). This enhances both the sensitivity and selectivity of the olfactory system. Finally, the information is sent into the brain. The brain receives a set of simplified nerve impulses as patterns of responses and further processes the signals to identify them as particular smells. This identification appears to be a learning process, with new smells to be recognized and remembered subconsciously in the individual memory in which the brain associates the collection of olfactory signals with the odor (Gibson et al. 1997).

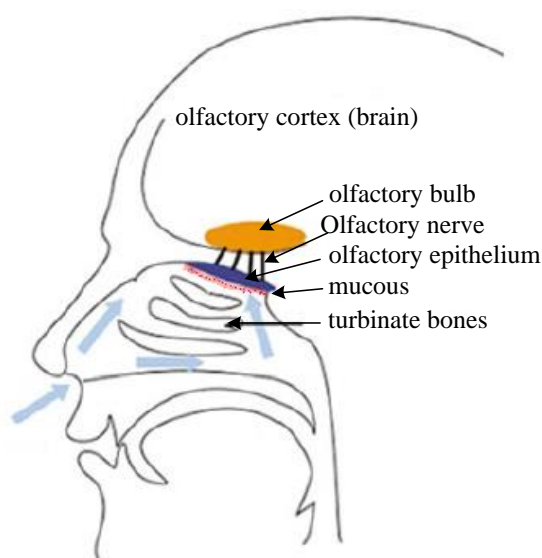


Fig. 2.2. Section through human nose representing some components of the olfactory system, adapted from Nagle et al. (1998) and Patel (2014).

The e-nose mimics the human olfaction system (see the comparison diagram between human olfaction and artificial olfaction in Fig. 2.3). Principally, a sampling unit delivers the odor molecules to a chamber where the sensor array is placed; the interaction between the sensors and the volatile compounds produce a change in the sensors response which then being interpreted by a set of pattern recognition system (PARC) which may act like the memory in our brain, creating a library of sensor responses (known as sensor profiles) (Patel 2014; Gibson et al. 1997; Nagle et al. 1998).



Similarly, as olfactory receptors, an e-nose employs an array of gas sensors. The compounds/ molecules structure (nature) of the sample are important in determining the sensors. This may requires sensors which non-specific and responsive to the shapes or structural features of the organic molecules (Gibson et al. 1997). Ideally, it would be helpful to define what these structural features were and select or design sensors used appropriately. At present, a more empirical approach is necessary, making use of available sensor types and attempting to modify sensor designs to meet the requirements of the e-nose. In general, the principle of sensing technology used to detect the molecules of chemicals is based on the measurement of the variation of electrical, thermal, optical, and mass changes of the active material due to the interaction between that and volatile compounds, such as Metal Oxide Semiconductors (MOS), Conducting Polymers (CP), Chemo-capacitors; MOS Field Effect Transistors (MOSFET), quartz Crystal Microbalance (QCM), surface Acoustic Wave (SAW), and SPR (Patel 2014).

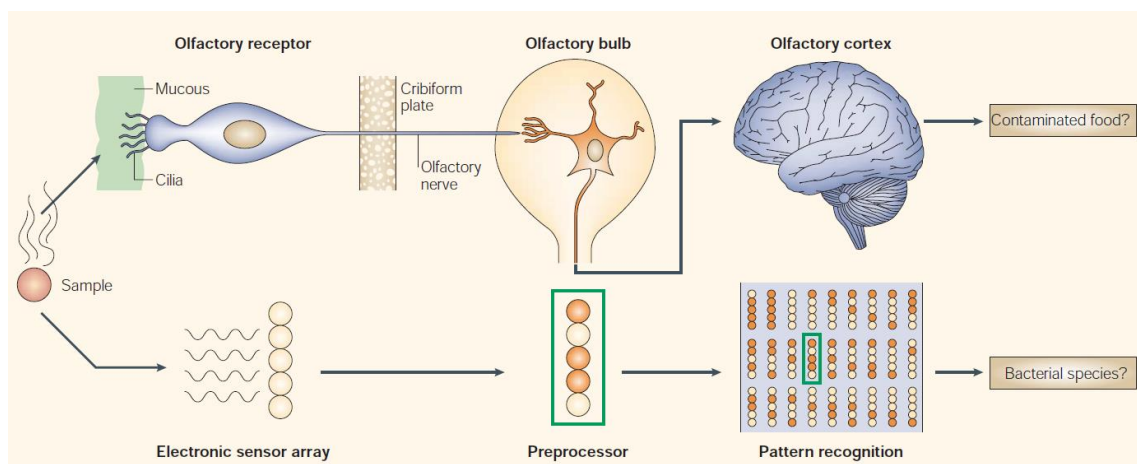


Fig. 2.3. Representing components mimics the functional units in human olfactory system (Turner & Magan 2004).

A series of response generated by the detector array is then fed into preprocessor on PARC as the olfactory bulb (a structure in the brain located just above the nasal cavity). This stage is to reduce the noise by compressing the signals and amplifying the output. This enhances both the sensitivity and selectivity of the e-nose system (Craven et al. 1996). The PARC system may include (i) the feature extraction step (preprocessing unit), which extracts useful information from the sensor responses to mimic the olfactory bulb and (ii) classifier or identifier unit, as identification library and detection software that serve as the brain to process input data from the sensor array for successive data analysis (Patel

2014). At this stage, multivariate statistical analyses and/or artificial neural network (ANN) can be employed for classifying samples, based on the pattern of the overall response generated by the array (Turner & Magan 2004).

### **2.3. Sample Handling and Measurement Methods**

Two things that could give significant effect on the e-nose performance are the sample handling (generating the sample vapor/odor) and measurement method (distributing and measuring the generated vapor/odor to sensor chamber). In principle the sample handling and the measurement method are the same. They are based on the movement of dynamism of vapor flow in such way inside a chamber. In implementation it may be combined in single sample handling and measurement method, eq. static headspace with static measurement. When the static system measures the odor/gas sample after the equilibrium is reached then it means the system is applying the static headspace in the static measurement at once.

There are two main odor sampling methods: Static Headspace Analysis (SHA) and Flow Injection Analysis (FIA) (Craven et al. 1996). In principle, these techniques is similar with commonly used method in Gas Chromatography analysis, known as Static Headspace (SH) and dynamic Headspace (DH) technique (Kolb & Ettre 2006). And there are two measurement methods: the Static System (SS) and the Sample Flow System (SFS).

The Static Headspace (Fig. 2.4) consists of two steps. First is equilibration, the sample (commonly in liquid form) is placed on a sealed and closed container having a gas volume above it, and left for a period of time so that the headspace becomes equilibrated/saturated with the sample. This vial is then left and thermostatted/agitated concurrently (if necessary) at a constant temperature to boost the equilibration. Second is sample delivery, this headspace is then transferred into the chamber containing the sensor array. It relates the measurement method, whether in static system or sample flow system. The SHA is the more popular and low-cost method since the principle is very simple.

On the other hand, the method of Flow Injection Analysis is usually automated and employs a carrier gas (e.g. clean air) constantly being pumped though the sensor chamber. The ratio of carrier gas and headspace volatiles can be controlled accurately. Nevertheless, due to dilution, the magnitude of sensor response to volatiles is much lower when compared against that obtained using the SHA technique (Craven et al. 1996). Because

the volume of the plumbing tube cannot be ignored, a technique similar to FIA is used to sample a few microliters of the liquid precisely. The automated system consists of a sample selector, a sample injector, and the measurement system. It selects the samples among several candidates, injects the sample liquid and measures the sensor responses after equilibrium. Since it takes time to measure the steady-state response due to the slow evaporation of the sample liquid, the automation is quite indispensable if many data need to be systematically measured. It seems that the mechanism of FIA is closely similar with the method of sample flow system (Fig. 2.6).

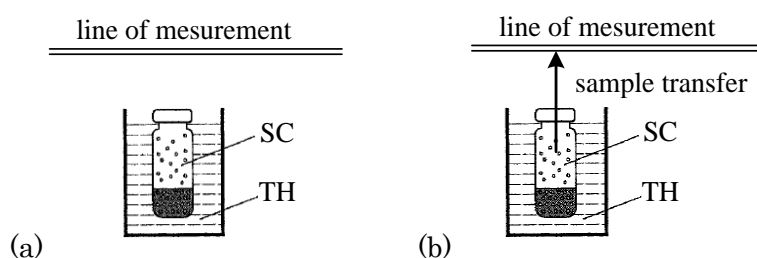


Fig. 2.4. Principles of static headspace when (a) equilibration and (b) sample delivery. SC=sample container, TH=thermostating, adapted from Nakamoto (2003).

As comparator, the DH method in Gas Chromatography, known as Purge and Trap method (Fig. 2.5), employs an absorbent agent to trap and contain the gases/volatiles resulted from absorption which then thermally desorbed and transferred to sensors. Thermal desorption from such a tube is the critical step, especially if combined with capillary columns for GC separation. There are three problems here: (a) the water existence, due to a lot of water also trapped vapor during adsorption, particularly from an aqueous sample; (b) time elapsed, due to the slow desorption; and (c) the flow problem, due to gas flow during desorption, which needed high purge flow to be used directly as carrier gas for capillary columns (Nakamoto 2003).

Moreover, the chamber of headspace has to be made of material with small adsorption coefficient to avoid gas reduction onto the internal wall. The whole chamber can be immersed in a temperature-controlled bath, thus the headspace can be kept at the same temperature and equilibrium relative humidity.

In the measurement method of static system (Fig. 2.6), there is no vapor flow around the sensor, and measurements are usually made on the steady-state responses of the sensors exposed to vapor at a fixed concentration and at a constant temperature.. The small volume of sample (gas or liquid) is injected into a chamber having a volume of

capacity, and is evaporated. Manual injection of the sample liquid by the syringe is the basic method, however it is possible to automate this procedure. While the sample flow system, also called dynamic chamber measurement (Barnes et al. 2006; Breuninger et al. 2012; Pape et al. 2008), the sensors are placed in the vapor flow, which allows the rapid exchange of vapor and hence many samples can be measured within a short time. The static system and sample flow system are closed units (Nakamoto 2003). Mostly the sample flow system measures the liquid sample.

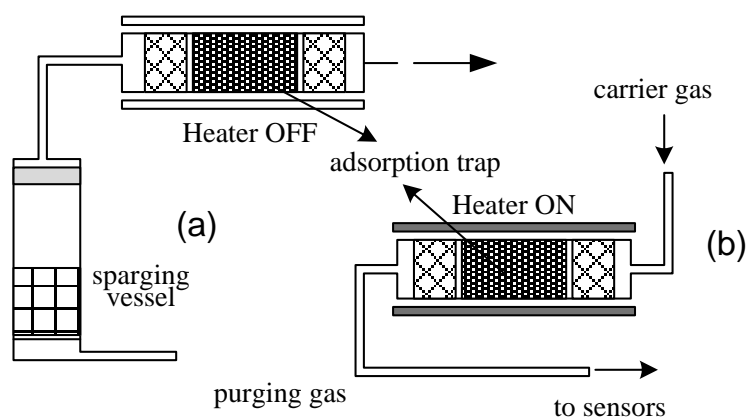


Fig. 2.5. Principle of Purge and Trap method in GC, (a) the adsorption of volatiles from the sample and (b) the desorption from the adsorption by back-flushing of the heated trapped volatiles, adapted from Nakamoto (2003).

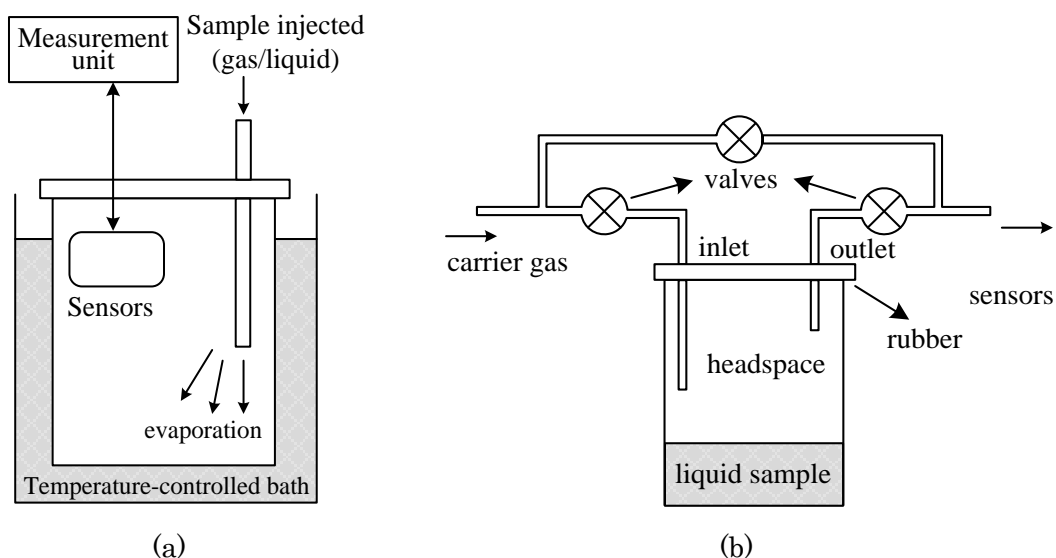


Fig. 2.6. Principle of (a) the static system and (b) the sampling of sample flow system, adapted from Nakamoto (2003).

## 2.4. MOS Gas Sensors Technology for E-Nose

A MOS (Metal Oxide Semiconductor) gas sensor, which categorized as a chemoresistive sensor, basically is formed from tin dioxide which sintered at high temperature to be transformed into a semiconductor. Hence, the material is very porous so that gases can easily pass through (Barsan et al. 2007). It works based on change of the resistance of a thin film upon adsorption of the gas molecules on the surface of a semiconductor. An its advance development leads manufacture of small size, simple, and compact MOS with various sensitivity (Wilson & Baietto 2009; Berna 2010). It is known as the simplest of gas sensors, and are widely used to make arrays for odor measurements (Nanto & Stetter 2003; Wilson & Baietto 2009). And, the MOS gas sensor is classified according to the conductance condition due to presence of gas, as n-type (conductance increases, e.g.,  $\text{SnO}_2$ ,  $\text{ZnO}$ , and  $\text{In}_2\text{O}_3$ ) or p-type conductance decreases, e.g.,  $\text{Cr}_2\text{O}_3$  and  $\text{CuO}$ . This classification is related to the (surface) conductivity type of the oxides, which is determined by the nature of the dominant charge carriers at the surface, that is, electrons or holes.

In general the working principle is that in air at high temperatures between  $150^\circ\text{C}$  and  $400^\circ\text{C}$  typically, oxygen is adsorbed on the surface of the metal oxides by trapping electrons from the bulk with the overall effect of increasing the resistance of the sensor (for n -type materials), or decreasing it (for p -type materials) (Nanto & Stetter 2003; Barsan et al. 2007).

The n-type semiconductors, especially  $\text{SnO}_2$ , are more suited and widely utilized as sensitive layer than p-type. There are two significant intrinsic properties of semiconductor that could be considered for base substrate in MOS gas sensor construction. They are the speed mobility of carrier (electrons/holes) and the chemical and thermal stability under operating conduction. The carrier mobility determines a proportionality constant of the change of the conductivity when a number of carriers changes due to gas–solid interactions. By having a high mobility of electron ( $160 \text{ cm}^2/\text{V.s}$ ) and the most stable chemical and thermal stability oxide among the n-type oxides lead to  $\text{SnO}_2$  being so important as a base semiconductor for gas sensors (Yamazoe et al. 2003). While on the opposite, the mobility of positive holes (p-type oxide) is usually much less (e.g.  $\text{TiO}_2$  has only  $0.4 \text{ cm}^2/\text{V.s}$ ), thus  $\text{TiO}_2$  is not preferable be employed to gas sensor, but instead as a

sensitive material for automotive air/fuel ratio sensors (Yamazoe et al. 2003).

The element of MOS gas sensor typically comprises of 5 main units as shown in Fig. 2.7, i.e. a *Sensitive layer* deposited over a *Substrate* provided with *Electrodes* in particular configuration for the measurement of the electrical characteristics. The device is generally heated by its own *Heater*; this one is separated from the sensing layer and the electrodes by an *Electrical insulating layer* (Barsan et al. 2007; Patel 2014). And, there are two basic configuration to construct MOS gas sensor (Fig. 2.8) that are commercially available (Yamazoe et al. 2003; Nanto & Stetter 2003).

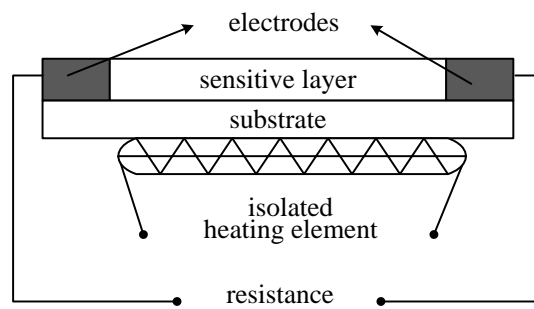


Fig. 2.7. Basic elements of MOS gas sensor, adapted from Patel (2014).

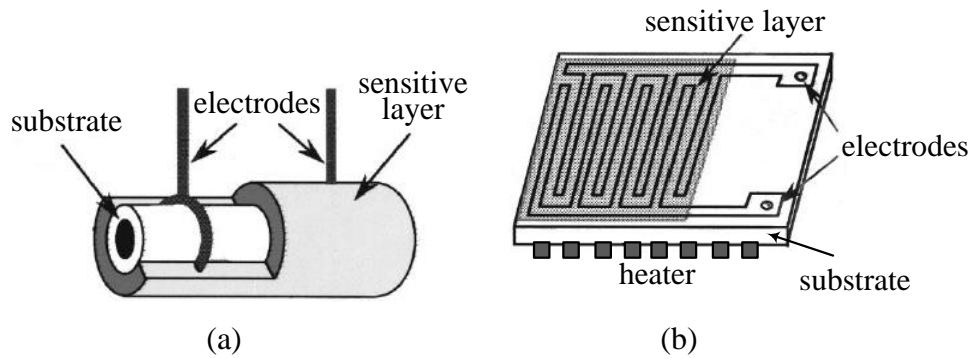
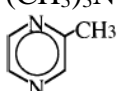


Fig. 2.8. The basic construction of (a) the sintering-type and (b) thin-film type of the MOS gas sensors, adapted from Yamazoe et al. (2003).

The most widely used semiconducting material as a gas sensor is  $\text{SnO}_2$  doped with small amounts of impurities and catalytic metal additives. By changing the choice of impurity and catalyst (known as sensitizer) and operating conditions such as temperature, many types of gas sensors using  $\text{SnO}_2$  have been developed. The gas selectivity depends on the kind and amount of catalyst. The type and amount of catalytic additives and concentration ranges of gas sensors using MOSs, have been reported by Yamazoe et al.

(2003), are listed in Table 2.1. However, mostly the MOS gas sensors provide relatively poor selectivity for gases and also behave responsive to other kinds of combustible gases.

Table 2.1. Doped additive materials in semiconductor oxide-based gas sensors (Yamazoe et al. 2003)

Base Oxide	Additives Sensitizer	Target	Concentration range
SnO <sub>2</sub>	Ag (3 wt%)	H <sub>2</sub> , C <sub>3</sub> H <sub>8</sub>	100–5000 ppm
WO <sub>3</sub>	Pd (0.3–1 wt%)	NO <sub>2</sub>	10–800 ppm
WO <sub>3</sub>	Au (0.8 wt%)	NH <sub>3</sub>	0.5–50 ppm
	Pt (0.4 wt%)		0.5–50 ppm
TiO <sub>2</sub>	Ru (0.5 wt%)	(CH <sub>3</sub> ) <sub>3</sub> N	300 ppm
WO <sub>3</sub>	Rh (0.4 wt%)		2–100 ppm
WO <sub>3</sub>	Ru (0.004 wt%)	NO	10–200 ppm
SnO <sub>2</sub>	ZnO (3 at%)	H <sub>2</sub> S, CH <sub>3</sub> SH	10 ppb–10 ppm
SnO <sub>2</sub>	CuO (5 wt%)	H <sub>2</sub> S	1–50 ppm
SnO <sub>2</sub>	La <sub>2</sub> O <sub>3</sub> (5 wt%)	C <sub>2</sub> H <sub>5</sub> OH	100–1000 ppm
SnO <sub>2</sub>	S (1 at%)+(Pd 1 wt%)	CH <sub>2</sub> FCF <sub>3</sub> (R-134a)	5–3000 ppm
In <sub>2</sub> O <sub>3</sub>	CeO <sub>2</sub> (3 at%)	O <sub>3</sub>	0.05–5 ppm
	Fe <sub>2</sub> O <sub>3</sub> (3 at%)		0.008–10 ppm
Pd–SnO <sub>2</sub> –Sb	SiO <sub>2</sub> coating	H <sub>2</sub>	100 ppm
SnO <sub>2</sub>	0.5Pt–Al <sub>2</sub> O <sub>3</sub> coating	C <sub>3</sub> H <sub>8</sub>	5000 ppm
In <sub>2</sub> O <sub>3</sub>	Rb <sub>2</sub> CO <sub>3</sub> (5 wt%)	CO	200–4000 ppm
In <sub>2</sub> O <sub>3</sub>	Au (0.04 wt%)–Co <sub>3</sub> O <sub>4</sub> (0.5 wt%)	CO	200–2000 ppm
Fe <sub>2</sub> O <sub>3</sub>	Pr <sub>6</sub> O <sub>11</sub> (5 wt%)	CH <sub>3</sub> SSCH <sub>3</sub>	5–50 ppm
ZnO	MoO <sub>3</sub> (5 wt%)	CH <sub>3</sub> COCH <sub>3</sub>	2–50 ppm
		WO <sub>3</sub> (5 wt%)	
ZnO	Er <sub>2</sub> O <sub>3</sub> (5 wt%)	C <sub>5</sub> H <sub>11</sub> CHO	1–20 ppm
		Gd <sub>2</sub> O <sub>3</sub> (5 wt%)	
Bi <sub>2</sub> O <sub>3</sub> –MoO <sub>3</sub>	Bi/Mo=1.0	C <sub>3</sub> H <sub>6</sub>	20–8000 ppm

The mechanism of MOS gas sensor could be understood by phenomenological and spectroscopic techniques, and the ionosorption is widely accepted mechanism approach in phenomenological technique (Barsan et al. 2007). It is agreed that the key agent in the mechanism of the semiconductor to response a reducing gas involves the concentration of adsorbed oxygen species such as O<sub>2</sub><sup>–</sup>, O<sup>2–</sup>, and O<sup>–</sup> (Barsan et al. 2007; Puzzovio 2008). They depend on the working temperature (described on Eq. 2.1), i.e. in molecular form (O<sub>2</sub><sup>–</sup>) at below 150°C and atomic (O<sup>2–</sup>, and O<sup>–</sup>) ions which more dominant at above 150°C, and O<sup>–</sup> is reckoned as the most reactive species when presence of reducing gases

while the  $O^{2-}$  is disregarded since such a high charge on the ion can give instability (Barsan et al. 2007; Puzzovio 2008).

The model of ionosorption process, adopted from Barsan et al.,(2007) and Puzzovio (2008),

$$\frac{\beta}{2}O_2(gas) + \alpha e^-(srf) \rightleftharpoons O_{\beta}^{\alpha-}(srf), \text{ as general equation} \quad \text{Eq. 2.1}$$

$$\text{when operates in low temperature, } O_2(gas) + e^-(srf) \rightleftharpoons O_2^-(ads) \quad \text{Eq. 2.2}$$

$$\text{when operates in high temperature, } \frac{1}{2}O_2(gas) + e^-(srf) \rightleftharpoons O^-(ads), \text{ or} \quad \text{Eq. 2.3}$$

$$O_2(gas) + 2e^-(srf) \rightleftharpoons 2O^-(ads), \text{ or} \quad \text{Eq. 2.4}$$

$$O_2^-(ads) + e^-(srf) \rightleftharpoons O_2^{2-}(ads) \rightleftharpoons 2O^-(ads)$$

And the model for a semiconductor gas sensor responses to composition of the gaseous mixture on high operating temperature is shown in Eq. 2.5 to 2.7 as reported by Nakata, Hashimoto, & Okunishi (2002) and Nakata et al. (2006).

$$S + \alpha e^-(srf) + 1/2O_2(gas) + \rightleftharpoons O^{\alpha-}(ads), \quad \text{Eq. 2.5}$$

$$O^{\alpha-}(ads) + g_x \rightarrow g_x O^{\alpha-}(ads), \quad \text{Eq. 2.6}$$

$$g_x O^{\alpha-}(ads) \rightarrow g_x O + \alpha e^-(srf) + S \quad \text{Eq. 2.7}$$

where, where S defines a surface adsorption site,  $e^-$  is a free electron,  $(\alpha, \beta=1 \text{ or } 2)$  is an ion absorbed oxygen,  $O(\text{sub})$  is an oxygen gas atom activated by sensor heating,  $g_x$  is a sample gas  $x$  in the bulk phase or,  $g_x O_{ad}^{m-}$  is  $g_x$  adsorbed on the oxidized sensor surface.

The schema of the ionosorption also could be depicted in structural and band model as shown in Fig. 2.9, exemplified with reducing gas CO. The presence of adsorbed oxygen ions leads to a band bending and the formation of a depletion layer (called space-charge layer) at the surface of tin oxide and to a high resistance. On the other words, by withdrawing the electron from the semiconductor surface, adsorbed oxygen gives rise up Schottky potential barriers at grain boundaries, and thus reduce the conductance of the sensor surface. When gas sensors exposure to CO, CO is oxidized by  $O^-$  and released electrons to the bulk materials. Together with the decrease of the number of surface  $O^-$ , the thickness of space-charge layer decreases (denoted by  $\Lambda_{air}$ ). Thus, the Schottky potential barrier (denoted by  $eV_{\text{surface}}$ ) between two grains is lowered and it would be easy for electrons to conduct in sensing layers through different grains. The temperature



dependence of this process arises in part from the differing stabilities of the surface oxygen species over different temperature ranges.

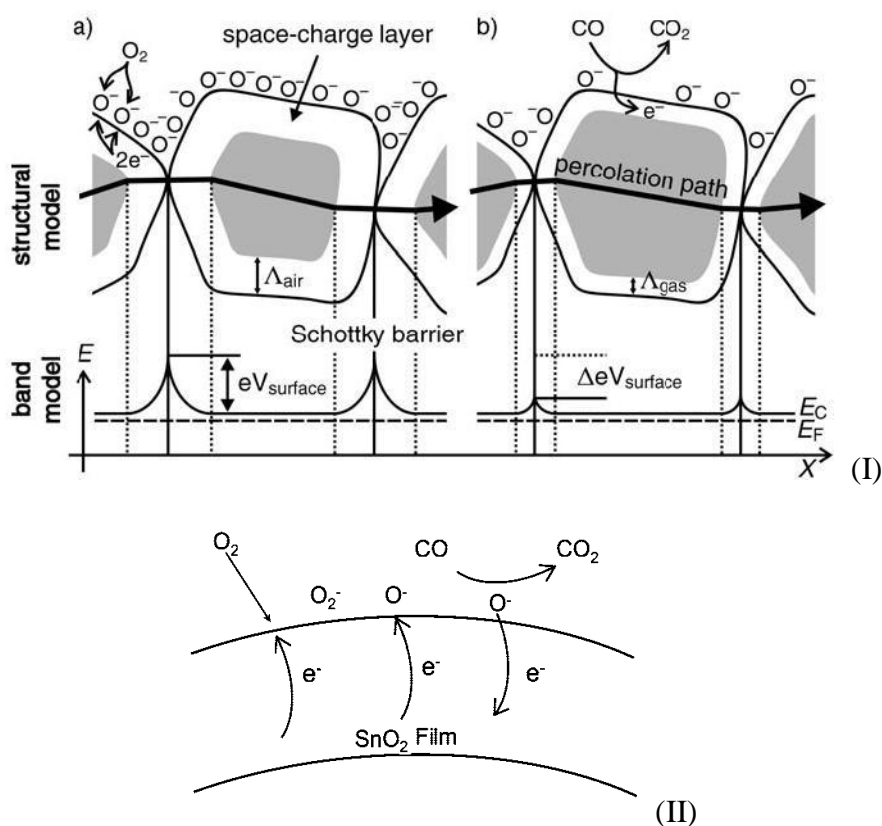


Fig. 2.9. (I) Schematic depiction of ionosorption in structural and band model for atmospheric O<sub>2</sub> interaction and CO gas sensing by SnO<sub>2</sub> where (a) with or (b) without CO existence (Wang et al. 2010), while (II) is the simplified model (Puzzovio 2008).

## 2.5. Pattern Recognition Tools in E-Nose (PARC)

Electronic nose employs a suitable and powerful kind of multivariate data analysis as pattern recognition to meet goal in determining the classification of the samples. It may function as data reduction, pattern classification, or clustering. Fig. 2.10 shows a summary of the available methods for the analysis of e-nose data, where MDS stand for (Multidimensional scaling), PCA (principal components analysis), SOM (self organizing maps), ICA (independent component analysis), CA (Cluster analysis), LDA (linear discriminate analysis), PLS (partial least squares), FSS (feature subset selection), PCR (principal component regression), MLR (multiple linear regression), CCR (canonical correlation regression), MLP (multilayer perception), RBF (radial basis function), PNN (probabilistic neural network), K-NN (K nearest neighbors), SVM (support vector

machines), ART (adaptive resonance theory), GA (genetic algorithm), HC (hierarchical clustering). In this project, the classification methods used were Principal Components Analysis (PCA) as preprocessing unit to display pattern of sensors responses and obtain more significant data in new little dimension, and Multi-Layer Perceptron Neural Network (MLPNN) as a supervised classifier.

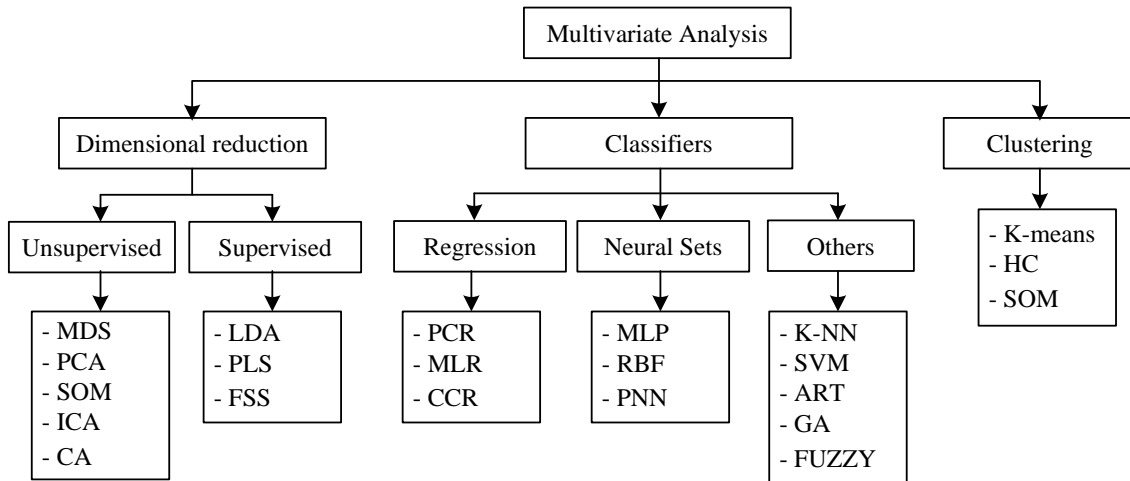


Fig. 2.10. Scheme of classification of multivariate analysis used in e-nose application (Patel 2014).

The PCA is a linear unsupervised method that has been widely used by various researchers to display the response of an EN to simple and complex odors. The PCA able to make a new projection of large dimension into few important Principal Components (PCs) which projects a dataset to a new coordinate system by determining the eigenvectors and eigenvalues of a matrix. It involves a calculation of a covariance matrix of a dataset to minimize the redundancy and maximize the variance (Hines et al. 2003; Patel 2014). The first two or three uncorrelated PCs normally hold most significant of variation present (over 90%) in all variables (Shurmer & Gardner 1992; Gardner 1991; Gardner et al. 2000). PCA is in the core a dimensionality reduction method for correlated data, such that a two-or three-dimensional plot able to represent an n-dimensional data. In the same degree order, each eigenvector associated with its eigenvalue determines the direction of its principle component (Hines et al. 2003), which means the eigenvector associated with the largest eigenvalue leads the direction of the first PC and the eigenvector associated with the second largest eigenvalue determines the second PC's.

Artificial Neural Network, mimics the cognitive processes of the human brain,

contains interconnected data processing algorithms that work in parallel and becomes the well-known and most evolved PARC includes for commercial software packages of electronic noses (Jamal et al. 2010). Recently, NNs have been widely used in wide application for odor recognition by using various NN algorithms paradigm and many evidences given by researchers that the three-layered networks have adopted this topology for implementing MLPs and provide sufficient computational degrees to solve any problem of classification (Hines et al. 2003; Jamal et al. 2010).

In a network, the architecture elements, known as Multi-Layer Perceptron (MLP), are organized in a regular form of three distinct groups of neurons: input, hidden, and output layers with 2 weight layers relate between input to hidden layer and hidden to output layer as shown in Fig. 2.11. MLP, as a three-layered feedforward Back-Propagation (BP) trained network, is the most popular architecture of neurons in classification to be applied to e-nose (Hines et al. 2003). The performances of the BP and BP with momentum algorithms in descending the weight space are highly dependent upon a suitable selection for learning rate and momentum factor (Fig. 2.12). They are generally adapted in each learning step (epoch) using global learning parameters. And among other accelerating methods for updating weight and biases, the search-then-converge-schedule (Eq. 2.8) is the most simple and popular method for adapting and accelerating the learning. Typically learning rate ( $\eta$ ) starts with a large value and gradually decreases it as the learning proceeds ( $t$ ) that similar with simulated annealing. The constant of search time ( $T$ ) of this schedule is a new free parameter that determined by trial and error.

$$\beta(t) = \frac{\beta(0)}{(1 + t/T)} \quad \text{Eq. 2.8}$$

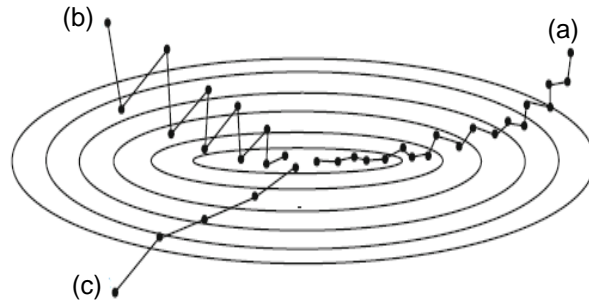


Fig. 2.11. Descent in weight space for (a) small learning rate, (b) large learning rate, and (c) large learning rate with momentum (Du & Swamy 2014).

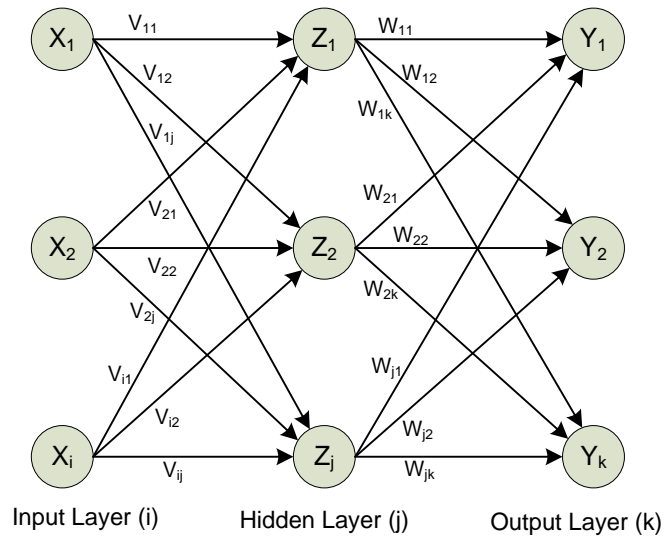


Fig. 2.12. The architecture of neural network with single hidden layer, adopted from Du & Swamy (2014).

## Chapter 3. Temperature Modulation with Specified Detection Point on Array MOS Gas Sensors

### 3.1. Introduction

Temperature modulation through oscillation of heater voltage on Metal-Oxide Semiconductor (MOS) gas sensor, also called dynamic measurement (Liu et al. 2007; Sun et al. 2004), has become most potential and established technique to be applied on MOS gas sensors than static temperature since it provides more information from a single sensor than static measurement (Sun et al. 2004). It also means that cyclic variation of temperature gives a unique signature for each gas, different type of modulation showed a slight difference signal response and amplitude (Huang et al. 2004; Ortega et al. 2001). Temperature modulation alters the kinetic of the sensor through changes in the operational temperature of device through applying modulated voltage on heater unit of MOS gas sensor. The operating modulation voltage, also consequently the operating temperature, of the sensor changes periodically either by square (rectangular) or triangular or sine waveform (Huang et al. 2004).

By using rectangular waveform, Dutta & Bhuyan (2012) has determined the optimal frequency applied for each sensor using theory of system identification based on best fit transfer function, pole-zero plot and the overshoot percentage. And, It is also reported the use of rectangular modulation to detect and distinguish the presence of two pesticide gases, a binary gas mixture (acephate and trichlorphon), in the ambient atmosphere (Huang et al. 2003).

This section presents an improved technique of temperature modulation on MOS gas sensor as an alternative attempt to increase selectivity and sensitivity as well, particularly for e-nose application. The technique implements rectangular heating Temperature Modulation with Specified Detection Point (Temperature Modulation-SDP). The principle is similar with general temperature modulation (Fig. 3.1.B), yet besides a modulation on Heater Unit ( $V_H$ ), it also modulates the Sensing Unit ( $V_C$ ) concurrently and in same phase with  $V_H$  (Fig. 3.1.C). The SDP means detection (acquiring) of MOS gas sensor output is put at specified point which associated to its temperature modulation on its heater. In this study, a rectangular temperature modulation-SDP is generated and

configured using Timer block in PSoC (Programmable System on Chip) CY8C28445-24PVXI. A single switching circuit is employed to drive either single or multi (array) sensors with similar type and characteristic. This technique allows to get the advantages of temperature modulation by only acquiring the change of resistance value (not the whole response). It suits to be implemented in a single chip (like a hybrid device, PSoC) by concomitantly generating modulation signal and acquiring the output at a constant point as well inside the chip. Generally it has a low rate of data transfer when used to acquire multi sensors and send them to outer device (computer), depended on time consuming of sequential process on multiplexing and digital conversion. It is also easy to construct the modulation since availability of required blocks to meet the desired modulation.

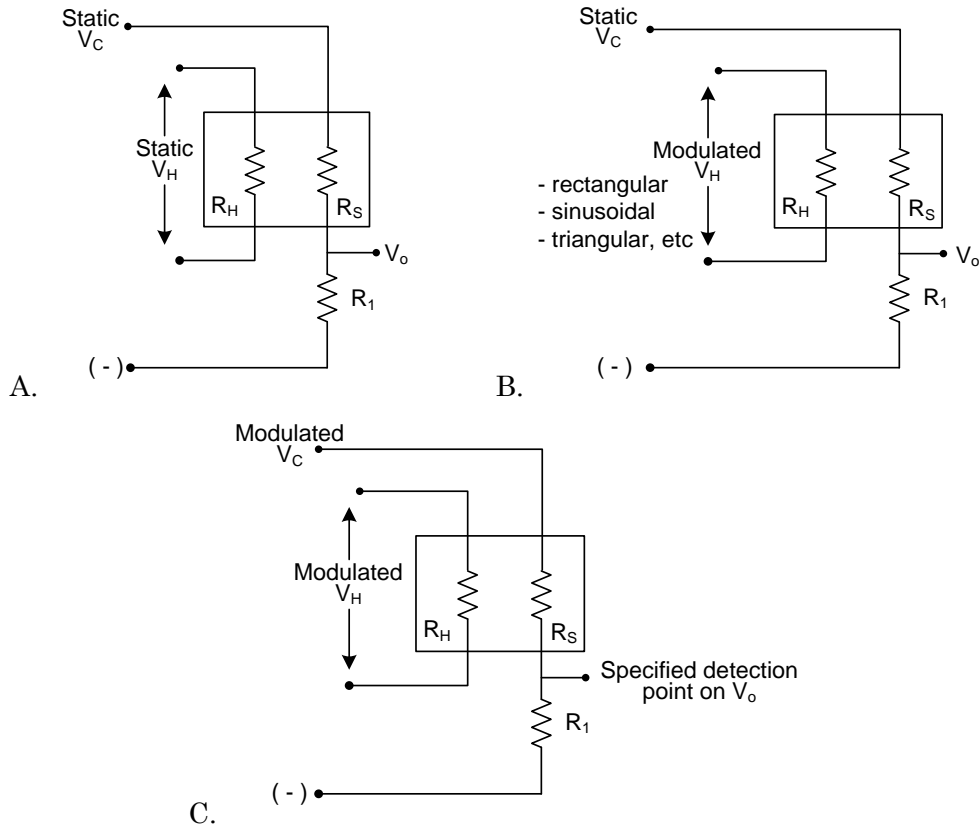


Fig. 3.1. Schematic-based comparison of typical working mode of MOS gas sensor: A. static temperature modulation, B. temperature modulation, and C. temperature modulation with specified detection point, where  $V_H$ =voltage of heater,  $V_C$ =voltage of sensing element, and  $V_o$ =voltage of output.

### 3.2. Design of Rectangular Temperature Modulation-SDP.

The temperature modulation-SDP design is based on required modulation which

applied on TGS 2444. As shown in Fig. 3.2.(a), TGS-2444 requires application of a 250 ms heating cycle ( $S_{VH}$ ) which comprised by 4.8 volt (high state) applied to the heater for the first 14 ms, then followed by 0 (low state) volt pulse for the remaining 236 ms. The  $S_{VC}$  cycle consists of low state applied for 2 ms at first, then by high state for 5ms and followed by low state for remaining 243 ms. For achieving optimal sensing, detection is measured after the center of  $S_{VH}$  pulse (Figaro Engineering Inc. 2011).

In my design (Fig. 3.2.(b)), compared with TGS-2444 detection time, on signal detection ( $S_{VC}$ ), an additional time after detection point is put so that detection point is in center of  $S_{VC}$  to ensure the acquisition system (PSOC based) have adequate time to acquire the sensor amplitude. The  $S_{VC}$  is positioned on midpoint 75% of "on/high" state of temperature modulation ( $S_{VH}$ ) whereas the detection point is laid on center of  $S_{VC}$  pulse.

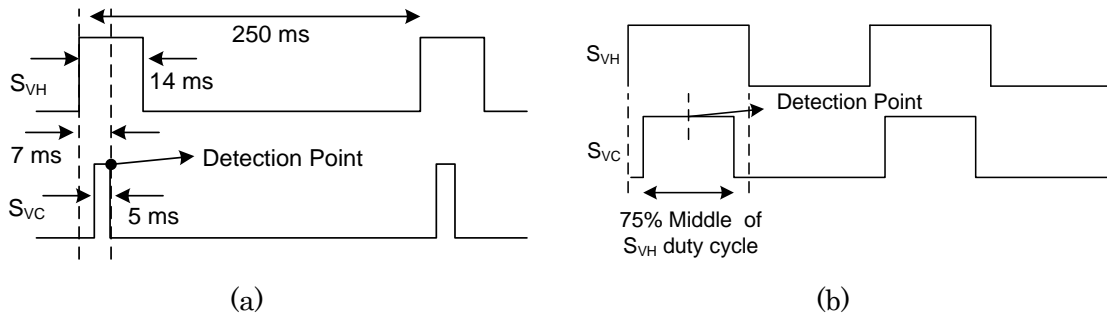


Fig. 3.2. The signal of (a) required modulation of TGS 2444 and (b) the designed temperature modulation-SDP.

Common temperature modulation-SDP (Fig. 3.3) is constructed that can be applied on array MOS gas sensor which has similar type and characteristic which employs the FET (Field Effect Transistor)-based switching circuit. It modulates and drives the array of TGS Sensors (manufactured by Figaro Engineering Inc.) and FIS sensors (manufactured by FIS Inc.) respectively since there is slight difference pin configuration on them. Both TGSs and FISs are configured in voltage divider as standard method for measuring resistance changes (Gutierrez-Osuna et al. 2003).

I configured the rectangular modulation signal for MOS gas sensors (TGSs and FISs) using PSOC CY8C28445-24PVXI (Programmable System on Chip). The PSoC is also configured to acquire array sensors and transmit data to computer wirelessly as well by employing Timer (signal to get data), Multiplexer, ADCs, and UART blocks. I employed internal main oscillator (IMO) in PSoC CY8C28445-24PVXI which is set at 5V/24 MHz ( $V_{cc}/SysClk$ ) to supply 12 MHz for CPU clock. Clock signal of IMO contains the jitter

around 200-300ps (Cypress 2010). However, in this research the timing error of detection point is negligible.

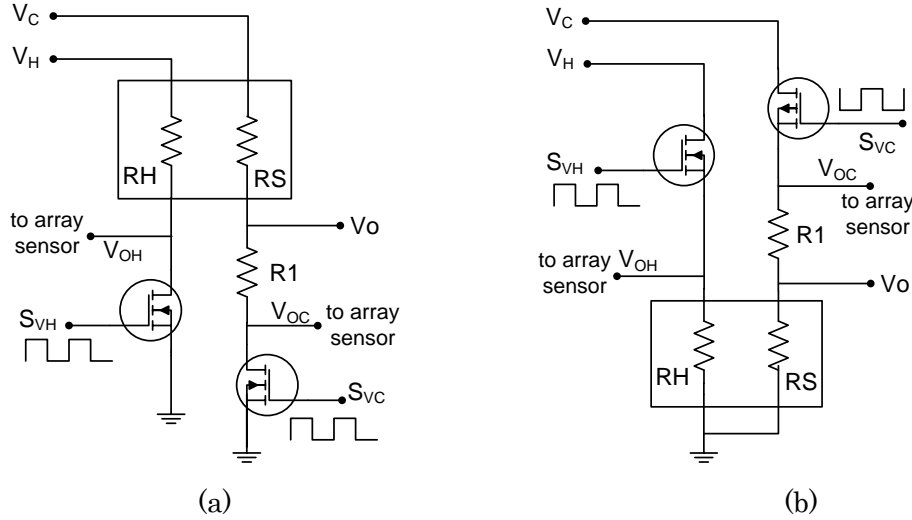


Fig. 3.3. Schematic of temperature modulation-SDP for array (a) TGS sensor and (b) FIS sensor with  $V_H$  is heater voltage,  $V_C$  is sensing circuit voltage,  $S_{VH}$  is modulation signal for  $V_H$ , and  $S_{VC}$  is modulation signal for  $V_C$ .

### 3.3. Experimental Design.

I tested 6 commercial MOS gas sensors (TGS-2444, TGS-2602, TGS-825, FIS-12A, FIS-30SB, and FIS-AQ1) and used 3 environment sensors (KE-25, LM35 and HSM30G). The diagram of PSOC-based system is shown in Fig. 3.4. The acquisition system transmits all data wirelessly through Radio Frequency using XBee serial communication (IEEE 802.15.4) Digi International Inc. I designed two temperature modulation-SDP timing generators by Timer8 block to provide fixed modulation and adjustable modulation that is set from acquisition software in Personal Computer (PC). Fixed modulation is only for TGS-2444 which recommended on is 4 Hz 5.6% of the temperature modulation (Figaro Engineering Inc. 2011), while adjustable modulation is provided for modulation on array of TGSs and FISs except TGS-2444.

Measurement and setting were adjusted and monitored automatically through developed software which built using Visual Studio VB Net 2012 that expanded from our previous work (Sudarmaji et al. 2013). It is functioned to monitor the initial conditioning of chamber oxygen level, to set the modulation signal, and to acquire output of all sensors.



The dynamic chamber measurement of system is shown in Fig. 3.5. The arrow represents the gas pipes and direction of flow. For analyte gas, the flow is helped by small air pump.

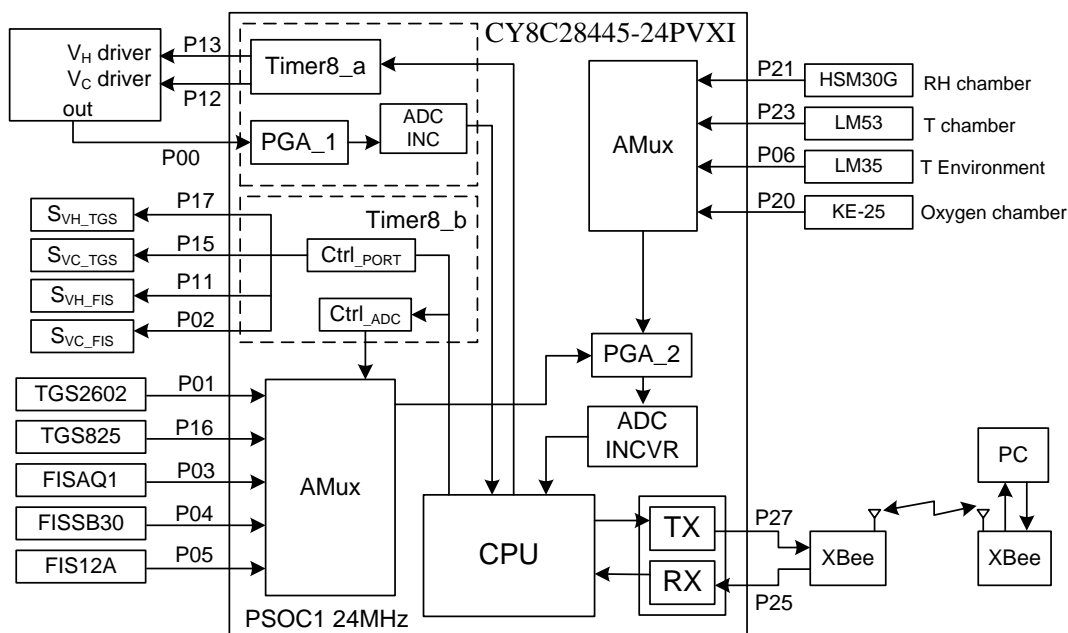


Fig. 3.4. Diagram block of system based on PSOC CY8C28445-24PVXI with pins configuration.

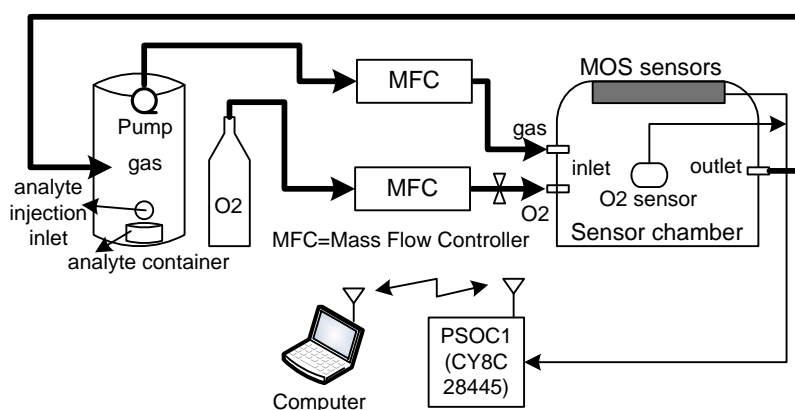


Fig. 3.5. Diagram of sample flow system (dynamic chamber) measurement to measure 3 various liquids (ammonia, ethanol, and toluene).

Initially, all MOS gas sensors are inactive (the voltage of heater and sensing element are on off mode). Then, oxygen concentration in chamber is measured and increased the concentration when under 21% by flowing oxygen into chamber constantly up to minimum recommended level of 21% (Figaro Engineering Inc. 2005). Both flow controller (Kofloc RK200/RK400) are tuned on rate of 0.4 liter per minute ( $0.67 \text{ cm}^3/\text{s}$ ).

After that, the gas sensors are activated and driven by certain modulation that chosen the frequency and duty cycle which set from PC. Then, the pump is turned on and waits the initial conditioning time of MOS sensors for 2 minutes plus certain steady time (15 or 30 minutes) for selectivity performance analysis. Next step is measuring the baseline for 1 minute, continued with injecting the analyte solution, and then measuring the analyte gas for 6 minutes. The hypodermic (Bolo-silicate hard glass) syringe 1 ml was used to inject the volume of solution.

Finally, the purging chamber is done for 10 minutes using two fans on cover of sensor and solution chamber. The (acquisition) software is connected to Microsoft Excel to store and process data, such as: (a) create file, read and write data, (b) create and show graph, and (c) determine average value of each sensor for each measurement mode (baseline and analyte sample measurement). The acquisition software creates automatically 2 worksheets to store 2 mode measurement at once cycle measurement.

I observed on 3 frequencies (0.25 Hz, 1 Hz, and 4 Hz) with 3 duty cycles (25%, 50%, and 75%) of temperature modulation-SDP and no modulation as comparator. No modulation means MOSs were driven using traditional technique, a static temperature. I therefore observed 10 modulations. Initial response and selectivity evaluation of array sensor was performed and visualized using statistical tool and Principal Component Analysis (PCA) to distinguish 3 analyte gases (Ammonia, Ethanol, and Toluene). The analyte concentration (in gas phase) was prepared in 5000 ppm that resulted from 1 ml injection of prepared solution.

The method of preparing accurate analyte in gas phase for volatile solution in air is described and applied by Chutia & Bhuyan (2012) and Uyanik & Tinkiliç (1999). By using Eq. 3.1, the necessary amount of analyte liquid in distilled water is calculated as prepared solution for once measurement. The liquid was then injected 1 ml of it into solution container to produce that gas concentration in total volume including (11x8x6) cm sensor chamber (528 ml), gas sample chamber (1800 ml), and piping (24 ml). As an example, It is calculated to be 0.344 ml of 99.5% liquid ethanol (molecular weight 46.07 g/mol and density 0.79 g/ml) added to 12 ml distilled water at laboratory pressure (1 atm) and temperature (293 °K) to produce 5000 ppm ethanol gas in volume 2352 ml. Table 1 shows the properties of analyte liquid used and calculation result of prepared solution. MOS gas sensors are presented by its resistance ( $R_s$ ) and sensitivity as defined Eq. 3.2

(Huang et al. 2003). The sensitivity is just the opposite of the relative based equation of baseline manipulation technique which able to eliminate the effect of multiplicative drift and provide a dimensionless response (Gutierrez-Osuna et al. 2003).

$$v_s = \frac{M_A \cdot C_{ppm} \cdot P \cdot V}{CAW \cdot D \cdot R \cdot T} \cdot v_p \cdot 10^{-6} \quad \text{Eq. 3.1}$$

where  $C_{ppm}$  denotes analyte gas concentration,  $M_A$  is molecular weight (g/mol),  $P$  is laboratory pressure (atm) which assumed = 1 atm,  $V$  is volume of total chamber ( $m^3$  or  $\mu L$ ),  $R$  is ideal gas constant (L atm/mol/°K),  $T$  is laboratory temperature (°K),  $CAW$  is Catalyst Altered Water (liquid concentration in %),  $D$  is solution density (g/ml),  $v_p$  is volume of prepared solution = 12 ml, and  $v_s$  is volume of solution (ml).

$$S = \frac{R_0}{R_g} \quad \text{Eq. 3.2}$$

where  $S$  defines sensitivity,  $R_0$  is sensor resistance of air and  $R_g$  is sensor resistance of analyte gas exposure.

Table 3.1. Properties of analyte liquids and their calculated portion in prepared solution.

Analyte Liquid	Density (g/ml)	Mol. weight (g/mol)	CAW (%)	$v_s^*)$ (ml)
Toluene $C_6H_5CH_3$	0.87	92.14	99	0.628
Ethanol $C_2H_5OH$	0.79	46.07	99.5	0.344
Ammonia $NH_3$	0.90	17.03	28	0.397

<sup>\*)</sup> in 12 ml prepared distilled-water

### 3.4. Results and Discussion.

#### 3.4.1. The Modulation and Sensor Response under Modulation.

All modulations applied on MOS gas sensor have been checked with oscilloscope Tektronix TDS 2024B (exemplified in Fig. 3.6) and they met the desired modulation as shown in Fig. 3.2(b). However, Fig. 3.6 only shows responses of three modulations, although ten modulations were generated and observed in the measurement in order to avoid cluttering in the graph. The measured frequency of  $V_{OH}$  was 0.2510 Hz and high state of  $V_{OC}$  is laid in middle 75% of high of  $V_{OH}$ . The acquiring of all MOS (in array) begins at middle of  $V_{OH}$  and takes 0.08s to complete it. The high state of  $V_{OH}$  of TGS and FIS were measured about 4.98 and 0.95 volt respectively and the  $V_{OC}$  of both TGS and FIS were 4.98 volt.

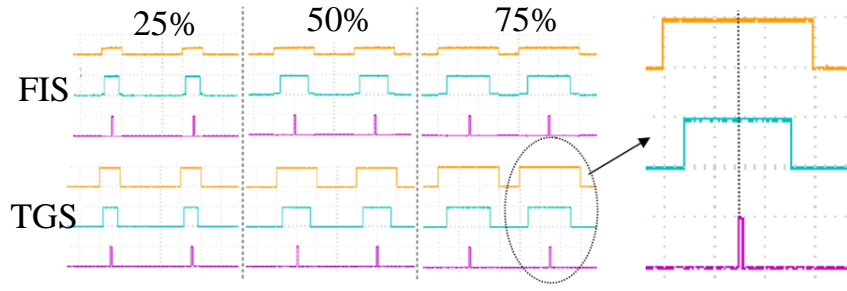


Fig. 3.6. Captured signal on MOS gas sensors under applied modulation of 0.25 Hz with duty cycle 25%, 50% and 75%, where:  $V_{OH}$  (top)= 2V/div of FIS;  $V_{OH}$  (top)= 2V/div of TGS;  $V_{OC}$  (middle) =5V/div; Time of detection Point (below) =5V/div; Time-Div= 1s.

Fig. 3.7 shows MOS gas sensor's original responses (amplitude (v) vs. time (s)), which taken and compiled from digital output of the oscilloscope, to observe gases under each rectangular modulation. The oscilloscope probes were pointed directly at pin of MOS's sensing elements. In Fig. 3.7(a), it seen that TGS2444 works on 4Hz modulation and responses sensitively to only ammonia gas since give similar response when sensed the air, ethanol gas, or toluene gas, but ammonia gas. As typical work of MOS gas sensor, the presence of ammonia gas leads the sensing layer's resistance of TGS2444 decreases depending on its concentration in the air.

Then, shown in Fig. 3.7(b)-(d), the responses of five sensors (TGS2602, TGS825, FISAQ1, FISSB30 and FIS12A) appear to differ in amplitude due to different types of gases and to differ in pattern caused the applied modulation on the sensors which serves as a signature of concerned gas. Temperature modulation leads to the generate response patterns, which may be characteristic of the species being detected. The figures show that even though the captured response was only at high state of modulated sensing element circuit as resulted from modulated heater, it remains provided significant characteristic feature to distinguish among ammonia, toluene, ethanol and clean air (no gas).

An important information of TGS2444 published by Figaro (manufacturer of TGS series) which contributes to performance of MOS gas sensors is application of modulated voltage of sensing element ( $V_{OC}$ ). Applying the  $V_{OC}$ , which is in phase with the modulation of  $V_H$ , may lead to prevent sensor from possible migration of heater materials into the sensing material which could causes long term drift of sensing material's resistance to higher values. It means that a pulsed- $V_C$  giving less force to drive migration

than a constant  $V_C$ , rendering negligible possibility of migration, particularly under high humidity and temperature operation (Figaro Engineering Inc. 2011).

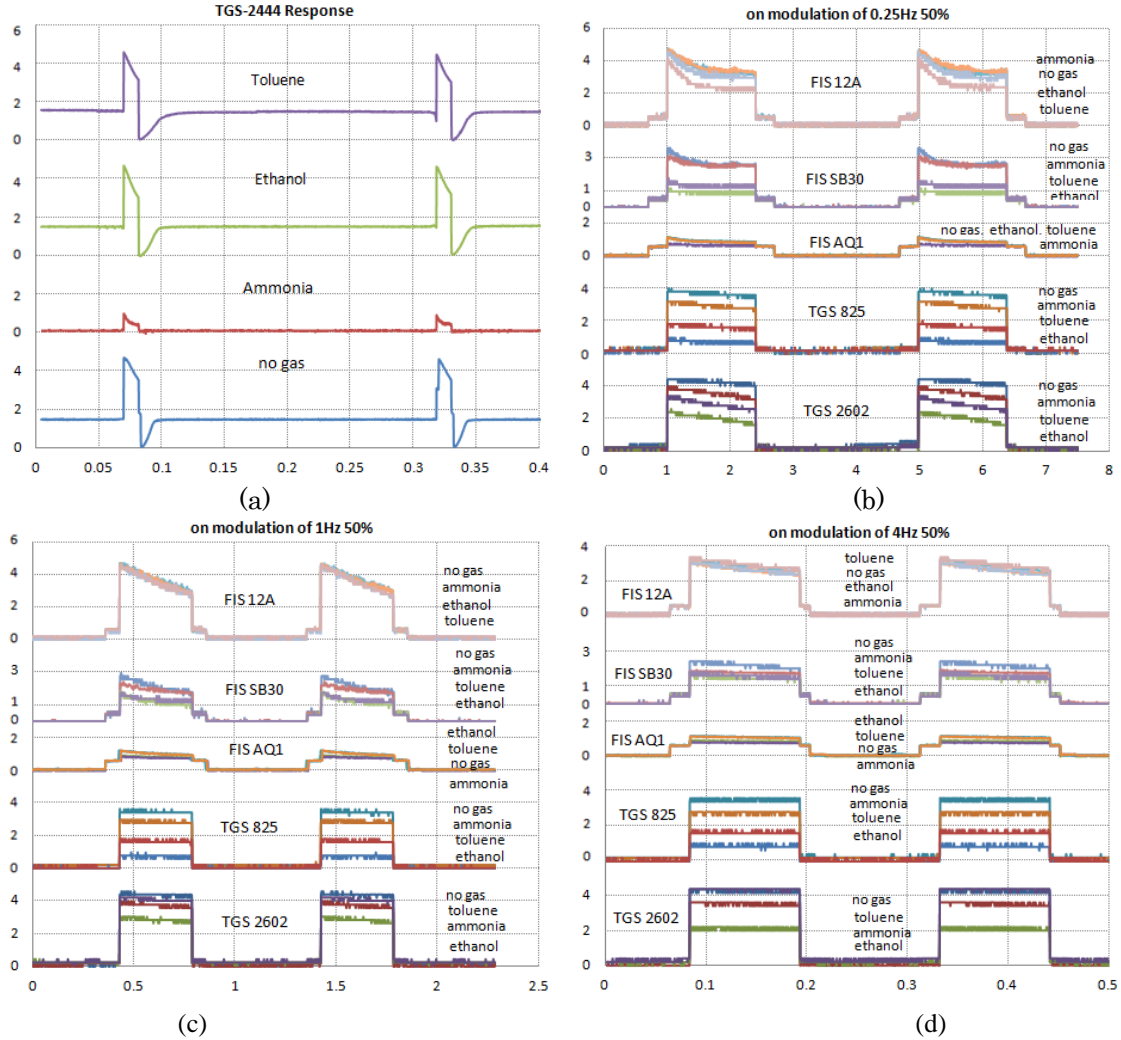


Fig. 3.7. Response of (a) TGS 2444, and the others (TGS2602, TGS830, FISAQ1, FIS SB30 and FIS12A) operated on (b) modulation 0.25 Hz, (c) modulation 1 Hz, and (d) modulation 4 Hz to air (no gas), ammonia, ethanol, and toluene gas.

It also seen in Fig. 3.7 (b)-(d) that as the lower frequency, the response waveform of the sensors becomes more sloping and distinct, notably the FISs. It is apparent that all MOS gas sensors, both TGSs and FISs, are more selective to differ gases at lower frequency. It is because sensor operates near (to meet) a quasi-isothermal behavior at multiple temperatures and, therefore, existing the equilibrium condition between adsorbed oxygen and volatile chemical compound of analyte gas (Chutia & Bhuyan 2014). Contrarily, at higher frequency sensor behaves non isothermal operation, therefore the information content is no longer in the shape of the dynamic signal but rather closely in

static (DC offset) mode, especially on TGS-825 and TGS-2602.

Primarily, the work of modulated temperature is supposed to alter the kinetics of both adsorption and reaction process at the surface of sensor while detecting reducing or oxidizing species in the presence of atmospheric oxygen. The well-known and accepted mechanism itself so-called ionosorption model. As described in Puzzovio (2008). The interaction between the surface of MOS and atmospheric oxygen causes the oxygen adsorption in form species of molecular ( $O_2^-$ ) and atomic ( $O^-$  and  $O^{2-}$ ) ions, where the atomic ions are more dominant at above 150 °C, and  $O^-$  is reckoned as the most reactive species when presence of reducing gases. The reactions of oxygen adsorption can be described by as Eq. 2.1 to Eq. 2.4.

In case of n-type semiconductor, e.g.  $SnO_2$ , the chemisorbed oxygen, which mainly as  $O^-$ , binds off electronic carriers and leads to the formation of a depletion layer at the surface. The electrons are drawn from ionized donors via the conduction band, so the charge carrier density at the interface between the oxidized layer and semiconductor is reduced and a (Schottky) potential barrier is created at grain boundaries. When the surface charge increases, the adsorption of further oxygen is hindered. The adsorption rate slows down because the charge is transferred to the adsorbate over that surface barrier, and the coverage saturates at a rather low value. At the junctions between the grains, the depletion layer and associated potential barrier cause high resistance contacts. Any presence of reducing gases will release the chemisorbed oxygen, lessen the surface oxygen concentration, and thus decrease the resistance.

As seen in Fig. 3.7, I perceive that MOS responses under a rectangular modulation mode were correlated to the different reaction kinetics of the interacting gases at its surface. In this way the reaction with the reducing and oxidizing gases was dramatically influenced, e.g. at higher temperatures (high voltage of  $V_s$ ) the response to gases such as ammonia, ethanol, and toluene exhibited their characteristic wave shape due to the reaction with certain oxygen species. The equations of Schottky barrier potential and Arrhenius in Nakata & Kashima (2010) show that conductance of semiconductor and rate constants respectively are depended on temperature, where the temperature of gas sensor surface is controlled by varying the voltage applied to its heater (Lee & Reedy 1999).

### 3.4.2. Environmental Circumstances and Initial Response.

KE-25, LM35DZ, and HSM20G was used to measure oxygen level in chamber, ambient temperature, and temperature and humidity in chamber respectively. The working ambient temperature during experiments was at 18 to 22°C and the oxygen concentration in the chamber was kept constant at round 21.8% (not changed by operation of sensors, as shown in Fig. 3.8). As assumed, it is also seen clearly that higher frequency and duty cycle of applied modulation in 30 minutes operation lead the increment of temperature significantly and humidity inside the chamber.

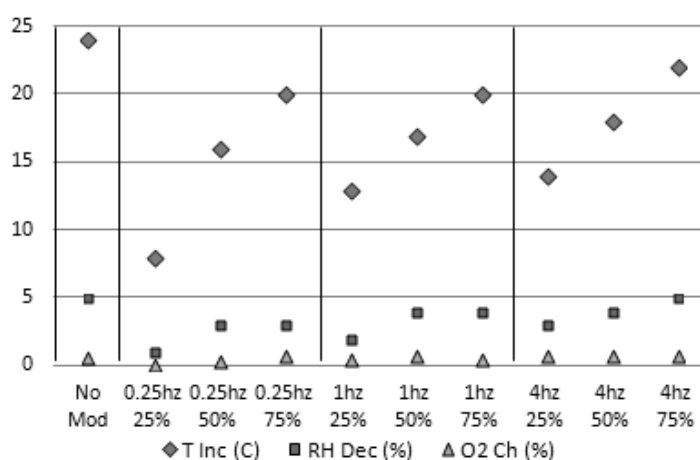


Fig. 3.8. Change of chamber environment (temperature, relative humidity, and oxygen concentration) after 30 minutes initial action.

The presence of minimum required ambient oxygen is essential to the sensor's operation which mean oxygen plays an important complementary role to reducing gases and its concentration effected to detection of combustibile or reducing gas which mediated by reaction with adsorbed oxygen on the sensor surface (Clifford & D.T. Tuma 1982). The behavior of steady-state conductance of MOS with temperature is greatly influenced by ambient oxygen concentration (Clifford & D T Tuma 1982) and the reduced oxygen pressure will lead the decrement of the sensor's resistance . Moreover, they also reported that the dynamic response of metal oxide gas sensor shows complex kinetics characterized by time constants which range, depends on ambient conditions. The long-term drift of the TGS resistance resulted from the diffusion of a native non-stoichiometric defect, an oxygen vacancy, evoked by changes in temperature or ambient oxygen pressure.

I tested initial action for 30 minutes on each temperature modulation with specified detection point by flowing natural air on measurement system. At a minute of initial

action, the resistance of TGSs was very high, i.e. 90 k $\Omega$  of TGS 2602 and 130 k $\Omega$  of TGS 825, then in second afterward dropped sharply which then toward its steady value in about 10 seconds. Other side, typically FISs have same responses. Yet, they have lower initial resistance, i.e. 20 k $\Omega$  of AQ1, 2.6 k $\Omega$  of SB30 and 25 k $\Omega$  of 12A, then gradually dropped in longer time (about 30 seconds) toward their steady value in first minute.

However, after a minute, as shown in Fig. 3.9, the steady state of both TGSs and FISs were slightly and gradually changed (mostly increased but FISAQ1 on all modulations with duty cycle of 25% were decreased) along with elapsed time during 30 minutes. Therefore, the baseline resistance was different to each temperature modulation. I found that higher frequency and duty cycle resulted in higher base-resistance. These increasing phenomena are potentially caused by heater temperature operation on MOS gas sensor and cumulative rising temperature in chamber. Typical curve of working heater temperature vs. resistance is shown in Fig. 3.10 where the responses increase and reach their maximums at a certain temperature, and then decreased rapidly with increasing the temperature (Malyshev & Pislyakov 2008). It is assumed that gas sensors with different compositions have similar shapes.

By using Eq. 3.3 in Zakrzewski et al. (2003) to determine working heater temperature from running voltage on heater and by calculating the effective voltage ( $V_{\text{eff}}$ , depend on its duty cycle) of modulated voltage operated on MOS gas sensors, I obtained that the effective working temperature of TGSs resulted from duty cycle modulation 25%, 50%, and 75% are 69 °C, 197 °C, and 325 °C respectively. Hence, it is clear that when a sensor is operated in the modulation mode using its recommended voltage  $V_s$  (e.g. 5 V of TGS and 0.9 V of FIS), the response ( $R_s$ ) tends to increase in higher frequency of operating modulation. Also from Fig. 3.9, I noticed that it takes more than a minute for MOS to reach its steady state condition. Overall, it seem takes minimum 10 minutes of initial action as base-resistance prior the measurement. It is called the quasi-steady state at each temperature modulation-SDP.

$$T_H = 102.83 * V_H - 58.79, \quad \text{Eq. 3.3}$$

where  $T_H$  (°C) is the working heater temperature,  $V_H$  (Volt) is the running voltage on heater.



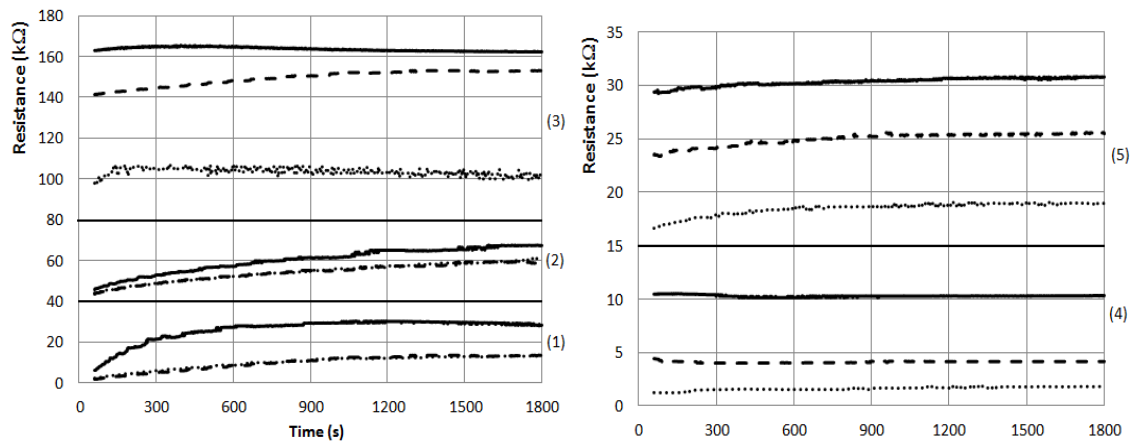


Fig. 3.9. Initial action responses of MOS sensors Resistance during 30 minutes after ready state conditioning (1 minute) of each MOS gas sensors: (1)=TGS-2602, (2)=TGS-825, (3)=FIS-12A, (4)=FIS-AQ1, and (5)=FIS-SB30 on modulation frequency: 0.25Hz (dotted), 1Hz (dashed) and 4Hz (solid). All modulation were on 50% duty cycle.

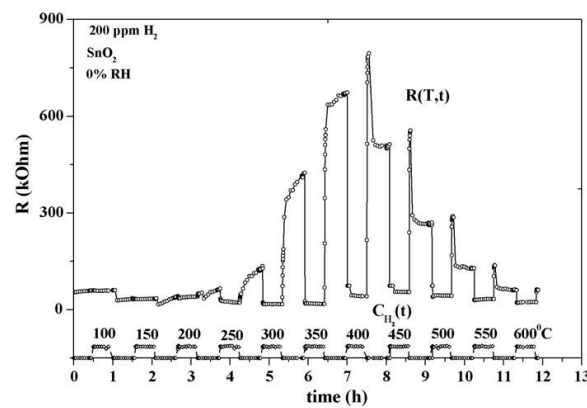


Fig. 3.10. The resistance responses of the SnO<sub>2</sub> sensor on 200 ppm H<sub>2</sub> pulses at various operating temperatures (Malyshev & Pislyakov 2008).

### 3.4.3. Selectivity Evaluation.

Test of Principal Component Analysis (PCA) was performed to evaluate selectivity performance in identifying the ammonia, ethanol, and toluene on each modulation. PCA is commonly used in electronic nose as feature extraction tool to test distinguish (selectivity) performance and a powerful linear classification technique that is usually employed in correlation with cluster analysis and visualization the difference in similarities or differences among the treatments (Gardner 1991; Hines et al. 2003). The large dimension of interrelated variables are reduces into few important principal components. The first two or three uncorrelated components hold most significant of

variation present in all variables and widely used in various application (Haddi et al. 2014; Shurmer & Gardner 1992; Gardner et al. 2000).

I observed 2 durations of quasi-steady state (i.e. 15 minutes and 30 minutes) prior the measurement and used each sensitivity value of MOS gas sensors to represent variables in PCA. Here, I only utilized 5 MOS gas sensors except TGS2444 in order to avoid ambiguous results since it is only sensitive to ammonia. The first three Principal Components (PC1, PC2, and PC3) are used, as at most together they usually contained over 90% of the variance within the data sets (Shurmer & Gardner 1992). Then, the Euclidean norm was determined as significant features to assess the fittest modulation which has highest selectivity to gas samples. Selectivity refers to characteristics that determine whether a sensor can respond selectively to a group of samples or even specifically to a single sample which can be indicated by how far the difference (distance) among responses on samples. Therefore, besides the PCA test on same modulation for array sensors, it is also performed PCA test on selected temperature modulation-SDP (shown in Table 3.2) of each MOS gas sensor based on the largest distance of sensitivity value among sample gases.

The variation value of sensitivity are shown in Fig. 3.11. Generally, Fig. 3.11 shows that most of sensors have highest sensitivity on ethanol gas and individually MOS gas sensor with its respectively modulation could discriminate among gases, and seemingly the modulation with duty cycle 75% leads higher selectivity on each frequency modulation. However, It also reveals that either on 15 minutes or 30 minutes quasi-steady state, individually TGS825 and FIS SB30 seem perform better selectivity (indicated by longer distance among sensitivity point) to differ ammonia, toluene and ethanol when not applied the modulation than applied by temperature modulation-SDP.

Table 3.2. Selected temperature modulation-SDP of MOS gas sensors based on their sensitivities for 15 minutes and 30 minutes quasi-steady state prior measurement.

Sensor	Selected Modulation	
	15 m	30 m
TGS2602	1 Hz 75%	0.25Hz 75%
TGS825	1 Hz 75%	4Hz 75%
FISAQ1	0.25hz 75%	0.25Hz 75%
FIS SB30	0.25hz 75%	0.25Hz 75%
FIS12A	0.25hz 50%	0.25Hz 25%

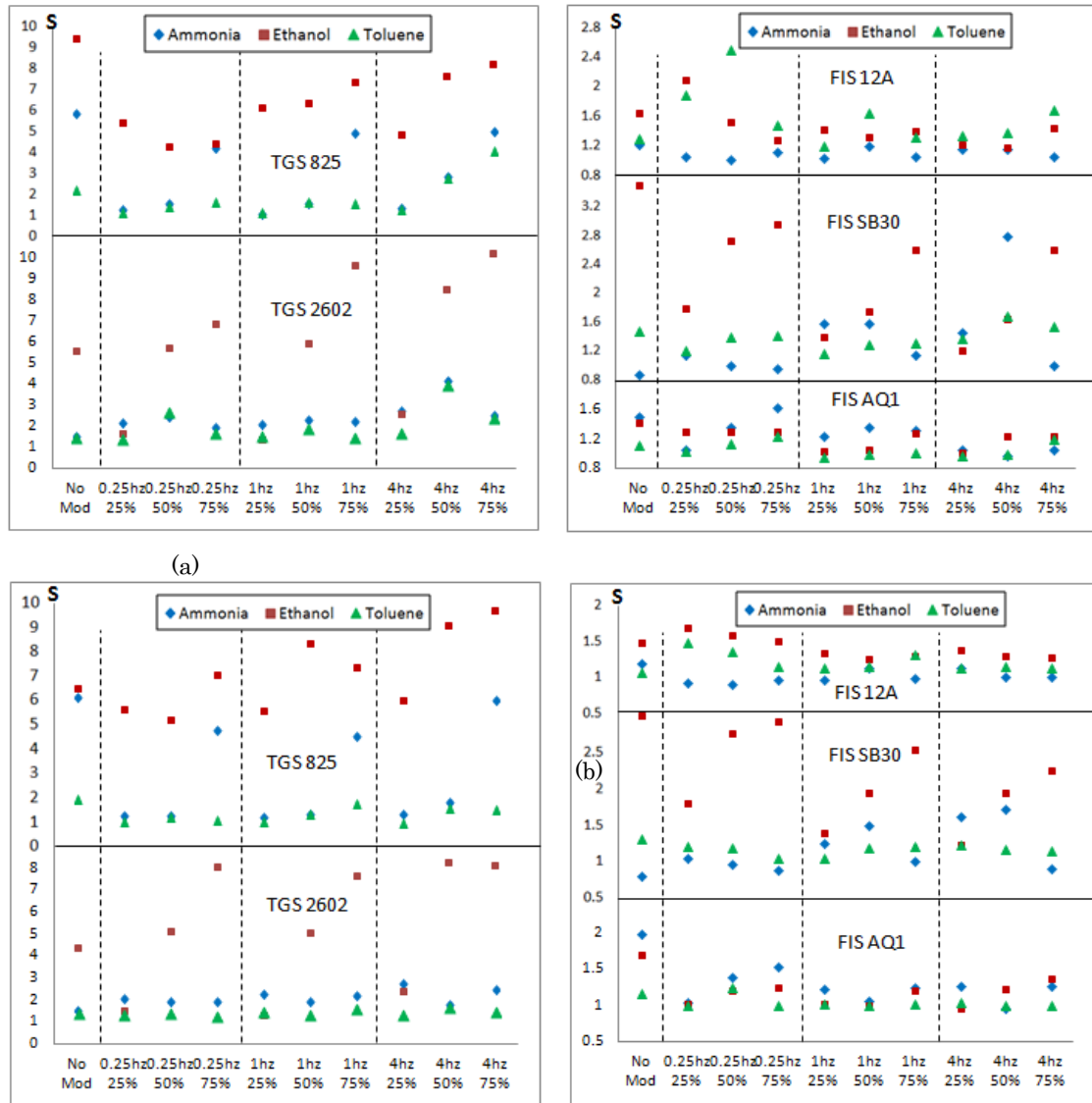


Fig. 3.11. Sensitivity variation of each MOS gas sensors and modulation upon exposure to various gases after (a) 15 minutes and (b) 30 minutes quasi-steady state

Table 3.2 implies that FISs individually performed best selectivity under temperature modulation-SDP at 0.25 Hz 75% of both 15 minutes and 30 minutes quasi-steady state to differ ammonia, toluene and ethanol, while TGS 2602 and TGS825 tend more varied. On array gas sensor which commonly used in e-nose application, the selected temperature modulation-SDP on each MOS gas sensor and measurement after 30 minutes quasi-steady state carried out better selectivity rather than single modulation on all gas sensors, as shown in Fig. 3.13. Moreover, compared to static (without modulation) mode (shown in Table 3.3 and Fig. 3.12), the selected modulation and 30 minutes quasi-steady state give highest increment of selectivity, up to 64.7%.

Table 3.3. Euclidean distance between Principal Component score of no modulation vs. selected modulation of 15 minutes and 30 minutes quasi-steady state.

Euclidean distance	15 minutes		30 minutes	
	w/o mod	w/ mod	w/o mod	w/ mod
Ammonia-Ethanol	6.005	8.103	3.630	7.50
Ethanol-Toluene	3.730	3.822	4.777	5.118
Ammonia-Toluene	8.558	10.198	6.176	11.408
Average	6.097	7.374	4.861	8.007
Increment	<b>20.9%</b>		<b>64.7%</b>	

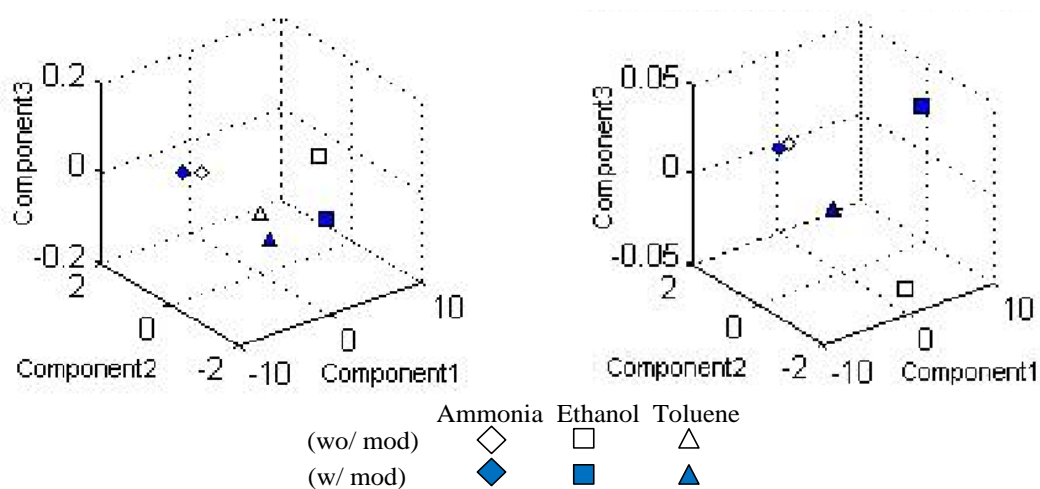


Fig. 3.12. Visualization of PCA plot of selected temperature modulation-SDP Vs without Modulation using 3 major PCs.

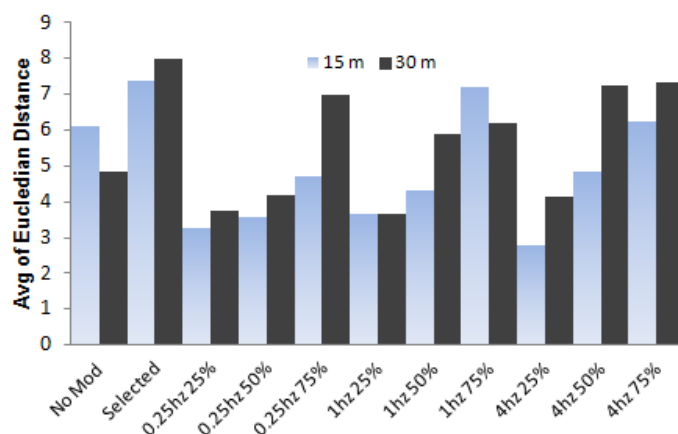


Fig. 3.13. Comparison of selectivity performance of array sensors among temperature modulation-SDP to distinguish three gases based on distance of Principal Component's score after 15 minutes and 30 minutes quasi-steady state.

However, Table 3.3 also shows that the Euclidean distance between Ammonia and Ethanol of 30 minutes quasi-steady state is lower than 15 minutes quasi-steady state. This

is strongly caused of two things: the higher increment of humidity (the presence water content) in sensor chamber, and the high solubility of Ethanol and Ammonia samples.

The operation of MOS gas sensor (especially when placed in a chamber) leads the increment of humidity inside the chamber (see Fig. 3.8) due to the working of heater on MOS gas sensor under the given modulation. Naturally, the longer operation (longer quasi-steady state) consequently will rise the higher increment of temperature and humidity. It means there more water content in air inside the chamber.

And, since the ethanol and ammonia have high solubility in water (Table 3.4), there will be more dissolved (bonded) sample gases in water vapor when much water contained in the air which can reduce the response and its sensitivity consequently. The solubility is determined by the Henry's Law constant (Sharpe 1964; Sander 1999; Sander 2015). Table 2 shows that the sequence of solubility among samples is Ethanol > Ammonia > Toluene (Sander 2015). That is why the selectivity of array MOS gas sensors, shown in the Euclidean distance, is less when sensing the Ethanol and Ammonia using 30 minutes quasi-steady state than 15 minutes quasi-steady state.

Therefore it may deduce that the longer quasi-steady state leads the higher humidity (water content) in sensor chamber and causes less sensitive/selectivity of MOS on high solubility sample. It seem that the long quasi-steady state is not suitable for the sample with high solubility (Henry's Law constant). Yet, the temperature modulation itself still may provide the higher selectivity even in long quasi-steady state, as seen in the comparison between no Mod and Mod in Table 3.3.

Table 3.4. Solubility, determined by Henry's Law constant, among Ammonia, Ethanol, and Toluene. (Sander 2015)

Sample	Henry's Law constant ( $\frac{mol}{m^3Pa}$ )
Ethanol C <sub>2</sub> H <sub>5</sub> OH	1.1 – 2.3
Ammonia NH <sub>3</sub>	$1.0 \times 10^{-1} - 7.7 \times 10^{-1}$
Toluene C <sub>6</sub> H <sub>5</sub> CH <sub>3</sub>	$1.7 \times 10^{-4} - 2.8 \times 10^{-3}$

*This page is intentionally left blank*

## **Chapter 4. Potential Use of Temperature Modulation-SDP on MOS Gas Sensors in Self-made E-Nose to Indicate Additional Nutrient in Soil.**

### **4.1. Introduction**

This chapter presents a performance test of the temperature modulation-SDP (Sudarmaji & Kitagawa 2015) to response a such complex compound in varies conditions, i.e. to identify soils and in various condition due to nutrient addition by capturing soil gaseous profiles using a self-made e-nose system. Soils, a complex mixture, are composed mostly of minerals and organic materials, water, air, and countless organisms (Carson et al. 2015; Soil Science Society of America 2010). Some evidences pointed that many gases and volatile organic compounds (VOCs) are found in the soil atmosphere in vary widely types and relative concentrations(De Cesare et al. 2011; Insam & Seewald 2010; Tassi et al. 2015; Peñuelas et al. 2014) that produced due to microbial activity (De Cesare et al. 2011) which influenced by environment conditions (Milchunas et al. 1988; Sherlock et al. 1994; Smith et al. 2003). Soil also known has a unique smell that can be sensed with human olfaction system. The smell molecules of soil are known as Geosmin and Methylisoborneol which mostly produced by bacteria belonging to the most genus *Streptomyces* that involves a number of enzymes (Wang & Cane 2008; Mei Wang & Cane 2008; Green et al. 1975). The existence and content of smell molecules and organic substances in different soil type and the composition of volatile substances of nutrient addition might result in a unique olfactory fingerprint, emitted from vaporized decomposition of organic matters and chemical reactions among others in static headspace at the certain conditions.

Accordingly, based on soil gaseous profiles (also called fingerprints) of the sensor responses corresponding to the samples, this paper aims to determine qualitatively the potential use of array MOS gas sensors which driven by temperature modulation-SDP. It drives the MOS gas sensors on certain driving modulation in self-made e-nose system to differ the soil type and indicate the presence/level of nutrient addition in soil on controlled environment condition.

In agriculture field, many results give the strong evidences of successful system

applications based on e-nose principle such as assessment of agriculture products quality (freshness, ripeness, contamination, spoilage), cultivar selection, preservation treatments, variety characteristics, plant pathology, and plant identification (Wilson & Baietto 2009). Particularly in soil analysis, though there were still few explorers, as reported by De Cesare et al. (2011), some relevant and successful examples of e-nose application on soil cases have been developed in recent years such as ammonium detection through ammonia measurement. They themselves measured the microbial activity in silty clay loam soil to distinguish different metabolic and growth phases of the inoculated bacteria during incubation and to discriminate between inoculated and non-inoculated ecosystems. The growth and activity of microbial was boosted by adding nutrient solutions into soil which incubated for 23 days.

The usage of an array of sensors in e-nose, where each commonly unspecific for single analyzed but also interact with substances belonging to other chemical classes (cross-selectivity) (Nanto & Stetter 2003), are altogether to provide a unique profile (also called fingerprint) for certain analyzed sample. This advantage of e-nose might be applied in situ measurement instead of the conventional method, namely The Gas Chromatography/Mass Spectrometry (GC/MS) which is well-known to separate, identify and quantify accurately the soil gaseous and volatile compounds (Smith & Dowdell 1973; Carter & Gregorich 2008) but required large labor space, and high expense and much time needed (Rappert & Müller 2005).

## **4.2. Experimental Materials and Methods**

### **4.2.1. The Self-made Electronic-Nose**

A system based on the principle of electronic-nose (Fig. 4.1) was built to capture and analyze the soil gaseous profiles. It mainly consisted of three components, (i) sensing element, consisted of 6 TGSs gas sensor (Table 4.1) which driven by a technique, temperature modulation with specified detection point to sense the soil's VOC, and 2 environment sensors (LM35 and HSM30G) to monitor the ambient temperature and temperature and humidity in sensor chamber, (ii) PSoC CY8C28445-24PVXI-based system, as interface system (data acquisition and front-end-like) for sensors, and (iii) data preprocessing (Principal Component Analysis, PCA) and pattern recognition tool (Neural



Network, NN) developed under Visual Studio 2012 to analyze the profiles of the array sensor responses corresponding to the soil samples.

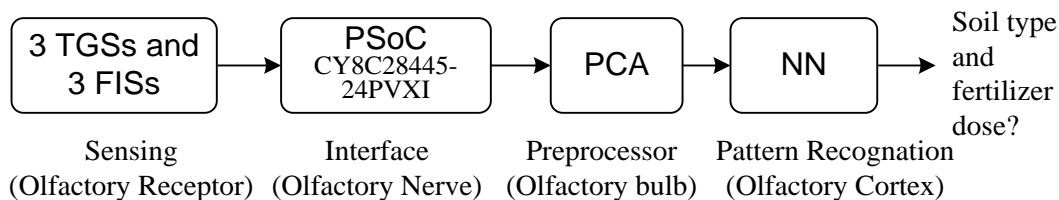


Fig. 4.1. Measurement diagram of soil vapor fingerprint based on e-nose principle.

The 6 MOS gas sensors used and the design of temperature modulation with specified detection point are exactly same with the previous work (Chapter 3). The sensors are designed by their manufacturers to sense the volatile compounds and expected to sense the soil volatiles, they are specified to detect a particular volatiles in low concentration range. In this study, the 0.25 Hz; 75% of temperature modulation-SDP was applied to drive both array of TGS and FIS gas sensors, except on TGS-2444 which driven at 4 Hz 5.6% as recommended by FIGARO Engineering Inc. (2011). This modulation setting (0.25 Hz; 75%) gave the highest selectivity performance on most of both TGS and FIS gas sensors used to distinguish among ammonia, toluene, and ethanol (Sudarmaji & Kitagawa 2015). Also similarly, for the setup and configuration of the PSoC CY8C28445-24PVXI (shown in Fig. 3.4) which acts as a core of the interface system which mainly functioned to acquire all sensors output, to communicate with computer wirelessly, and to generate desired modulation signals. It connects wirelessly through Radio Frequency using XBee (IEEE 802.15.4) serial communication interfaced by a developed program under Visual Basic.Net 2012.

Table 4.1. MOS gas sensors used and typical gas target <sup>\*)</sup>.

No	Sensor	Gas Target	Working Range
1	TGS2444	Ammonia	1-100ppm
2	TGS2602	Air Contaminant	1-30 ppm of EtOH
3	TGS825	Hydrogen Sulfide	5-100 ppm
4	FIS12A	Methane	300-7,000 ppm
5	FIS30SB	Alcohol	1-100 ppm
6	FISAQ1	VOC (air quality)	10-10,000 ppm

<sup>\*)</sup> based on product datasheet from Figaro Engineering Inc. and FIS Inc.

I applied 2 (two) famous and powerful data processing tools which commonly used in E-Nose to imitate the work of an olfactory bulb and olfactory cortex in mammalian nose

system (Turner & Magan 2004), i.e. PCA and NN respectively. They are built using Visual Studio VB Net 2012 and compared their results using PCA and NN function in Matlab 7.12.0 (R2011a). The PCA software is constructed by utilizing PCA routine in open-source Accord.NET Framework 2.10.

The NN with a single hidden layer and an appropriate hidden layer activation function are capable of accurate approximation to an arbitrary function and its derivatives (Hornik et al. 1989; Hornik et al. 1990). The Neural Network was developed based on Backpropagation (BP) learning method in Multi-Layer Perceptron Neural Network (MLPNN) architecture by employing a log-sigmoid activation function. Basically the BP algorithm is a generalization of the delta rule (Least-Mean Squares algorithm), also called the *generalized delta rule* (Rumelhart et al. 1986; Du & Swamy 2014). It uses a gradient search technique to minimize a cost function equivalent to the Mean Square Error (MSE) between actual network outputs and the desired (target) output. The BP propagates the MSE to backward through the network and the weights (and biases) are then adjusted by a gradient descent based algorithm. Thus, a closed-loop control system is established in network. BP algorithm might be applied in many layers of MLP.

#### **4.2.2. Soil Preparation and Treatment.**

The soils (sandy loam and sand soil) were derived from the top 15 cm and land without prior soil management. Sandy clay loam soil was taken from land around Kanazawa University (36°32'46.3380"N, 136°42'11.5452"E), while sand soil was taken from around coastal area of Uchinada Beach (36°38'39.19"N, 136°37'37.88"E), a sand hill on Sea of Japan, which is located about 17 km from Kanazawa University. The collected soil samples were crushed and sieved manually at <2 mm after plant derbies, turfs, and gravels were carefully removed.

As soil treatments, I added commercial fermentation compost, produced by Wakayama Organic Productive Union, into soil as organic nutrient addition. In the specifications, it contains Nitrogen 2.54/ Phosphoric acid 0.56/ Potash 0.56/ Humus acid 17.1/ Carbon-nitrogen ratio 9.6/ number of actinomycetes 21 million per gram/ pH 6.8. The composts were put at average and high doses as recommended in practical application, i.e. 20 and 30 ton ha<sup>-1</sup> DM (Dry Matter) respectively (Haber et al. 2010). Thus, I added fertilizer at rate 0, 15, and 22.5 mg/g soil sample corresponding nearly to 0, 20, and 30 ton ha<sup>-1</sup> DM

respectively by considering that it is generally assumed that in 1 ha soil area, 15 cm deep, contains 2Mkg despite bulk density of soil varies considerably (King 1911; Conklin 2014).

The soil and compost samples were put into LLDPE (Linear low-density polyethylene) plastic bag and sealed with paraffin. Then, it was stored them in refrigerator at  $5\pm0.5^{\circ}\text{C}$  to inactivate microbial activity in soil. This temperature is known as biologic zero temperature, which recognized that most microbes in soil become relatively inactive at temperature below  $5^{\circ}\text{C}$  (Malone & Williams 2010; Rabenhorst 2005). Prior being used, the samples were air-dried up to room temperature.

#### 4.2.3. Soil Gaseous Sampling and Headspace Condition.

The critical stage in e-nose measurement is gas sampling, i.e. to collect and provide sufficient concentration of volatile compound that represent the condition of sample/analytical substance to be detected by sensors used. I applied a Static Headspace (SH) technique (Fig. 4.2), commonly used in GC, to acquire the soil gaseous profiles. It is simple, low-cost, and more flexible in adapting to varying sample properties because the headspace is directly transported to the measuring chamber, guaranteeing sample integrity. In SH, sample is placed in a closed vial and remains closed to reach equilibrium state. Simply, it needs to determine mostly only the physical parameters (i.e., time and temperature) to achieve the necessary state of equilibrium (Kolb & Ettre 2006).

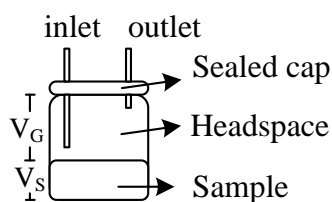


Fig. 4.2. Static headspace design for saturated soil samples.

The samples in SH is prepared into solution since soil might contains many soluble substances in water. In case the solid sample is able to be dissolved in water, the determination can be simplified using the solution approach. Solution has bigger diffusion coefficient than solid, thus it takes shorter diffusion and consequently equilibration times, where time of diffusion depends on the diameter and thickness of particles, and the shortest equilibration times are also found with liquid samples of low viscosity (e.g., aqueous solutions) (Kolb & Ettre 2006).

Moreover, the water content of soil samples is conditioned into saturation state (i.e. slightly above 100% of wet based water content) by adding the ultra-pure water and specified the phase ratio of SH into 1.5. And the mass of soil sample is determined using Eq. 4.1 to define the mass of pure water and compost addition, where  $m_s$  expresses mass of soil (g),  $V_v$  is volume of headspace vial (ml),  $\rho_s$  is bulk density of soil (sandy loam = 1.44 g/ml and sand = 1.51 g/ml) (Yu et al. 1993),  $\rho_w$  is density of pure water = 0.998 g/ml,  $\beta$  ( $V_G/V_S$ ) is phase ratio in SH, and  $w_c$  is water content (in fractional number). Table 4.2 resumes the properties of parameters used and calculation results.

$$m_s = \frac{V_v \times \rho_s \times \rho_w}{(\beta + 1) \times (\rho_w + w_c \times \rho_s)} \quad \text{Eq. 4.1}$$

The headspace equilibration in SH is optimized by both agitating (i.e. stirring) and thermostating concurrently for all samples on the same phase ratio. Thermostating may lead to reduce the equilibration time since the diffusion coefficient is proportional to the absolute temperature, and continuous agitation of the sample during the equilibrating is the better and recommended way to speed up equilibration time, especially for of non-polar VOCs in aqueous solutions (Kolb & Ettre 2006). I set 30 minutes, 60°C, and 200 rpm of equilibration time, temperature, and stirring frequency respectively. Those values (except stirring frequency) gave the optimum responses to analyze of fumigants 1,3-dichloropropene (1,3-D) and methyl isothiocyanate (MITC) in Soil and Water Samples using Gas Chromatography Methods. (Gan et al. 1998). Moreover, others results also showed that temperature and time of equilibration improved the sensitivity and optimized the equilibration (Yilmazcan et al. 2013; Wu et al. 1998; Lebrun et al. 2008). However, generally the optimized parameters of equilibration for headspace analysis should be selected depending on the compound studied and chemical class.

The Corning PC-4200D is utilized to heat and stir the sample in the headspace vial and used 90 ml glass container with sealed cap as headspace vial which is put inside the 500 ml open beaker filled with 100 ml water (Fig. 4.3). It aims to maintain the equilibrium relative humidity the same as the soil sample (Bastos & Magan 2007). And, the soil gaseous sampling in static headspace was conducted inside a room with controlled-temperature. By those ways, all soil samples were under the same treatments and environmental conditions when produced patterns of soil gaseous compounds that to be

captured and studied due to the soil type and nutrient addition. In practical use, I set the temperature regulator of Corning at 110°C to maintain the water temperature in beaker at  $60\pm1^{\circ}\text{C}$ , where at this point the surface temperature of ceramic was at  $87\pm1^{\circ}\text{C}$ .

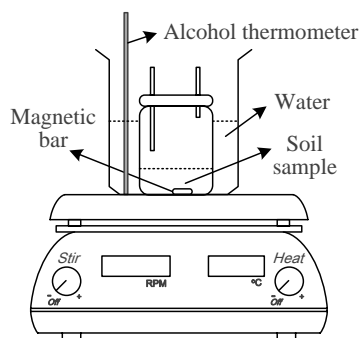


Fig. 4.3. Headspace conditioning with heating and stirring using The Corning PC-420D in SH sampling, the layout of Corning modified from (Corning Inc. 2007).

Table 4.2. Properties of samples of soil, fertilizer, water, and static headspace condition.

Properties of SH	Value
Volume of SH Vial	90 ml
Bulk density of sandy loam soil	1.44 g/ml
Bulk density of sand soil	1.52 g/ml
Phase ratio	1.5
Water content	1
Density of pure water	0.998 g/ml
Equilibration temperature	60°C
Equilibration time	30 minutes
Mass of sandy loam soil	21.22 g
- mass of compost adding at 20 ton/ha	0.318 g
- mass of compost adding at 30 ton/ha	0.477 g
Mass of sand soil	21.63 g
- mass of compost adding at 20 ton/ha	0.324 g
- mass of compost adding at 30 ton/ha	0.287 g

#### 4.2.4. Measurement Procedures.

The measurement of soil gaseous profiles are performed using close measurement method by switching between the reference gas (filtered air with silica gel) as baseline ( $R_0$ ) and the soil gaseous profiles as analyte ( $R_g$ ). The gas is delivered by utilizing a pump which located at the side of the system as usually used in many transferring an analyte of the headspace gas directly into a sensor chamber. The flow direction and rate of gas are controlled by 3-way valve and The Koflok mass flow controller (MFC) respectively in which the 3-way valves were switched manually and the MFCs are adjusted at 0.3 liter

per minute. As shown in Fig. 4.4 the reference gas flows through point a (valve 1), point c (valve-2), and point e (valve-3), while the analyte gas flows through point b (valve-1), point d (valve-2), and point e (valve-3). The purging of sensor chamber is in open measurement mode by disconnecting the hose of inlet pump from valve-2, directing the valve-3 to point f, and turning on the purge pump.

The PSOC based unit as interface, controlled by computer, generates a temperature modulation signal to activate/drive or deactivate MOS gas sensor and received a set of digital data to be analyzed. The temperature modulation is on 0.25 Hz; 75% duty cycle to drive all MOS gas sensors. This frequency resulted in the higher selectivity to differentiate among ammonia, toluene and ethanol (Sudarmaji & Kitagawa 2015). As initial action at first time turning on, the system turned on operating in reference measurement mode for one hour to allow the MOS gas sensors reach stabilized. The gas sensors are expressed in resistance and the profiles is defined by its Sensitivity (Eq. 3.2) (Huang et al. 2003; Arshak et al. 2004).

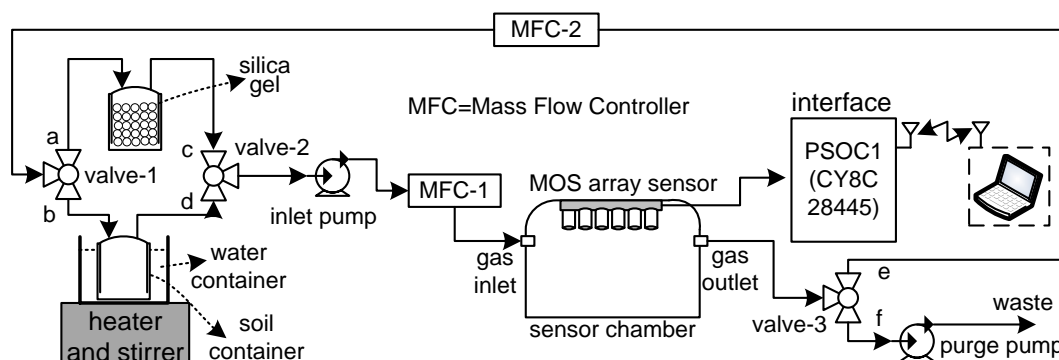


Fig. 4.4. Experimental setup to capture the soil gaseous compounds using static headspace extraction in sample flow system (close) measurement.

The  $R_0$  is measured after 30 minutes of quasi-steady state time for MOS gas sensor (concurrently with the time of thermostating) and then the  $R_g$  is measured right after the 3-way valve are switched. The measurement cycle timing of the  $R_0$  phase,  $R_g$  phase, and purging phase are set on 1 minute, 1 minute, and 5 minutes (including the flush time of gas hoses) respectively. Therefore, the total cycle time per sample was 37 min. The sampling period of both  $R_0$  and  $R_g$  measurement are 2 seconds, obtained respectively 30 data of  $R_0$  and  $R_g$  per measurement cycle. I tested 2 types of soil with 3 compost adding levels and each sample/treatment was replicated five replicates. Concisely, the

measurement steps from soil preparation until identification could be shown in Fig. 4.5.

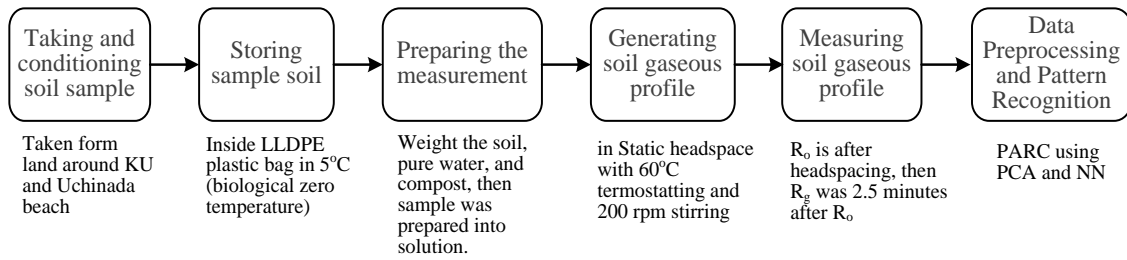


Fig. 4.5. Measurement steps to indicate the nutrient level based on soil gaseous profiles.

### 4.3. Results and Discussion.

#### 4.3.1. Initial Measurement.

Initially, I observed  $R_g$  for 5 minutes after  $R_0$  measurement, as shown in Fig. 4.6, to know the response of each sensor and obtain the best starting measurement time for  $R_g$  measurement since it was assumed the gas distribution is not spread evenly. It shows that most sensor has similar response (except TGS2602 and TGS2444) to the flow and distribution of gas produced in the headspace, but reaches a different stability time. Particularly on TGS2444, even though it seem most distinct (more ripples) among the others, yet it still shows its typical response. When it is expressed in ppm (part per million) using graphical calibration in its datasheet (Figaro Engineering Inc. 2011), the values lie around 2 ppm. While the resistance of TGS2620 suddenly dropped then toward its stability response.

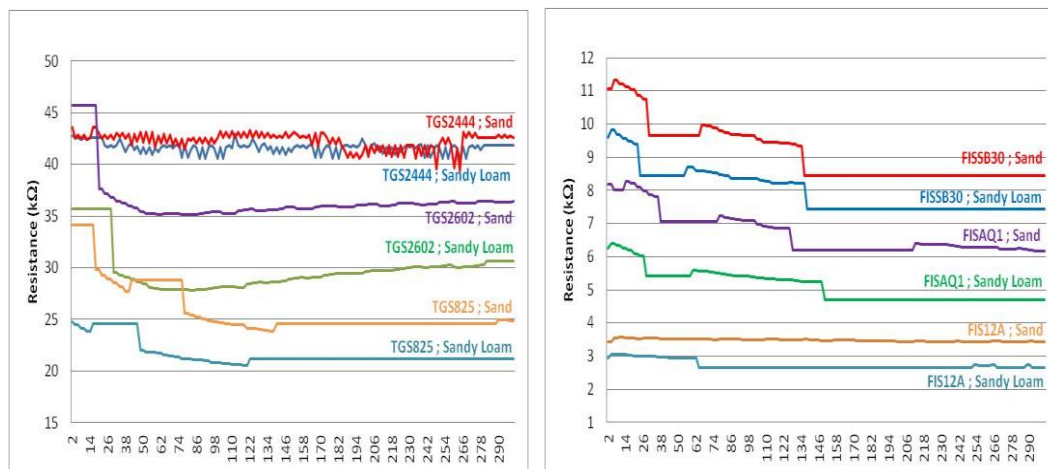


Fig. 4.6. The response of TGSs and FISs to soil samples (sandy loam soil and sand soil) without compost addition under 0.25 Hz; 75% modulation in 5 minutes.

Significantly, it seem that overall sensors reached a stable state after  $\pm 150$  s ( $\pm 2.5$  minutes) which strongly indicate they sensing stably the flow of gas that have been spread evenly in the close measurement system. Therefore I took this time be the starting point of  $R_g$  measurement.

#### 4.3.2. Sensor Responses and soil gaseous profiles.

A MOS gas sensor driven by temperature modulation will behave a unique characteristic response depends on the given modulation signal and amplitude (Huang et al. 2004; Ortega et al. 2001; Sun et al. 2004; Chutia & Bhuyan 2012). Temperature modulation leads to generate a pattern, which may be a characteristic of the species being detected. In our previous work, lower frequency of DC square/rectangular modulation provided more slope and distinct shape, and selected modulation gave higher sensitivity than static temperature, and in our extended design of temperature modulation, the specified detection point ensures a same measurement points at each output shape (Fig. 4.7). Moreover, the modulation on sensing element  $R_s$  associated (in same phase) with temperature modulation may lead to prevent sensor from possible migration of heater materials into the sensing material which could causes long term drift of sensing material's resistance to higher values (Figaro Engineering Inc. 2011). It means that a pulsed- $S_{VC}$  would be giving less force to drive migration than a constant voltage, rendering negligible possibility of migration, particularly under high humidity and temperature operation. This benefit contributes to performance of MOS gas sensors when operates in such application with increasing in humidity and temperature as like in this work.

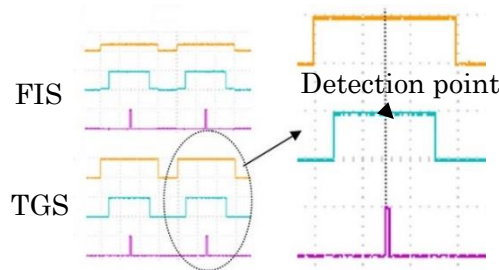


Fig. 4.7. 0.25 Hz; 75% Modulation signals of TGS and FIS, orange:  $S_{VH}$ , blue:  $S_{VC}$ , and purple: time of detection point, captured by Oscilloscope Tektronix TDS 2024B: 5V/div except for  $S_{VH}$  of FIS at 2V/div (Sudarmaji & Kitagawa 2015).



I found that during all measurement the temperature in sensor chamber was slightly increased ( $\pm 2^\circ\text{C}$ ) while the humidity was increased higher ( $\pm 7\%$ ) during  $R_0$  and  $R_g$  measurement (Table 4.3), which strongly due to the heat and water vapor respectively produced during thermostating in SH. The ambient temperature in controlled-temperature room during all measurement was  $20.5^\circ\text{C} \pm 0.4$ . Water molecules, present in the humid air, electronically interact with the effective surface of the sensing element upon chemisorption and cause changes in  $R_g$ .

Table 4.3. Sensor chamber circumstances during  $R_0$  and  $R_g$  measurement.

Measurement	Temperature ( $^\circ\text{C}$ )		Humidity (%)	
	$R_0$	$R_g$	$R_0$	$R_g$
Sandy loam	39.9	41.4	24.0	31.2
Sand	35.8	37.7	23.8	30.6
Overall	37.8	39.6	23.9	30.9

I also found that the  $R_0$  had slightly variations as shown in Fig. 4.8. These drift seem to be an inevitable thing in oxide type sensor since its mechanism operation was depends on the heater temperature and the sensing layer strongly effected by temperature changes around sensor as well. The heater power lead a variation of the ambient temperature causes fluctuations in the operating temperature. This alters both the population of the charge carriers within the grains of the oxide semiconductor and the average thermal energy of the carriers which are to overcome the potential barriers established at the grain boundaries (Wang et al. 2010). So that it seem that almost all MOS gas sensors to be replicate dependent since varied over time (Knobloch et al. 2009). However the drift tends to smaller than static temperature operation when operated in a chamber.

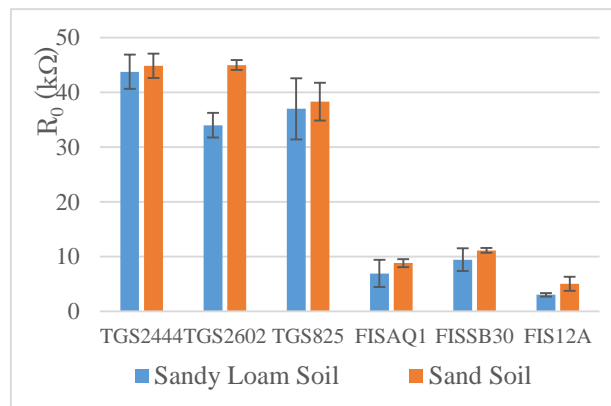


Fig. 4.8. Variation of baseline resistance expressed in standard deviation from mean value during measurement.

Individual soil gaseous profiles on each soil type shown in Fig. 4.9. It reveals that the array of gas sensors were able to sense the soil gases and/or volatiles resulted from different samples, and as well indicates that the method of the optimized SH seem suitable to provide/accumulate the concentration sufficiently. Those individual responses indicate that the technique of temperature modulation-SDP led the sensors to sense differently the amounts and types of soil gaseous compounds produced and released inside the SH atmosphere which corresponded to the soil type and doses of nutrient addition.

Moreover, As shown in Fig. 4.9, for most of the MOS gas sensors but TGS2602 the Sensitivity to the nutrient addition (20T/Ha and 30T/Ha) was higher than without nutrient addition whether for the same soil type or between sandy loam and sand. Sandy loam soil usually have more holding capacity of water and nutrient, along with lower bulk density than sand soil, thus lead to have more organic matter content (Amador & Atoyan 2012; Chaudhari et al. 2013) and microorganism (Hamarashid et al. 2010). In addition, the use of a flow system (usually employing a pump) in sample detection causes cooling of the sensor surface, reducing the high increment of temperature and humidity inside such a sensor chamber (heat dissipation) (Figaro Engineering Inc. 2005), thus also influences its response.

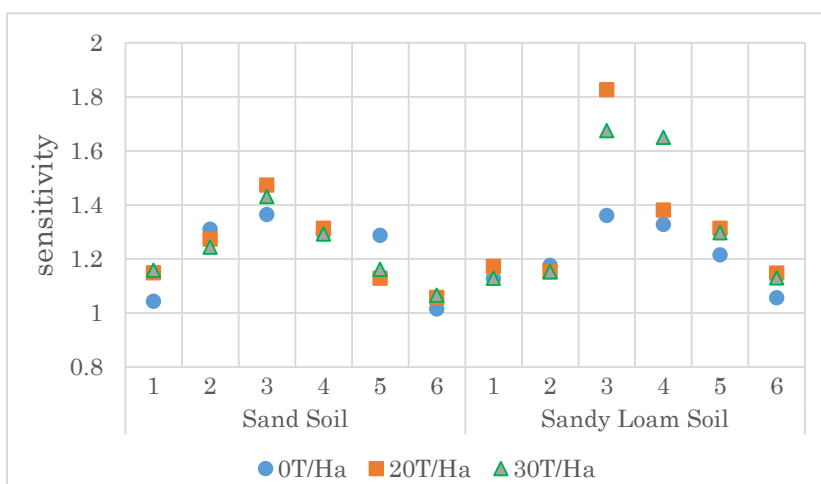


Fig. 4.9. Individual Sensitivity of sensor, average of 5 replicates, to 3 level of compost adding in different soil, 1:TGS2444, 2:TGS2602, 3: TGS825, 4: FISAQ1, 5: FISSB30, and 6: FIS12A.

The chart also shows that the highest concentration during the headspace process was hydrogen sulfide ( $H_2S$ ). It highly indicated there much acid sulfate materials in soil samples. This gas is produced by some bacterial actions upon organic matter with the aid

of the sulfates oxygen contained as an oxidation in low oxygen level (like flooded soil) which depends on ambient conditions such as temperature, humidity, and the concentration of certain metal ions (Elion 1927; Chou et al. 2014). And, soils may absorb amounts of  $H_2S$  from the air through atmospheric deposition, migration of mobilized pore water, or sulfuric material from spills and leaks, then retaining most of it in the form of elemental sulfur as sediment (Chou et al. 2014). The result also shows that the sandy loam soil provided higher concentration than sand soil since it contained higher organic matter.

However, It is also observed that there was an overlapping response in differing level of compost addition (Fig. 4.10), especially between in dose 20T/ha and 30T/ha, in which this phenomena also shown in the other sensors. However, it may be reduced by new dimension projecting using PCA as commonly used in E-nose.

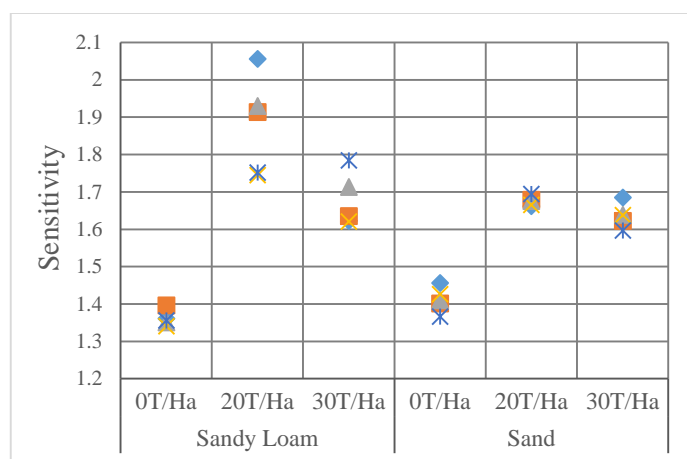


Fig. 4.10. Experiment result of TGS 825 responses to compost dose (Ton/Ha) in sandy loam and sand soil for 5 replicates.

#### 4.3.3. Soil Discrimination under different nutrient addition.

The PCA was applied to plot the soil gaseous profiles and shows the selectivity of MOS gas sensors used to discriminate the soil type various dose of nutrient addition. It offers an advantage that the classification of unknowns is processed much faster through reducing detection time since it projects of large origin dimensional data into new and lower dimensional subspace (Hines et al. 2003).

Fig. 4.12(a) shows the PCA plot of discrimination of two soils, both without addition of compost. It shows a distinct zone of patterns volatile production between sandy loam

soil and sand soil, where the principal component (PC)-1 accounts higher differentiation of cluster than PC-2. PC-1 and PC-2 cumulatively account for 78.32% of the variance within the data set (Table 4.4).

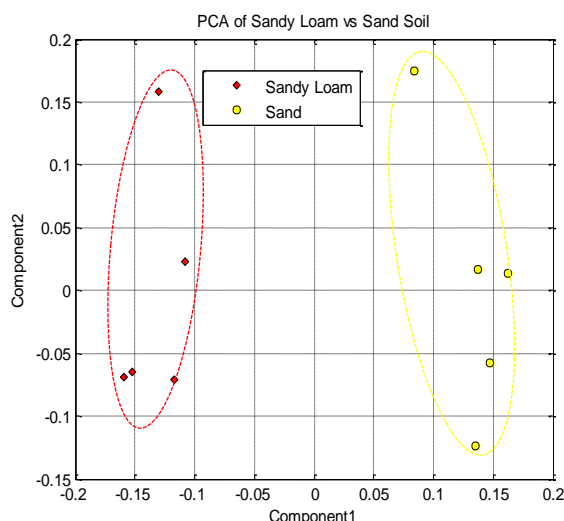


Fig. 4.11. PCA plot between sandy loam and sand soil in without compost addition.

While generally Fig. 4.12 show that the PCA plots by PC-1 and PC-2, which account about 64% and 83% cumulatively of the variance in the input variables, allow to discriminate distinctly type of soil and to differ between soil condition whether with or without compost (nutrient) addition as indicated by separately blue zone, even when differentiating irrespective of soil type. It was only for sandy loam soil (Fig. 4.12(a)) the level of compost were able to be classified clearly into three groups as predefined previously while for sand soil (shown red and yellow zone in Fig. 4.12(b)) there were miss-identification between soil with dose 20T/Ha and to 30T/Ha. Fig. 4.12(c) shows there no clear classification (black zone) when identifying soil with dose 20T/Ha and to 30T/Ha irrespective of soil type. Overall Fig. 4.12 shows that the highest level of differentiation was found along PC-1 on clusters between of the soil with nutrient addition and without nutrient addition, whereas that between addition of 20T/Ha and 30T/Ha were placed in mainly along PC-2.

Finally, I determined the performance of NN as decision unit of e-nose to classify the level of nutrient addition in soil based on indicator the error (MSE) achieved resulted from the training process. I employed three principal components (PCs) as new dimension to distinguish between headspace volatiles released from soil samples and as the input of

neural network since they represent more than 90% of divergence samples data (Table 4.4). I designed the architecture of MLPNN that comprises 3 layer (single hidden layer). All the weights in the network are updated using the global adapted learning parameter  $\eta$  which updated by search-then-converge schedule. It is a simple and non-adaptive annealing schedule. Typically, it starts with a large  $\eta$  and gradually decreases it as the learning proceeds which the process of adapting  $\eta$  is similar to that in simulated annealing (Du & Swamy 2014). The characteristic time of this schedule is a new free parameter that must be determined by trial and error the search time constant. The algorithm escapes from a shallow local minimum in early training and converges into a deeper, possibly global minimum.

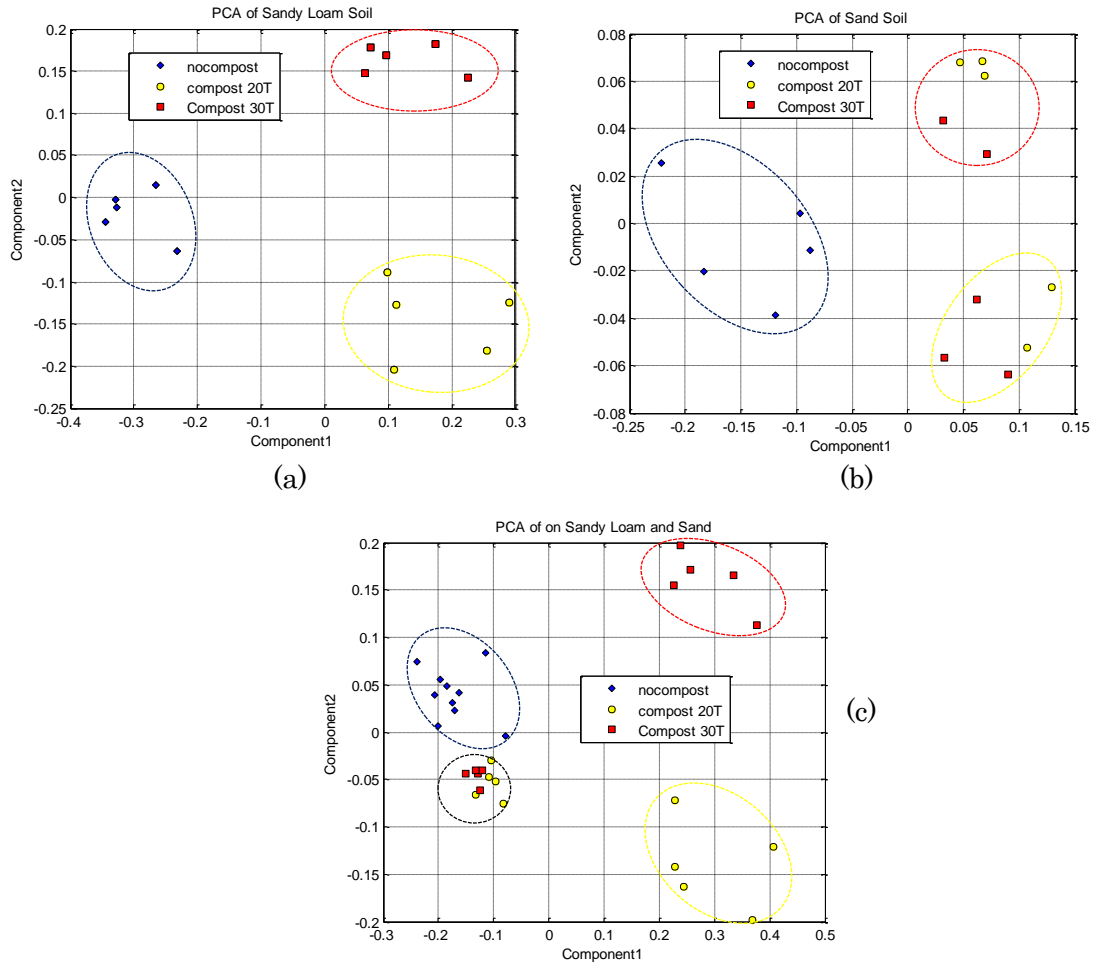


Fig. 4.12. PCA plot between sandy loam and sand soil both without compost addition, and soil gaseous pattern projection mapped in 2 PCs for each soil sample to differ the level of compost addition of (b) sand, (c) sandy loam, (d) irrespective of soil type.

Table 4.4. Cumulative proportion of 3 PCs resulted from 6 sensors used.

PC	cumulative PCs proportion			
	SL*	S*	SL+S*	Soil diff*
PC1	64.27%	75.61%	66.53%	52.69%
PC2	86.34%	88.96%	80.69%	78.32%
PC3	93.73%	93.73%	89.18%	90.38%

\* SL=Sandy Loam; S=Sand; Soil diff= between sandy loam and sand soil.

In learning, I took the learning parameters of BP as follow: maximum epoch is  $10^4$ , error target is  $10^{-5}$ , initial learning rate is 0.8 and the constant of search time in search-then-converge annealing learning rate is 700. Our NN software keeps the results (MSE in each epoch, achieved final weights and biases, and outputs) in excel format.

I determined the optimum number of neuron in hidden layer by Singular Value Decomposition (SVD) analysis of its output in each training dataset (Santos et al. 2010; Tamura 1997). By input from 3 PCs and considering resulted SVD value, I choose 6 neuron in hidden layer to differ among the pre-described three categorized fertilizer levels in soil sample, thus the neuron number architecture of MLPNN is 3-6-3 of respectively input, hidden, and output layer. It also meets the general suggestion by Hecht-Nielsen (1987) *in* (Nakamura et al. 1994) that it should less than  $2n + 1$  the number of hidden neurons, where  $n$  is the number of inputs. A small number of hidden neurons does not lead complex input-output reactions modelling in network. I also trained the NN by input directly from sensors output (without preprocessing/PCA) with the same hidden layer (6-6-3 NN architecture). The achieved MSE of training results (Table 4.5) show that PCA helps improving the NN classification to differ level of compost addition in soil. The all application of trained data shows successful recognitions to indicate level of nutrient addition in soil as well.

Table 4.5. MSE achieved by 6 neuron of hidden layer to discriminate 3 level of compost addition in soil.

Soil type	MSE of with PCA	MSE of without PCA
Sand	4.204e-04	3.490e-03
Sandy Loam	1.226e-04	5.024e-04
Regardless of type	2.678e-03	4.080e-03

## Chapter 5. Conclusion.

### 5.1. Conclusions.

This dissertation has presented an application of new technique (temperature modulation-SDP) on MOS gas sensor in such non-parametric biological system to distinguish the soil type and indicate the different dose of nutrient addition in soil. The conclusions obtained from this study are as follow:

1. A new technique to enhance the sensitivity of MOS gas sensor, called the temperature modulation-SDP (Specified Detection Point), has been successfully developed using a common switching circuit employing FET (Field Effect Transistor) to drive a single or array of MOSs, where in this study I use a rectangular (square) modulation signal generated by PSoC CY8C28445-24PVXI. The response shapes of MOS gas sensor due to temperature modulation-SDP seem in accordance with the modulation given, where each modulation provides a particular response and at lower frequency has more sloping and distinct characteristic. In first test to discriminate 3 gases (Toluene, Ethanol and Ammonia), it led higher selectivity on 75% duty cycle of modulation on each tested frequency modulation (0.25 Hz, 1 Hz, and 4 Hz) and most gas sensors especially the FISs performed highest selectivity under 0.25 Hz modulation. And, the PCA plot indicated that selected temperature modulation-SDP for array sensor leads the increment of selectivity up to 64.7 % compared with static temperature mode in distinction of those gases.
2. The self-made measurement system based on e-nose principle has been developed to get the soil gaseous profiles that comprises of:
  - a. 6 MOS (3 TGS and 3 FIS) gas sensors, driven with temperature modulation-SDP, and 3 environment sensors.
  - b. The PSoC CY8C28445-24PVXI as a hearth of wireless interface and acquisition system for the measurement system.
  - c. The Patten recognition (PARC) tools consist of Principal Component Analysis (PCA) as preprocessor and Multi-Layer Perceptron Neural Network (MLPNN) as recognition/identifier unit.

The soil gaseous was generated in a static headspace with 60°C thermostating and 200 rpm stirring to optimize and measured upon a sample flow system (dynamic chamber) measurement.

3. It is strongly suggested to determine the starting time of analyte ( $R_g$ ) measurement since different stable state of MOS gas sensor response. I found, it took about 150 seconds ( $\pm 2.5$  minutes) for most gas sensors used reach stable response state to measure soil gaseous profile in our sample flow system measurement.
4. It was found that the highest concentration of soil gaseous compound in the static headspace was hydrogen sulfide, indicated with highest Sensitivity of TGS-825 which specially designed to sense more sensitively the hydrogen sulfide.
5. The 6 selected commercial MOS gas sensor applied in e-nose system were promising for use in the indicating the presence of additional nutrients in soil and their dose as well since they could response and provided the (unique) soil gaseous profiles resulted from a static headspace in certain condition.
6. The PCA helps improving the NN classification to differ level of compost addition in soil and the discrimination results of PCA and NN are closely in accordance, as in this study was found that PCA discriminates clearly between sandy loam and sand soil, and could distinguish between soil condition whether with or without compost (nutrient) addition.
7. The optimum architecture of MLPNN with single hidden layer was 3-6-3 with PCA as prior data preprocessor. The first three principal components account over 90% cumulatively of the variance in the 6 MOS gas sensors input. This architecture may give better identification while distinguishing the soil type or the dose of nutrient in soil, even with irrespective the type of soil. By backpropagation learning algorithm, it resulted a successful identification as shown by the MSE achieved (e.g. The MSE was  $1.226 \times 10^{-4}$  when learning at maximum epoch is  $10^4$  for the nutrient level in sandy loam soil).



## 5.2. Future Works.

This technique, temperature modulation-SDP, can be applied in any MOS gas sensor since principally a MOS gas sensor consists of heater and sensing element. It was also proved that temperature modulation provides more unique and distinct response, and could increase the selectivity and sensitivity. Hence, this e-nose (i.e. measurement system) could be implemented for in-situ measurement of soil atmosphere and environmental applications, and its possibility for correlation to macro nutrient or others specific parameters related to soil fertility and comparison to conventional methods.

However in this study, by PCA analysis the 6 MOS gas sensor used still indicated a cross-grouping to differ between the soil with nutrient adding in normal dose (20T/Ha) and high dose (30T/Ha). Therefore it needs further observation on the modulation itself or usage of other MOS gas sensors, mainly those high response to hydrogen sulfide, air contaminant, and alcohol (the hydroxyl functional group  $-OH$ ) group or other organic compound group which indicated had high response in this research results. On the pattern recognition side, besides PCA and MLPNN, many other advance of multivariate statistical analysis, whether for dimensional reduction, classification, or clustering, are also reliable to treat the data sets produced by the MOS gas sensor in e-nose system to obtain best result.

And, other promising applications are the soil toxicity detection due to excessive usage of fertilizer and pesticide, and/or monitoring the pesticide bioremediation program. The process of remediating of contaminated soils involves inducing airflow in the subsurface with an applied vacuum, and thus enhancing the in situ volatilization of contaminants. The process itself takes advantage of the volatility of the contaminants to allow mass transfer from adsorbed, dissolved, and free phases in the soil to the vapor phase, where it is removed under vacuum and treated above ground. Depending on the applications and the type of sample to be analyzed, the choice of sensor array can be crucial for the good performance of the system.

***This page is intentionally left blank***

## Acknowledgments

Firstly I would like to say Alhamdulillah Rabbil ‘Alamin for His blessing so that I am able to finish this dissertation and all achievement in my doctoral study at Kanazawa University. Here, I am very grateful to whom has been contributed directly and indirectly during my study.

My sincere and warm thanks to my lovely wife (Nur Rohmah) and children (Syifa, Bayyin, Barru, and Sakhi), my beloved parents, and all my family for their constant support and great understanding over years. My special thank goes to Mbah Kuat for protecting and caring my sweethearts, passing our long distance and difficult periods.

I deeply thank to my supervisor, Prof. Akio Kitagawa. His immeasurable support, guidance, and patience are the most significant and meaningful for both my study and live in Kanazawa. Prof. Kitagawa has provided me the outstanding environment and materials for conducting my research, and as well has supervised me with his high ability, ethic, and work culture. I also would like to express my gratitude to Prof. Junichi Akita who has shared his laboratory and has given some fruitful discussions and especially constructive comments at my progress seminars. Further, I thank to all members of Micro-Electronic Laboratory (MeRL) and Interface Device Laboratory (ifDL) since October 2012 to March 2016 for helping during my research and nice friendship. My big thank goes to Kawai-san for a year being my tutor with friendly helps in my settling period in Kanazawa and to Imamura-san for many helps during over last 3 months prior my return to Indonesia.

I am very grateful to DIKTI (Indonesian Directorate General of Higher Education) for the doctoral scholarship and to KU-DIKTI staffs (especially to Ms. Maiko) for supporting and managing the affairs of all Indonesian-DIKTI awardees.

Last, but not least, I thank to my friends in Kanazawa University, who join in the KU-DIKTI and PPI Ishikawa groups, especially to my best friend (Romy), for all valuable support and encouragement throughout my study.

Thank You. ありがとうございます。

*This page is intentionally left blank*

## References

- Aleixandre, M. & Gerboles, M., 2012. Review of small commercial sensors for indicative monitoring of ambient gas. *Chemical Engineering Transactions*, 30(SEPTEMBER 2012), pp.169–174.
- Amador, J.A. & Atoyan, J.A., 2012. Structure and Composition of Leachfield Bacterial Communities: Role of Soil Texture, Depth and Septic Tank Effluent Inputs. , pp.707–719.
- Arshak, K. et al., 2004. A review of gas sensors employed in electronic nose applications. *Sensor Review*, 24(2), pp.181–198. Available at: <http://www.emeraldinsight.com/doi/abs/10.1108/02602280410525977>.
- Barnes, I. et al., 2006. Dynamic Chamber System to Measure Gaseous Compounds Emissions and Atmospheric-Biospheric Interactions. *Environmental Simulation Chambers: Application to Atmospheric Chemical Processes*, 62, pp.97–109. Available at: [http://dx.doi.org/10.1007/1-4020-4232-9\\_7](http://dx.doi.org/10.1007/1-4020-4232-9_7).
- Barsan, N., Koziej, D. & Weimar, U., 2007. Metal oxide-based gas sensor research: How to? *Sensors and Actuators B: Chemical*, 121(1), pp.18–35. Available at: <http://linkinghub.elsevier.com/retrieve/pii/S0925400506006204>.
- Bastos, A.C. & Magan, N., 2006. Potential of an electronic nose for the early detection and differentiation between *Streptomyces* in potable water. *Sensors and Actuators B: Chemical*, 116(1-2), pp.151–155. Available at: <http://linkinghub.elsevier.com/retrieve/pii/S0925400506001778>.
- Bastos, A.C. & Magan, N., 2007. Soil volatile fingerprints: Use for discrimination between soil types under different environmental conditions. *Sensors and Actuators, B: Chemical*, 125(2), pp.556–562.
- Bermak, A. et al., 2005. Pattern Recognition Techniques for Odor Discrimination in Gas Sensor Array. *The Encyclopedia of Sensors*, X, pp.1–17.

- Berna, A., 2010. Metal Oxide Sensors for Electronic Noses and Their Application to Food Analysis. *Sensors*, 10(4), pp.3882–3910. Available at: <http://www.mdpi.com/1424-8220/10/4/3882/>.
- Breuninger, C. et al., 2012. The dynamic chamber method: trace gas exchange fluxes ( $\text{NO}$ ,  $\text{NO}_2$ ,  $\text{O}_3$ ) between plants and the atmosphere in the laboratory and in the field. *Atmospheric Measurement Techniques*, 5(5), pp.955–989. Available at: <http://www.atmos-meas-tech.net/5/955/2012/>.
- Carlo, S. Di & Falasconi, M., 2012. Drift Correction Methods for Gas Chemical Sensors in Artificial Olfaction Systems: Techniques and Challenges. *Advances in Chemical Sensors*, pp.305–326. Available at: [http://porto.polito.it/2474783/1/2012\\_InTech\\_Drift.pdf](http://porto.polito.it/2474783/1/2012_InTech_Drift.pdf).
- Carson, T., Bachmann, C.M. & Salvaggio, C., 2015. Soil signature simulation of complex mixtures and particle size distributions. *Optical Engineering*, 54(9), p.094103. Available at: <http://opticalengineering.spiedigitallibrary.org/article.aspx?doi=10.1117/1.OE.54.9.094103>.
- Carter, M.R. & Gregorich, E.G. eds., 2008. *Soil Sampling and Methods of Analysis: 2nd ed.*, Boca Raton, FL: CRC Press Taylor & Francis Group. Available at: [http://books.google.com/books?hl=en&lr=&id=54lYLSV49zIC&oi=fnd&pg=PA1&dq=Soil+Sampling+and+Methods+of+Analysis&ots=K1nH1IM0xO&sig=v\\_ZPJHbvR5f9hCz7blw6hgazb9wYnhttp://books.google.com/books?hl=en&lr=&id=54lYLSV49zIC&oi=fnd&pg=PA1&dq=Soil+sampling+and+metho](http://books.google.com/books?hl=en&lr=&id=54lYLSV49zIC&oi=fnd&pg=PA1&dq=Soil+Sampling+and+Methods+of+Analysis&ots=K1nH1IM0xO&sig=v_ZPJHbvR5f9hCz7blw6hgazb9wYnhttp://books.google.com/books?hl=en&lr=&id=54lYLSV49zIC&oi=fnd&pg=PA1&dq=Soil+sampling+and+metho).
- De Cesare, F. et al., 2011. Use of electronic nose technology to measure soil microbial activity through biogenic volatile organic compounds and gases release. *Soil Biology and Biochemistry*, 43(10), pp.2094–2107. Available at: <http://dx.doi.org/10.1016/j.soilbio.2011.06.009>.
- Chaudhari, P.R. et al., 2013. Soil Bulk Density as related to Soil Texture , Organic Matter Content and available total Nutrients of Coimbatore Soil. *International Journal of Scientific and Resaerch Publications*, 3(2), pp.1–8.

- Chou, S. et al., 2014. *Draft Toxicological Profile for Hydrogen Sulfide and Carboxyl Sulfide*, Atlanta, Georgia. Available at: <http://www.atsdr.cdc.gov/toxprofiles/tp114.pdf>.
- Chutia, R. & Bhuyan, M., 2014. Best Frequency for Temperature Modulation of Tin Oxide Gas Sensor for Chemical Vapor Identification. , 6(2), pp.1158–1166.
- Chutia, R. & Bhuyan, M., 2012. Study of temperature modulated tin oxide gas sensor and identification of chemicals. In *Proceedings of 2nd National Conference on Computational Intelligence and Signal Processing (CISP 2012)*. Guwahati, India, pp. 181–184.
- Clifford, P.K. & Tuma, D.T., 1982. Characteristics of semiconductor gas sensors I. Steady state gas response. *Sensors and Actuators*, 3, pp.233–254.
- Clifford, P.K. & Tuma, D.T., 1982. Characteristics of semiconductor gas sensors II. transient response to temperature change. *Sensors and Actuators*, 3(0), pp.255–281. Available at: <http://www.sciencedirect.com/science/article/pii/0250687482800279>.
- Conklin, A.R., 2014. *Introduction to Soil Chemistry: Analysis and Instrumentation* 2nd ed. A. R. Conklin, ed., Hoboken, NJ, USA: John Wiley & Sons, Inc. Available at: <http://doi.wiley.com/10.1002/9781118773383>.
- Corning Inc., 2007. *Instruction Manual: For All Hot Plates , Stirrers , and Stirrer / Hot Plates with Digital Displays and for the 6795PR Temperature Controller*, Chelmsford St. Lowell, MA. Available at: [http://csmedia2.corning.com/LifeSciences/media/pdf/hotplate\\_digital.pdf](http://csmedia2.corning.com/LifeSciences/media/pdf/hotplate_digital.pdf).
- Craven, M. a., Gardner, J.W. & Bartlett, P.N., 1996. Electronic noses — development and future prospects. *TrAC Trends in Analytical Chemistry*, 15(9), pp.486–493.
- Cypress, 2010. *Programmable System-on-Chip (PSoC): CY8C28243/ CY8C28403/ CY8C28413/ CY8C28433/ CY8C28445/ CY8C28452/ CY8C28513/ CY8C28533/ CY8C28545/ CY8C28623/ CY8C28643/ CY8C28645*, San Jose, CA. Available at: <http://www.cypress.com/?docID=50827>.
- Del, R. et al., 2007. Continuous monitoring of odours from a composting plant using

- electronic noses. *Waste Management*, 27(3), pp.389–397.
- Doran, J.W., 2002. Soil health and global sustainability: translating science into practice. *Agriculture, Ecosystems & Environment*, 88(2), pp.119–127.
- Du, K. & Swamy, M.N.S., 2014. *Neural Networks and Statistical Learning*, London: Springer London. Available at: <http://link.springer.com/10.1007/978-1-4471-5571-3>.
- Dutta, N. & Bhuyan, M., 2012. Optimal Temperature Modulation of MOS Gas Sensors by System Identification. *International Journal of Signal Processing, Image Processing and Pattern Recognition*, 5(2), pp.17–28.
- Elion, L., 1927. Formation of Hydrogen Sulfide by the Natural Reduction of Sulfates. *Industrial & Engineering Chemistry*, 19(12), pp.1368–1368. Available at: <http://pubs.acs.org/doi/abs/10.1021/ie50216a022>.
- Figaro Engineering Inc., 2011. *Data sheet TGS 2444 for the detection of Ammonia*, Available at: [http://www.figaro.co.jp/en/data/pdf/20091110142953\\_64.pdf](http://www.figaro.co.jp/en/data/pdf/20091110142953_64.pdf).
- Figaro Engineering Inc., 2005. *General Information For TGS Sensors: Technical Information on Usage of TGS Sensors for Toxic and Explosive Gas Leak Detectors*, Available at: [http://www.figarosensor.com/products/common\(1104\).pdf](http://www.figarosensor.com/products/common(1104).pdf).
- Gan, J., Papiernik, S. & Yates, S.R., 1998. Static Headspace and Gas Chromatographic Analysis of Fumigant Residues in Soil and Water. *Journal of Agricultural and Food Chemistry*, 46(3), pp.986–990.
- Gardner, J.W. et al., 2000. An electronic nose system for monitoring the quality of potable water. *Sensors and Actuators B: Chemical*, 69(3), pp.336–341.
- Gardner, J.W., 1991. Detection of vapours and odours from a multisensor array using pattern recognition Part 1. Principal component and cluster analysis. *Sensors and Actuators B: Chemical*, 4(1-2), pp.109–115.
- Gibson, T.D. et al., 1997. Detection and simultaneous identification of microorganisms from headspace samples using an electronic nose. *Sensors and Actuators B:*



- Chemical*, 44, pp.413–422.
- Green, G.H., Blincoe , C. & Weeth, H.J., 1975. Geosmin and Methylisoborneol in Garden Soil. *Exp. Stn. Bull. Nevada Agricultural Experiment Station Journal Series*, (337).
- Gutierrez-Osuna, R. et al., 2003. Introduction to Chemosensors. In T. C. Pearce et al., eds. *Handbook of Machine Olfaction*. Weinheim: WILEY-VCH Verlag GmbH {&} Co. KGaA, pp. 133–160.
- Haber, N. et al., 2010. Sustainable Compost Application in Agriculture. , (April 2008), p.38.
- Haddi, Z. et al., 2014. A hybrid system based on an electronic nose coupled with an electronic tongue for the characterization of moroccan waters. *Sensors & Transducers*, 27(May), pp.190–197.
- Hamarashid, N.H., Othman, M.A. & Hussain, M.-A.H., 2010. Effects of Soil Texture on Chemical Compositions , Microbial Populations and Carbon Mineralization in Soil. *The Egyptian Journal of Experimental Biology*, 6(July 2008), pp.59–64.
- Hecht-Nielsen, R., 1987. Kolmogorov's mapping neural network existence theorem. In *Proceedings of the IEEE First Annual International Conference on Neural Networks III*. New York, pp. 11–13.
- Hellebrand, H.J., Beuche, H. & Dammer, K.-H., 2002. Sensor requirements in Precision Farming. *Scientia Agriculturae Bohemica*, 33(3), pp.114–119. Available at: <http://www.atb-potsdam.de/hauptseite-deutsch/Institut/abteilungen/Abt2/Mitarbeiter/jhellebrand/jhellebrand/Publikat/Sensor.pdf>.
- Hierlemann, A. & Gutierrez-Osuna, R., 2008. Higher-order chemical sensing. *Chemical Reviews*, 108(2), pp.563–613.
- Hines, E.L. et al., 2003. Pattern Analysis for Electronic Noses. In T. C. Pearce et al., eds. *Handbook of Machine Olfaction*. Weinheim: WILEY-VCH Verlag GmbH & Co. KGaA, pp. 133–160.

- Hornik, K., Stinchcombe, M. & White, H., 1989. Multilayer feedforward networks are universal approximators. *Neural Networks*, 2(5), pp.359–366.
- Hornik, K., Stinchcombe, M. & White, H., 1990. Universal approximation of an unknown mapping and its derivatives using multilayer feedforward networks. *Neural Networks*, 3, pp.551–560.
- Huang, X. et al., 2004. Gas sensing behavior of a single tin dioxide sensor under dynamic temperature modulation. *Sensors and Actuators, B: Chemical*, 99(2-3), pp.444–450.
- Huang, X. et al., 2003. Rectangular mode of operation for detecting pesticide residue by using a single SnO<sub>2</sub>-based gas sensor. *Sensors and Actuators B: Chemical*, 96(3), pp.630–635. Available at: <http://linkinghub.elsevier.com/retrieve/pii/S0925400503006737>.
- Insam, H. & Seewald, M.S.A., 2010. Volatile organic compounds (VOCs) in soils. *Biology and Fertility of Soils*, 46(3), pp.199–213. Available at: <http://link.springer.com/10.1007/s00374-010-0442-3>.
- Jamal, M. et al., 2010. Artificial neural network based E-nose and their analytical applications in various field. *11th International Conference on Control, Automation, Robotics and Vision, ICARCV 2010*, (December), pp.691–698.
- King, F.H., 1911. Investigations in soil management, being three of six papers on the influence of soil management upon the influence of soil management upon the water-soluble salts in soils and the yield of crops, by F. H. King. , p.188. Available at: <http://www.biodiversitylibrary.org/item/72721>.
- Knobloch, H. et al., 2009. Methodological variation in headspace analysis of liquid samples using electronic nose. *Sensors and Actuators, B: Chemical*, 139(2), pp.353–360.
- Kolb, B. & Ettre, L.S., 2006. *Static ssss Headspace – Gas Chromatography : Theory and Practice Second Edition* 2nd ed., Hoboken, NJ: John Wiley & Sons, Inc.
- Lamers, L.P.M. et al., 2013. Sulfide as a soil phytotoxin-a review. *Frontiers in Plant Science*, 4(July), p.268. Available at:

<http://www.pubmedcentral.nih.gov/articlerender.fcgi?artid=3717504&tool=pmcentrez&rendertype=abstract> <Go to ISI>://WOS:000330760000001.

- Lebrun, M. et al., 2008. Discrimination of mango fruit maturity by volatiles using the electronic nose and gas chromatography. *Postharvest Biology and Technology*, 48(1), pp.122–131.
- Lee, A.P. & Reedy, B.J., 1999. Temperature modulation in semiconductor gas sensing. *Sensors and Actuators, B: Chemical*, 60(1), pp.35–42.
- Lee, W.S. et al., 2010. Sensing technologies for precision specialty crop production. *Computers and Electronics in Agriculture*, 74(1), pp.2–33. Available at: <http://linkinghub.elsevier.com/retrieve/pii/S0168169910001493>.
- Leff, J.W. & Fierer, N., 2008. Volatile organic compound (VOC) emissions from soil and litter samples. *Soil Biology and Biochemistry*, 40(7), pp.1629–1636. Available at: <http://linkinghub.elsevier.com/retrieve/pii/S0038071708000746>.
- Li, C., 2000. Modeling trace gas emissions from agricultural ecosystems. *Nutrient Cycling in Agroecosystems*, 58(2), pp.259–276. Available at: <http://link.springer.com/article/10.1023/A:1009859006242>.
- Liu, J., Huang, X. & Meng, F., 2007. The Dynamic Measurements of SnO<sub>2</sub> Gas sensors and their Applications. In D. K. Aswal & S. K. Gupta, eds. *Science and Technology of Chemiresistor Gas Sensors*. New York, NY, USA: Nova Science Publishers, pp. 177–214.
- Malone, K. & Williams, H., 2010. *Growing Season Definition and Use in Wetland Delineation: A Literature Review*, Nacogdoches, Texas. Available at: <http://www.dtic.mil/cgi-bin/GetTRDoc?AD=ADA527538>.
- Malyshev, V. V. & Pislyakov, a. V., 2008. Investigation of gas-sensitivity of sensor structures to hydrogen in a wide range of temperature, concentration and humidity of gas medium. *Sensors and Actuators, B: Chemical*, 134, pp.913–921.
- Mei Wang, C. & Cane, D.E., 2008. NIH Public Access. *J Am Chem Soc*, 29(6), pp.997–1003.

- Meixner, H. & Lampe, U., 1996. Metal oxide sensors. *Sensors and Actuators B: Chemical*, 33(1-3), pp.198–202. Available at: <http://www.sciencedirect.com/science/article/pii/S0925400596800980>.
- Milchunas, D.G. et al., 1988. Factors influencing ammonia volatilization from urea in soils of the shortgrass steppe. *Journal of Atmospheric Chemistry*, 6(March 1986), pp.323–340.
- Mosier, a. R., 1998. Soil processes and global change. *Biology and Fertility of Soils*, 27(3), pp.221–229.
- Nagle, H.T., Gutierrez-Osuna, R. & Schiffman, S.S., 1998. The how and why of electronic noses. *Spectrum, IEEE*, 35(9), pp.22–31.
- Nakamoto, T., 2003. Odor Handling and Delivery Systems. In T. C. Pearce et al., eds. *Handbook of Machine Olfaction*. Weinheim: WILEY-VCH Verlag GmbH & Co. KGaA, pp. 55–78.
- Nakamura, M., Mines, R. & Kreinovich, V., 1994. Guaranteed Intervals for Kolmogorov's Theorem ( and Their Possible Relation to Neural Networks ). *Materials Research*, (9), pp.1–13.
- Nakata, S., Hashimoto, T. & Okunishi, H., 2002. Evaluation of the responses of a semiconductor gas sensor to gaseous mixtures under the application of temperature modulation. *The Analyst*, 127(12), pp.1642–8. Available at: <http://www.ncbi.nlm.nih.gov/pubmed/12537374>.
- Nakata, S. & Kashima, K., 2010. Distinguishing Among Gases with a Semiconductor Sensor Depending on the Frequency Modulation of a Cyclic Temperature. *Electroanalysis*, 22(14), pp.1573–1580. Available at: <http://doi.wiley.com/10.1002/elan.201000034>.
- Nakata, S., Okunishi, H. & Nakashima, Y., 2006. Distinction of gases with a semiconductor sensor under a cyclic temperature modulation with second-harmonic heating. *Sensors and Actuators B: Chemical*, 119(2), pp.556–561. Available at: <http://linkinghub.elsevier.com/retrieve/pii/S0925400506000281>.

- Nanto, H. & Stetter, J.R., 2003. Introduction to Chemosensors. In T. C. Pearce et al., eds. *Handbook of Machine Olfaction*. Weinheim: WILEY-VCH Verlag GmbH & Co. KGaA, pp. 79–104.
- Ortega, A. et al., 2001. An intelligent detector based on temperature modulation of a gas sensor with a digital signal processor. *Sensors and Actuators, B: Chemical*, 78(1-3), pp.32–39.
- Page, T. et al., 2005. Spatial Variability of Soil Phosphorus in Relation to the Topographic Index and Critical Source Areas. *Journal of Environmental Quality*, 34(6), p.2263. Available at: <http://www.ncbi.nlm.nih.gov/pubmed/16275728> ~~¥n~~ <https://www.agronomy.org/publications/jeq/abstracts/34/6/2263>.
- Pape, L. et al., 2008. An automated dynamic chamber system for surface exchange measurement of non-reactive and reactive trace gases of grassland ecosystems. *Biogeosciences Discussions*, 5(4), pp.3157–3219.
- Patel, H.K., 2014. *The Electronic Nose: Artificial Olfaction Technology* E. Greenbaum, ed., New Delhi: Springer. Available at: <http://link.springer.com/10.1007/978-81-322-1548-6>.
- Peñuelas, J. et al., 2014. Biogenic volatile emissions from the soil. *Plant, Cell & Environment*, 37(8), pp.1866–1891. Available at: <http://doi.wiley.com/10.1111/pce.12340>.
- Puzzovio, D., 2008. *Surface interaction mechanisms in metal-oxide semiconductors for alkane detection*. Università degli Studi di Ferrara. Available at: [http://eprints.unife.it/59/1/Tesi\\_Delia\\_Puzzovio.pdf](http://eprints.unife.it/59/1/Tesi_Delia_Puzzovio.pdf).
- Rabenhorst, M.C., 2005. Biologic Zero: A Soil Temperature Concept. *Wetlands*, 25(3), pp.616–621. Available at: [http://dx.doi.org/10.1672/0277-5212\(2005\)025\[0616:BZASTC\]2.0.CO](http://dx.doi.org/10.1672/0277-5212(2005)025[0616:BZASTC]2.0.CO).
- Rappert, S. & Müller, R., 2005. Odor compounds in waste gas emissions from agricultural operations and food industries. *Waste Management*, 25(9), pp.887–907. Available

- at: <http://linkinghub.elsevier.com/retrieve/pii/S0956053X05001820>.
- Rincón, M. et al., 2010. Gas sensor array for VOC's monitoring in soils contamination. *Ingeniería*, 14(1), pp.45–54.
- Rumelhart, D.E., Hinton, G.E. & Williams, R.J., 1986. Learning internal representations by error propagation. In D. E. Rumelhart & J. L. McClelland, eds. *Parallel Distributed Processing: Explorations in the Microstructure of Cognition, 1: Foundation*. Cambridge: MIT Press, pp. 318–362.
- Sander, R., 1999. Compilation of Henry ' s Law Constants for Inorganic and Organic Species of Potential Importance in Environmental Chemistry. *Database*, 20(1), p.107. Available at: <http://www.mpch-mainz.mpg.de/~sander/res/henry.html>.
- Sander, R., 2015. Compilation of Henry's law constants (version 4.0) for water as solvent. *Atmospheric Chemistry and Physics*, 15(8), pp.4399–4981.
- Santos, J., Barreto, G. a & Medeiros, C., 2010. Estimating the Number of Hidden Neurons of the MLP Using Singular Value Decomposition and Principal Components Analysis: A Novel Approach. *2010 Eleventh Brazilian Symposium on Neural Networks*, pp.19–24. Available at: <http://ieeexplore.ieee.org/lpdocs/epic03/wrapper.htm?arnumber=5715207>.
- Scaglia, B. et al., 2011. Odours and volatile organic compounds emitted from municipal solid waste at different stage of decomposition and relationship with biological stability. *Bioresource Technology*, 102(7), pp.4638–4645. Available at: <http://dx.doi.org/10.1016/j.biortech.2011.01.016>.
- Schiffman, S.S. & Pearce, T.C., 2003. Introduction to Olfaction: Perception, Anatomy, Physiology, and Molecular Biology. In T. C. Pearce et al., eds. *Handbook of Machine Olfaction*. Weinheim: WILEY-VCH Verlag GmbH Co. KGaA, pp. 133–160.
- Sharpe, A.G., 1964. Solubility explained. *Education in chemistry*, 1, pp.75–82.
- Sherlock, R.R. et al., 1994. Estimating ammonia volatilization from unsaturated urea fertilized and urine affected soils by an indirect method. *Fertilizer Research*, 40(3),

pp.197–205.

Shurmer, H. V & Gardner, J.W., 1992. Odor Discrimination With an Electronic Nose. *Sensors and Actuators B-Chemical*, 8, pp.1–11.

Smith, K.A. et al., 2003. Exchange of greenhouse gases between soil and atmosphere: Interactions of soil physical factors and biological processes. *European Journal of Soil Science*, 54(4), pp.779–791.

Smith, K.A. & Dowdell, R.J., 1973. Gas Chromatographic Analysis of the Soil Atmosphere: Automatic Analysis of Gas Samples For O<sub>2</sub>, N<sub>2</sub>, Ar, CO<sub>2</sub>, N<sub>2</sub>O and C<sub>1</sub>-C<sub>4</sub> Hydrocarbons. *Journal of Chromatographic Science*, 11(12), pp.655–658. Available at: <http://chromsci.oxfordjournals.org/cgi/doi/10.1093/chromsci/11.12.655>.

Soil Science Society of America, 2010. Soils - Overview. *Water Resources*, pp.1–13. Available at: <https://www.soils.org/files/about-soils/soils-overview.pdf>.

Stahl, P.D. & Parkin, T.B., 1996. Microbial Production of Volatile Organic Compounds in Soil Microcosms. *Soil Science Society of America Journal*, 60(3), p.821. Available at: <https://www.soils.org/publications/sssaj/abstracts/60/3/SS0600030821>.

Sudarmaji, A. & Kitagawa, A., 2015. Sensors & Transducers Temperature Modulation with Specified Detection Point on Metal Oxide Semiconductor Gas Sensors for E-Nose Application. *Sensors & Transducers*, 186(3), pp.93–103.

Sudarmaji, A., Kitagawa, A. & Akita, J., 2013. Design of Wireless Measurement of Soil Gases and Soil Environment Based on Programmable System-on-Chip (PSOC). In *The International Symposium on Agricultural and Biosystem Engineering (ISABE)*. Yogyakarta: Jurusan Teknik Pertanian Fakultas Teknologi Pertanian UGM, pp. E5–1–E5–13.

Sudduth, K.A., Hummel, J.W. & Birrell, S.J., 1997. Sensors for Site-Specific Management. *The State of Site-Specific Management for Agriculture*, (January), pp.183–210. Available at: <http://www.ars.usda.gov/sp2UserFiles/Place/36221500/cswq-0267-sudduth.pdf>.

- Sun, Y. et al., 2004. Study of Influencing Factors of Dynamic Measurements Based on SnO<sub>2</sub> Gas Sensor. *Sensors*, 4, pp.95–104.
- Tamura, S., 1997. Method of Determining an Optimal Number of Neurons Contained in Hidden Layers of a Neural Network. , p.16.
- Tassi, F. et al., 2015. Volatile organic compounds (VOCs) in soil gases from Solfatara crater (Campi Flegrei, southern Italy): Geogenic source(s) vs. biogeochemical processes. *Applied Geochemistry*, 56, pp.37–49. Available at: <http://dx.doi.org/10.1016/j.apgeochem.2015.02.005>.
- Turner, A.P. & Magan, N., 2004. Electronic noses and disease diagnostics. *Nature reviews. Microbiology*, 2(2), pp.161–166.
- Uyanik, A. & Tinkiliç, N., 1999. Preparing Accurate Standard Gas Mixtures of Volatile Substances at Low Concentration Levels. *The Chemical Educator*, 4(4), pp.141–143. Available at: <http://dx.doi.org/10.1007/s00897990313a>.
- Vadas, P. a, Kleinman, P.J. a & Sharpley, a N., 2004. A simple method to predict dissolved phosphorus in runoff from surface-applied manures. *Journal of environmental quality*, 33(2), pp.749–56. Available at: <http://www.ncbi.nlm.nih.gov/pubmed/15074829>.
- Vass, A. a. et al., 2008. Odor analysis of decomposing buried human remains. *Journal of Forensic Sciences*, 53(2), pp.384–391.
- Wang, C. et al., 2010. Metal Oxide Gas Sensors: Sensitivity and Influencing Factors. *Sensors*, 10(3), pp.2088–2106. Available at: <http://www.mdpi.com/1424-8220/10/3/2088/>.
- Wang, C.M. & Cane, D.E., 2008. Biochemistry and molecular genetics of the biosynthesis of the earthy odorant methylisoborneol in *Streptomyces coelicolor*. *Journal of the American Chemical Society*, 130(28), pp.8908–8909.
- Wheatley, R.E., Millar, S.E. & Griffiths, D.W., 1996. The production of volatile organic compounds during nitrogen transformations in soils. *Plant and Soil*, 181(1), pp.163–167. Available at:



<http://dx.doi.org/10.1007/BF00011303>¥n<http://www.springerlink.com/content/m8u2523040747663/>.

- Wilson, A.. & Baietto, M., 2009. Applications and advances in electronic-nose technologies. *Sensors*, 9(7), pp.5099–5148. Available at: <http://www.pubmedcentral.nih.gov/articlerender.fcgi?artid=3274163&tool=pmcentrez&rendertype=abstract>.
- Wu, Y., Hamouz, F. & Schnepf, M., 1998. Factors Affecting Static Headspace-Gas Chromatographic Analysis of Lipid Oxidation in Precooked Meat. , 8561(98), pp.3677–3682.
- Yamazoe, N., Sakai, G. & Shimanoe, K., 2003. Oxide semiconductor gas sensors. *Catalysis Surveys from Asia*, 7(1), pp.63–75. Available at: <http://www.springerlink.com/index/gx42551010532137.pdf>.
- Yilmazcan, O. et al., 2013. Optimization of Static Head-Space Gas Chromatography - Mass Spectrometry-Conditions for the Determination of Benzene , Toluene , Ethyl benzene , Xylene , and Styrene in Model Solutions. *Ekoloji*, 22(89), pp.76–83.
- Yu, C. et al., 1993. *Data Collection Handbook to Support Modeling Impacts of Radioactive Material In Soil*, Argonne, Illinois. Available at: [https://web.evs.anl.gov/resrad/documents/data\\_collection\\_1993.pdf](https://web.evs.anl.gov/resrad/documents/data_collection_1993.pdf).
- Zakrzewski, J. et al., 2003. Improving Sensitivity and Selectivity of SnO<sub>2</sub> Gas Sensors by Temperature Variation. In *IEEE International Workshop on Intelligent Data Acquisition and Advanced Computing Systems: Technology and Applications*. Lviv, Ukraine, pp. 296–299.

*This page is intentionally left blank*

## Publication List

Sudarmaji, A., Kitagawa, A. & Akita, J., 2013. Design of Wireless Measurement of Soil Gases and Soil Environment Based on Programmable System-on-Chip (PSOC). In *The International Symposium on Agricultural and Biosystem Engineering (ISABE)*. Yogyakarta: Jurusan Teknik Pertanian Fakultas Teknologi Pertanian UGM, pp. E5–1–E5–13.

Sudarmaji, A. & Kitagawa, A., 2015. Temperature Modulation with Specified Detection Point on Metal Oxide Semiconductor Gas Sensors for E-Nose Application. *Sensors & Transducers*, 186(3), pp.93–103.

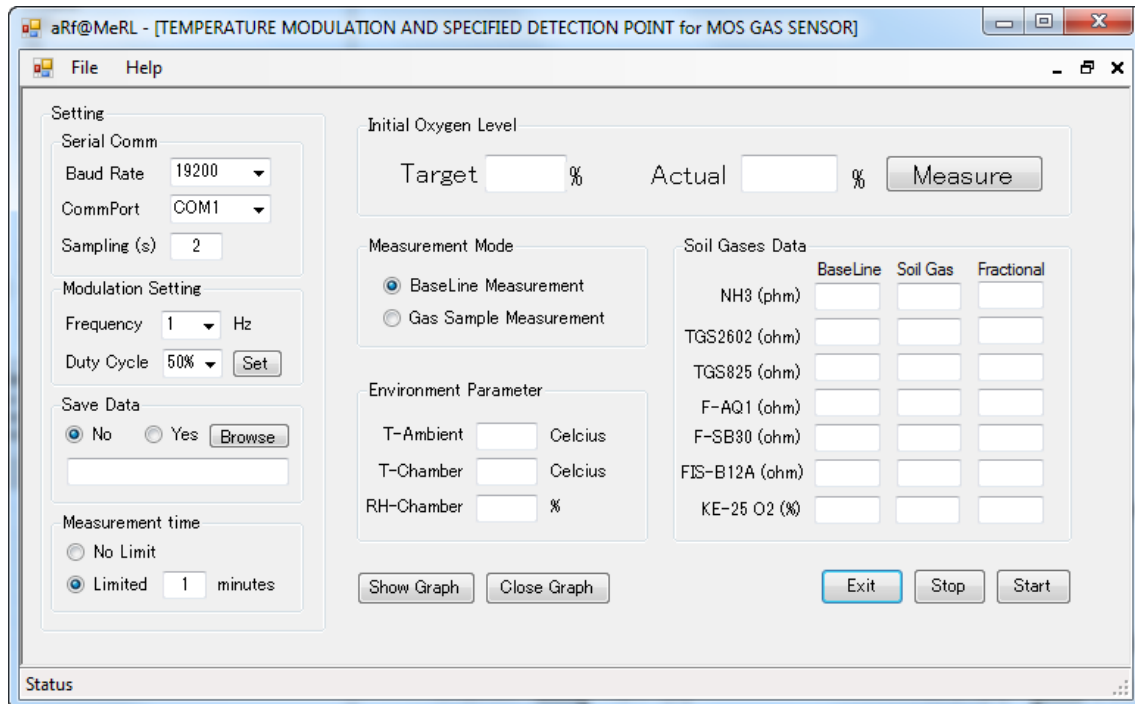
Sudarmaji, A. & Kitagawa, A., 2016. Application of Temperature Modulation-SDP on MOS Gas Sensors: Capturing Soil Gaseous Profile for Discrimination of Soil under Different Nutrient Addition. *Journal of Sensors*, 2016, pp.1–11. Available at: <http://www.hindawi.com/journals/js/2016/1035902/>.

***This page is intentionally left blank***

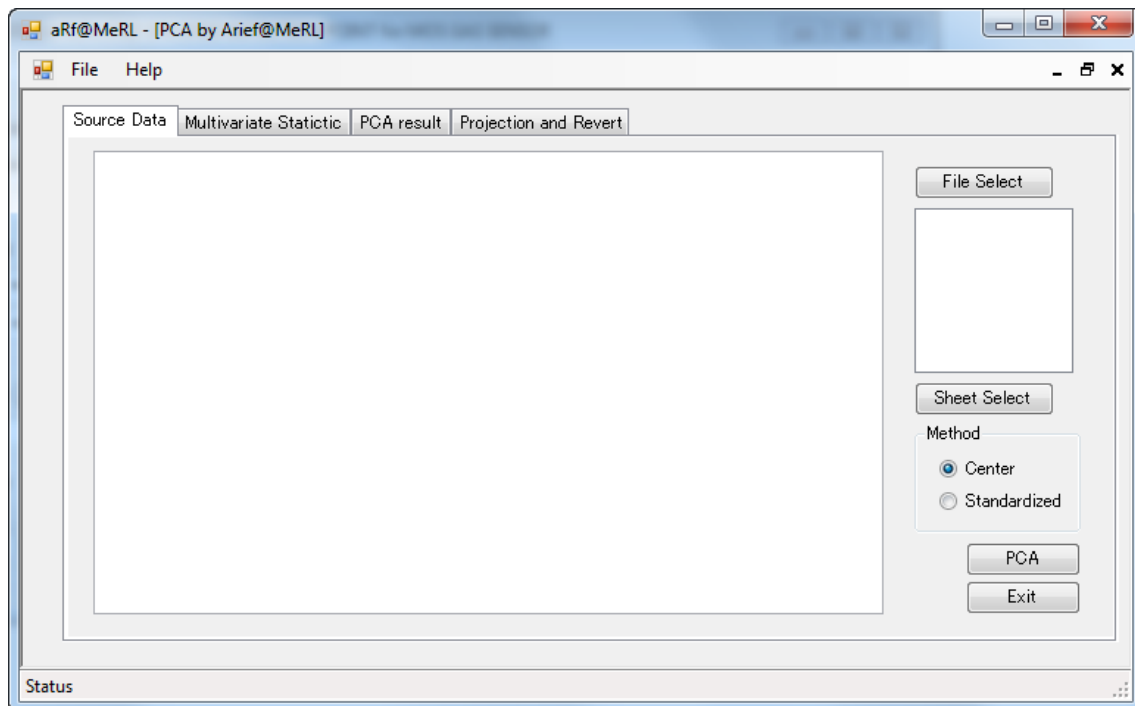
# **Appendix**

## Appendix A. Interface Display of Software.

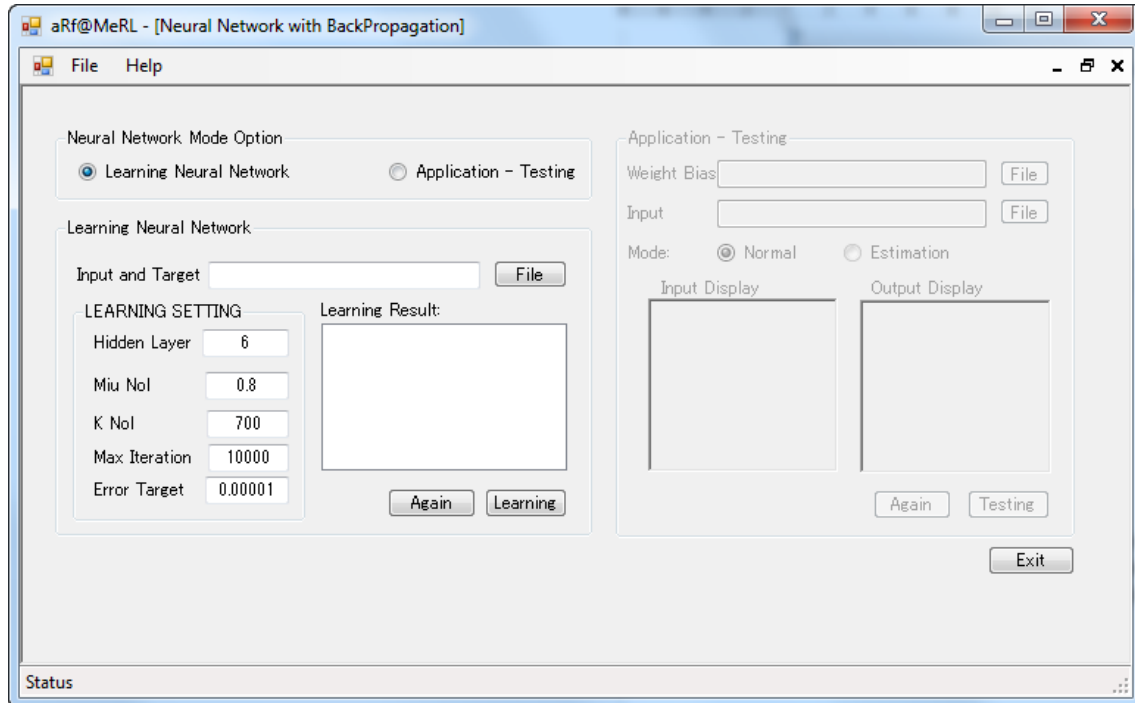
1. Interface of acquisition for setting of modulation and acquiring of sensors.



2. Interface of PCA software

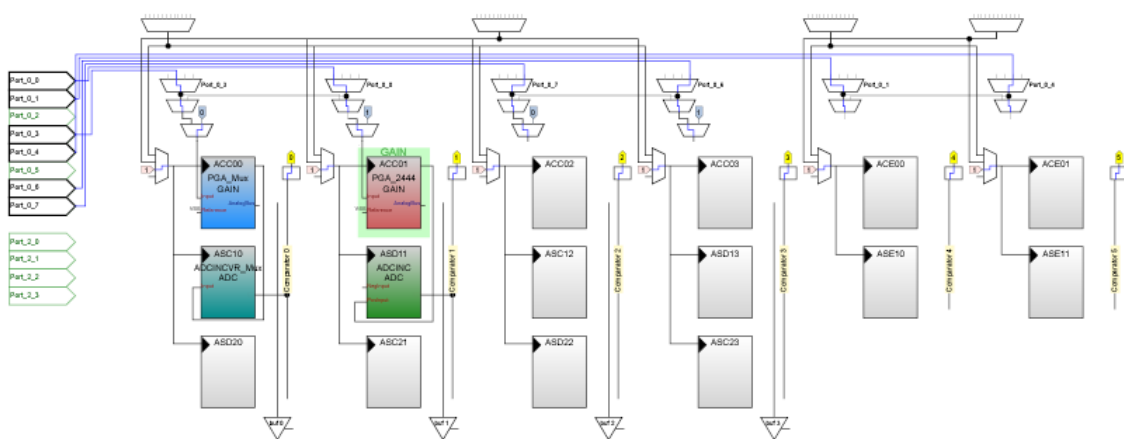
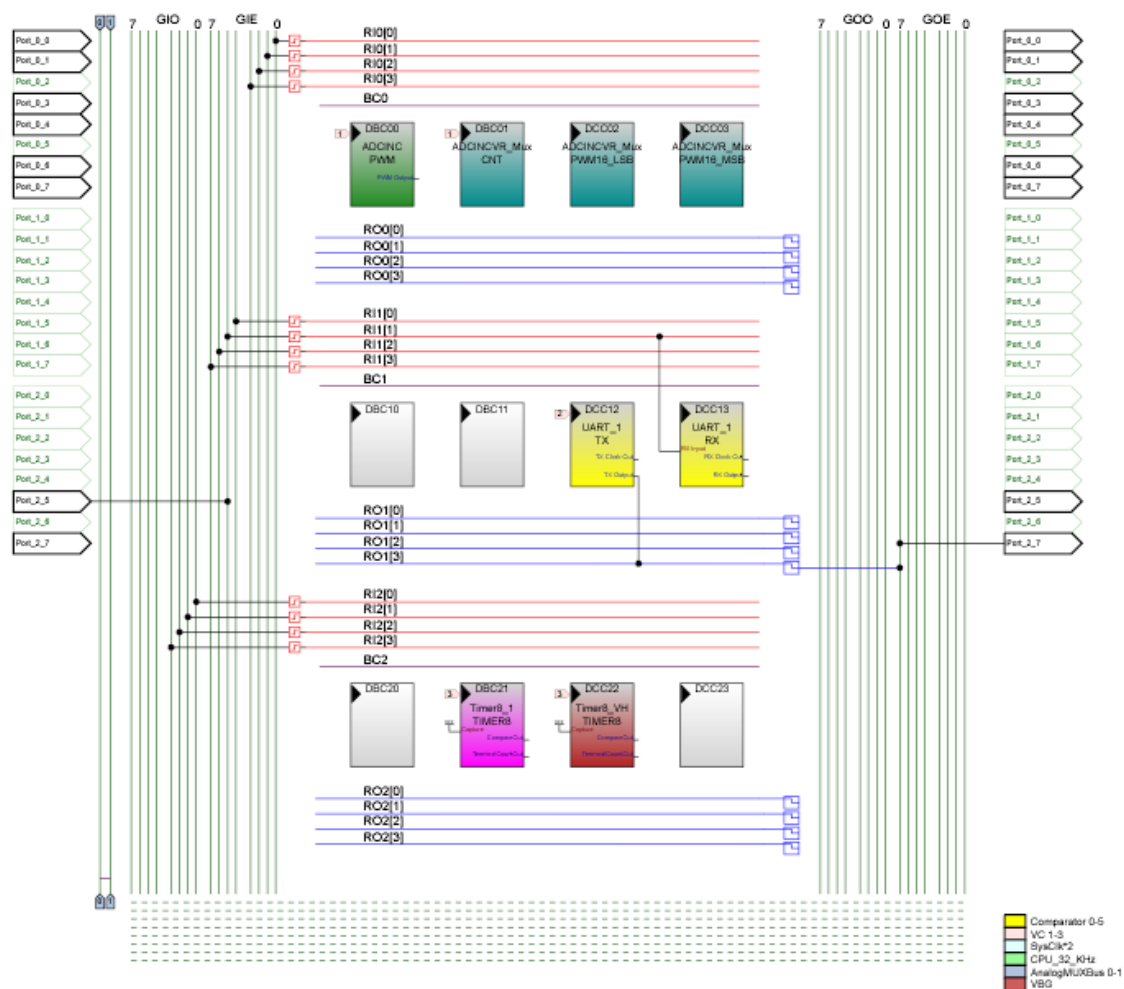


### 3. Interface of Neural Network software



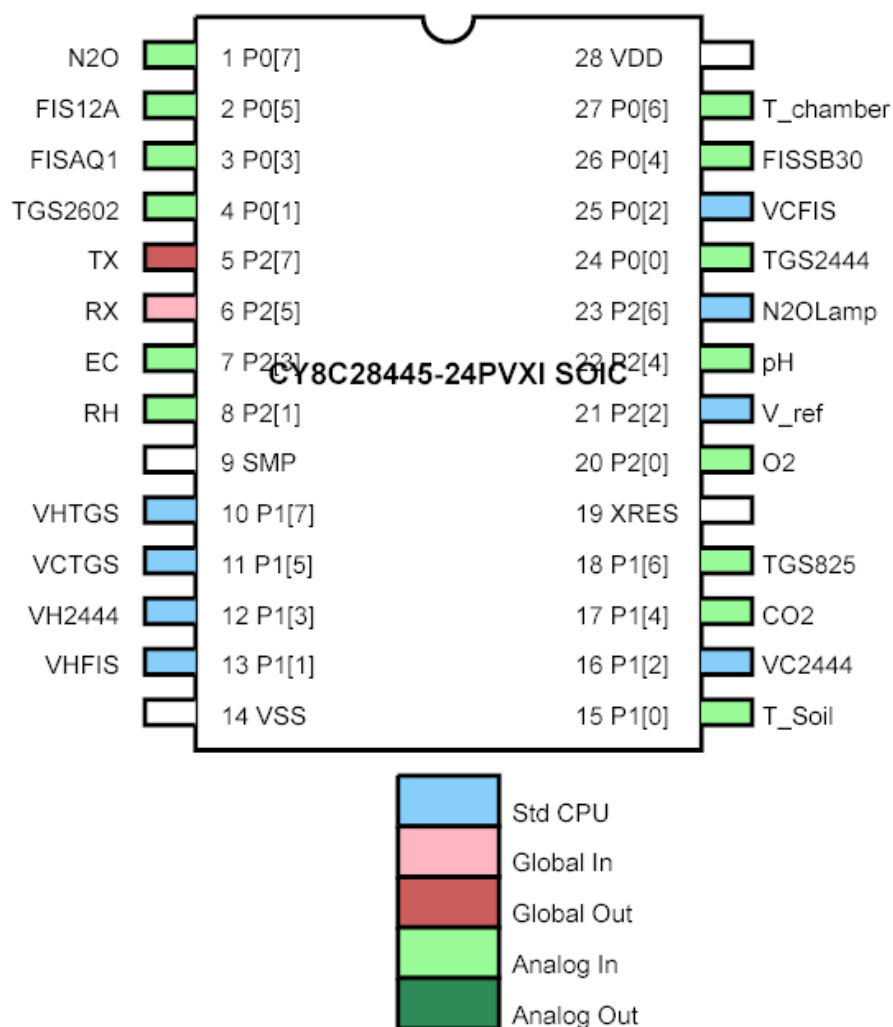
## Appendix B. Design of PSoC CY8C28445-24PVXI.

#### A. Usage of Analog and Digital blocks on PSoC CY8C28445-24PVXI.

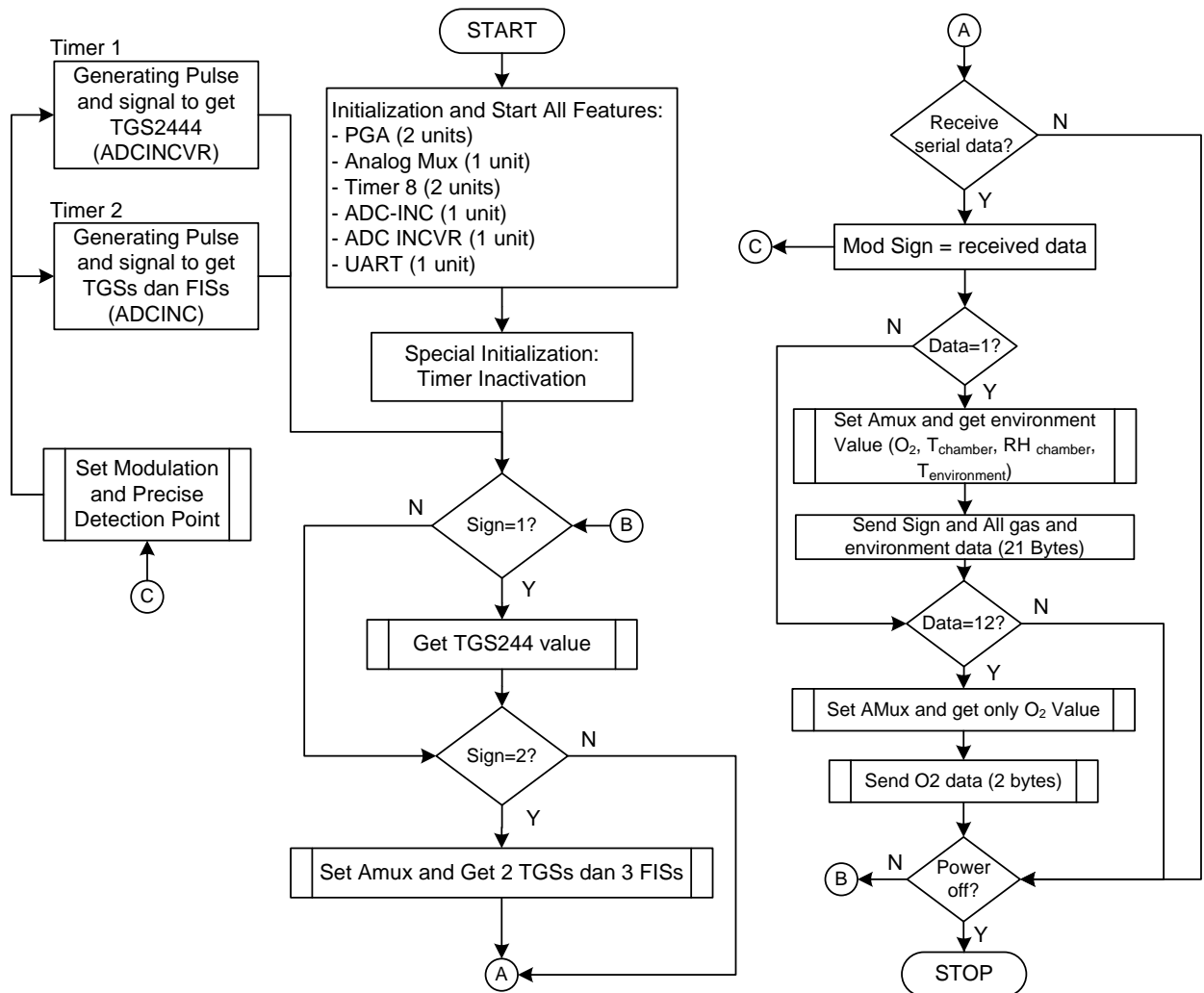




## B. Pin configuration on PSoC CY8C28445-24PVXI



C. General flowchart of PSoC CY8C28445-24PVXI firmware.



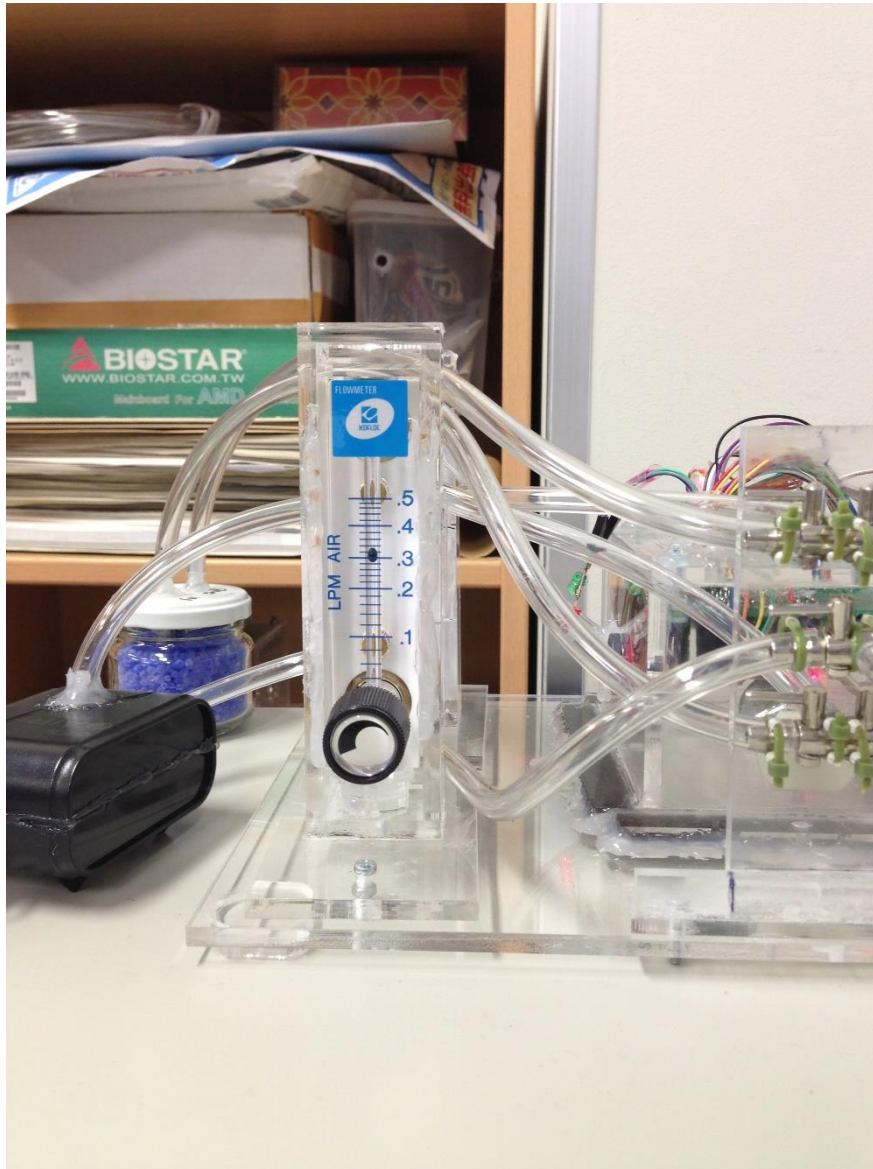
## Appendix C. Experimental documentation.



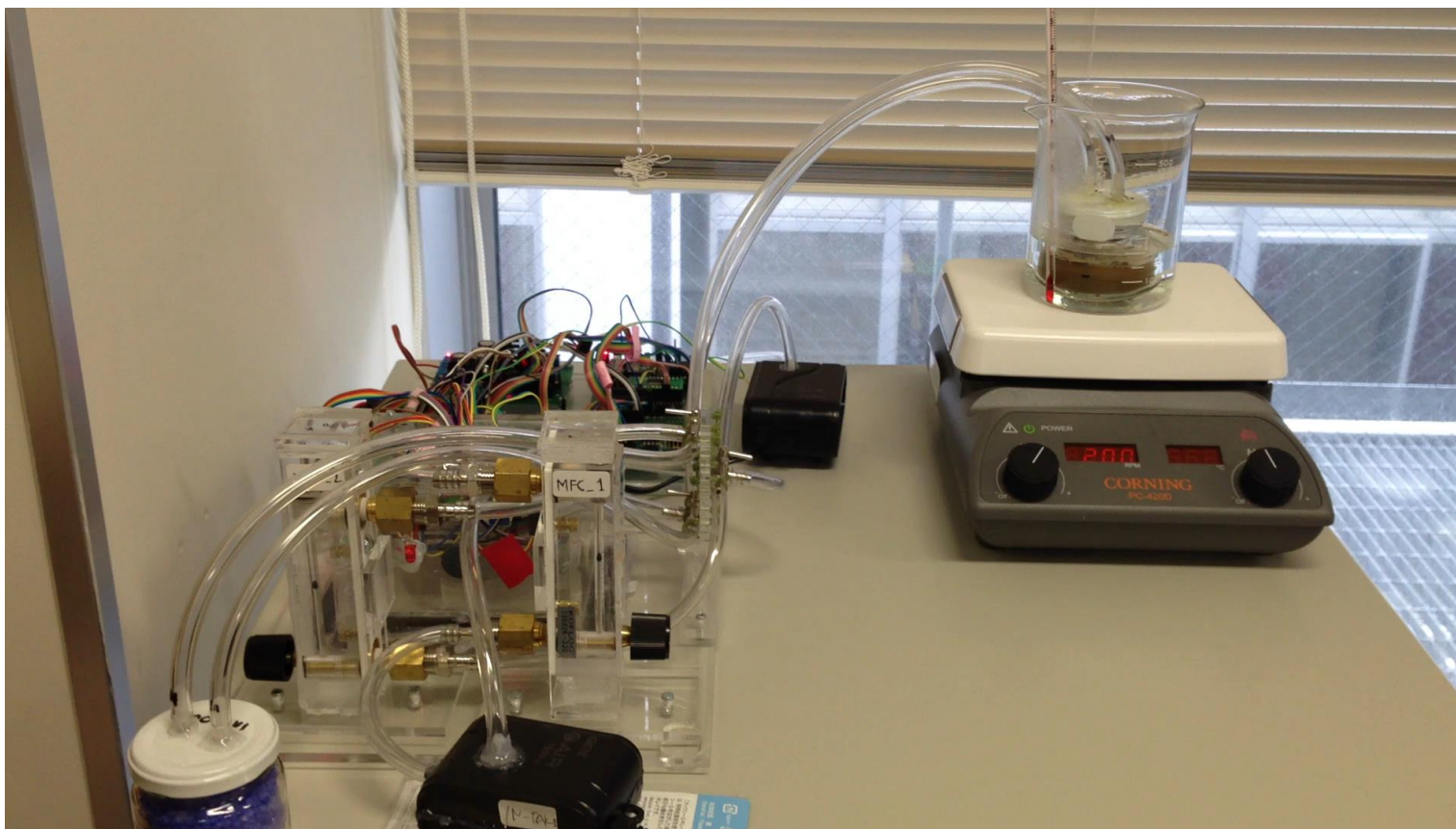
Weighting the compost for nutrient addition at normal dose



Weighting the compost for nutrient addition at high dose.



Controlled air/gas flow at 0.3 liter per minute.



Capturing soil gaseous profile using thermostating and stirring on static headspace under controlled circumstance.